Experimental approaches to study nuclear structure far from the stability: part 1

THE UNIVERSITY OF TENNESSEE KNOXVILLE

Exotic beam summer school 2026

Part 1

- Why nuclear structure in exotic nuclei?
- Radioactive ion-beam facilities
- Access nuclear structure via β-decay methods

Part 2

- Techniques for studying nuclear ground states
- Nuclear excitations and related measurements

Exotic isotopes dominate the chart of nuclei

- 3499 isotopes have been discovered by May 2026
- ~250 isotopes are known to be stable (<10% of the total), the rest are radioactive
- The properties of exotic isotopes give the full picture of how protons and neutrons are bound together inside an atomic nucleus

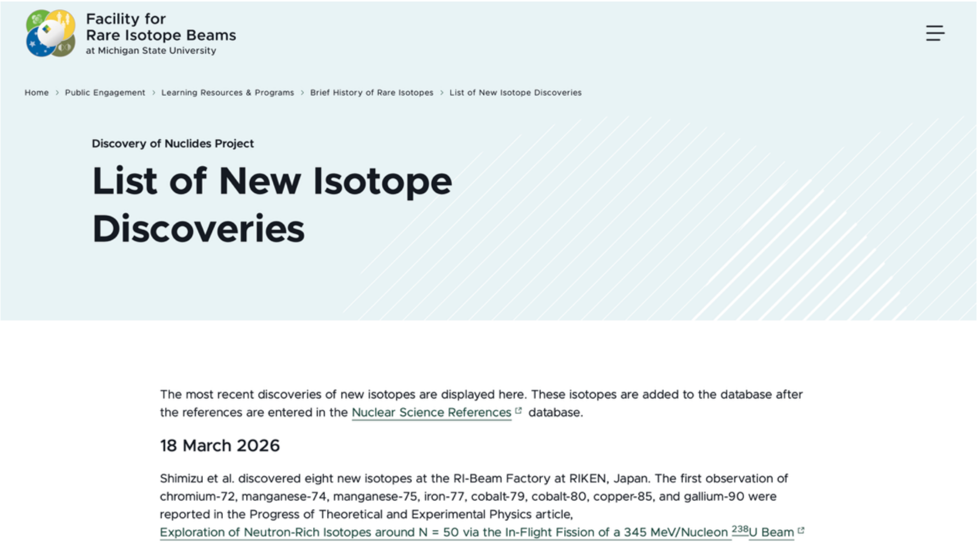
Facility for Rare Isotope Beams at Michigan State University

Home › Public Engagement › Learning Resources & Programs › Brief History of Rare Isotopes › List of New Isotope Discoveries

Discovery of Nuclides Project

List of New Isotope Discoveries

The most recent discoveries of new isotopes are displayed here. These isotopes are added to the database after the references are entered in the Nuclear Science References database.

18 March 2026

Shimizu et al. discovered eight new isotopes at the RI-Beam Factory at RIKEN, Japan. The first observation of chromium-72, manganese-74, manganese-75, iron-77, cobalt-79, cobalt-80, copper-85, and gallium-90 were reported in the Progress of Theoretical and Experimental Physics article, Exploration of Neutron-Rich Isotopes around N = 50 via the In-Flight Fission of a 345 MeV/Nucleon ^{238}U Beam

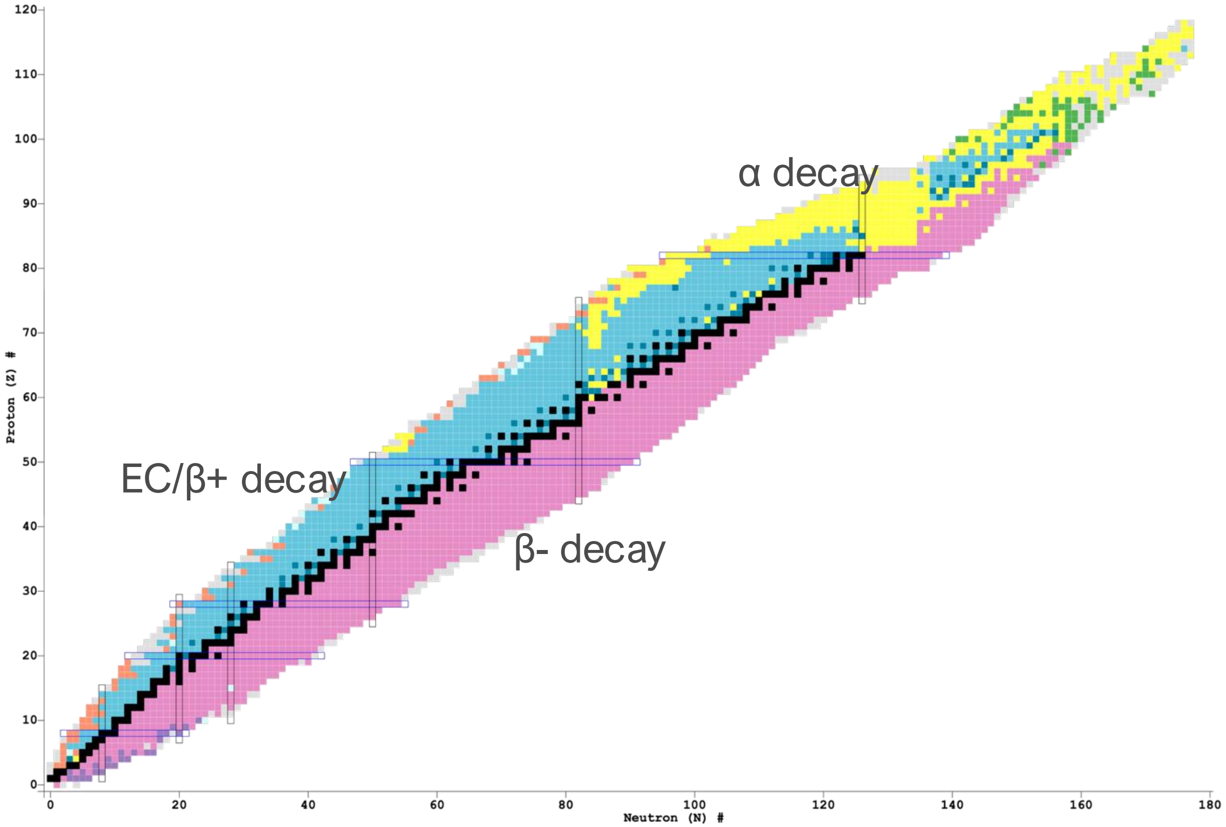

https://frib.msu.edu/public-engagement/learning-resources-and-programs/brief-history-of-rare-isotopes/list-of-new-isotope-discoveries

Exotic isotop

- 3499 isotopes have been c
- ~250 isotopes are known t total), the rest are radioact
- The properties of exotic isc picture of how protons and together inside an atomic r

Facility for Rare Isotope Beams at Michigan State University

Home › Public Engagement › Learning Resources & Programs › Brief History of Rare Isotopes › List of New Is

Discovery of Nuclides Project

List of New Isotope Discoveries

The most recent discoveries of new isotopes are displayed h the references are entered in the Nuclear Science Reference

18 March 2026

Shimizu et al. discovered eight new isotopes at the RI-Beam chromium-72, manganese-74, manganese-75, iron-77, cobalt reported in the Progress of Theoretical and Experimental Ph Exploration of Neutron-Rich Isotopes around N = 50 via the

Isotopes of Nickel (35 total)

In the table below click on an isotope symbol for more information about its discovery. When quoting the abstracts please cit the abstract as: "FRIB Nuclear Data Group, *Discovery of Nuclides Project*, Isotope Database, doi:10.11578/frib/2279152". Newly discovered isotopes will be included after the references are entered in the NSR database.

go to search page

Isotope	First Author	Lab	Country	Year	Reference
^{60}Ni	F. W. Aston	Cambridge	United Kingdom	1921	1921AS04
^{61}Ni	F. W. Aston	Cambridge	United Kingdom	1934	1934AS04
^{62}Ni	F. W. Aston	Cambridge	United Kingdom	1934	1934AS04
^{63}Ni	A. R. Brosi	Oak Ridge	USA	1951	1951BR05
^{64}Ni	J. de Gier	Amsterdam	Netherlands	1935	1935DE08
^{65}Ni	J. A. Swartout	Oak Ridge	USA	1946	1946SW01
^{66}Ni	R. H. Goeckermann	Berkeley	USA	1948	1948GO29
^{67}Ni	R. T. Kouzes	Princeton	USA	1978	1978KO28
^{68}Ni	T. S. Bhatia	Heidelberg	Germany	1977	1977BH03
^{69}Ni	P. Dessagne	Orsay	France	1984	1984DE33
^{70}Ni	P. Armbruster	Grenoble	France	1987	1987AR21
^{71}Ni	P. Armbruster	Grenoble	France	1987	1987AR21
^{72}Ni	P. Armbruster	Grenoble	France	1987	1987AR21
^{73}Ni	P. Armbruster	Grenoble	France	1987	1987AR21
^{74}Ni	P. Armbruster	Grenoble	France	1987	1987AR21
^{75}Ni	M. Weber	Darmstadt	Germany	1992	1992WE04
^{76}Ni	Ch. Engelmann	Darmstadt	Germany	1995	1995EN07
^{77}Ni	Ch. Engelmann	Darmstadt	Germany	1995	1995EN07
^{78}Ni	Ch. Engelmann	Darmstadt	Germany	1995	1995EN07
^{79}Ni	T. Ohnishi	RIKEN	Japan	2010	2010OH02
^{80}Ni	Z. Y. Xu	RIKEN	Japan	2014	2014XU07
^{81}Ni	T. Sumikama	RIKEN	Japan	2017	2017SU15
^{82}Ni	T. Sumikama	RIKEN	Japan	2017	2017SU15

decay

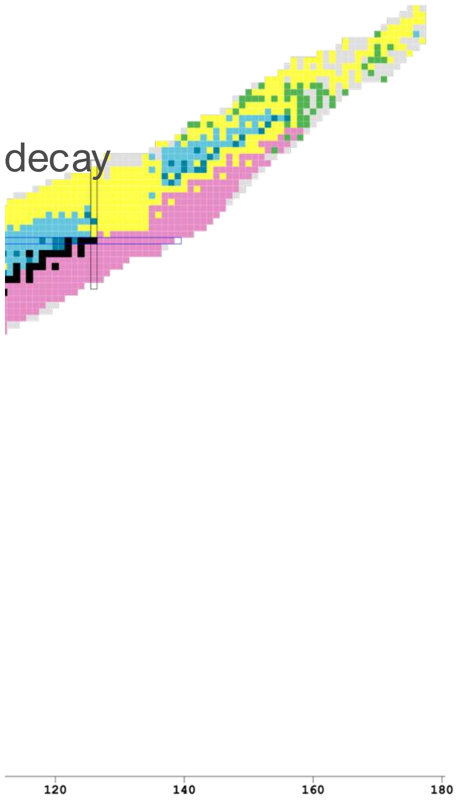

ning-resources-and-
f-new-isotope-discoveries

Nuclear shell model and spin-orbital splitting

ΔB = Binding energy (experiment) – Weizsaecker-Bethe mass formula

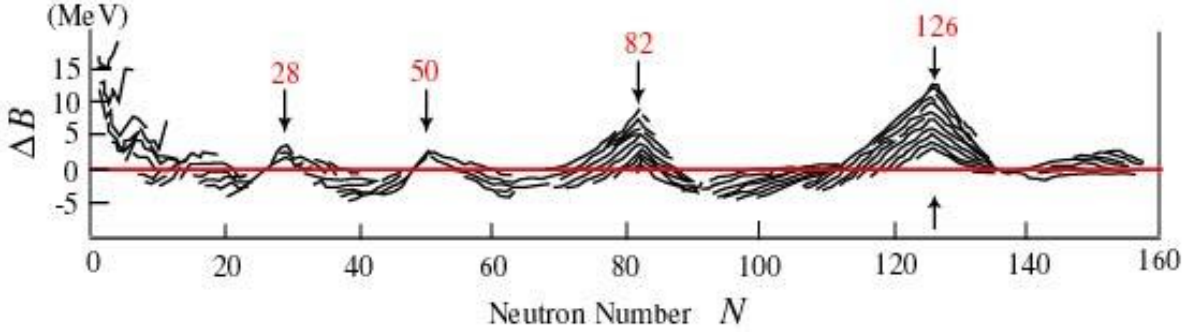

Ragnarsson and Nilsson, 1995

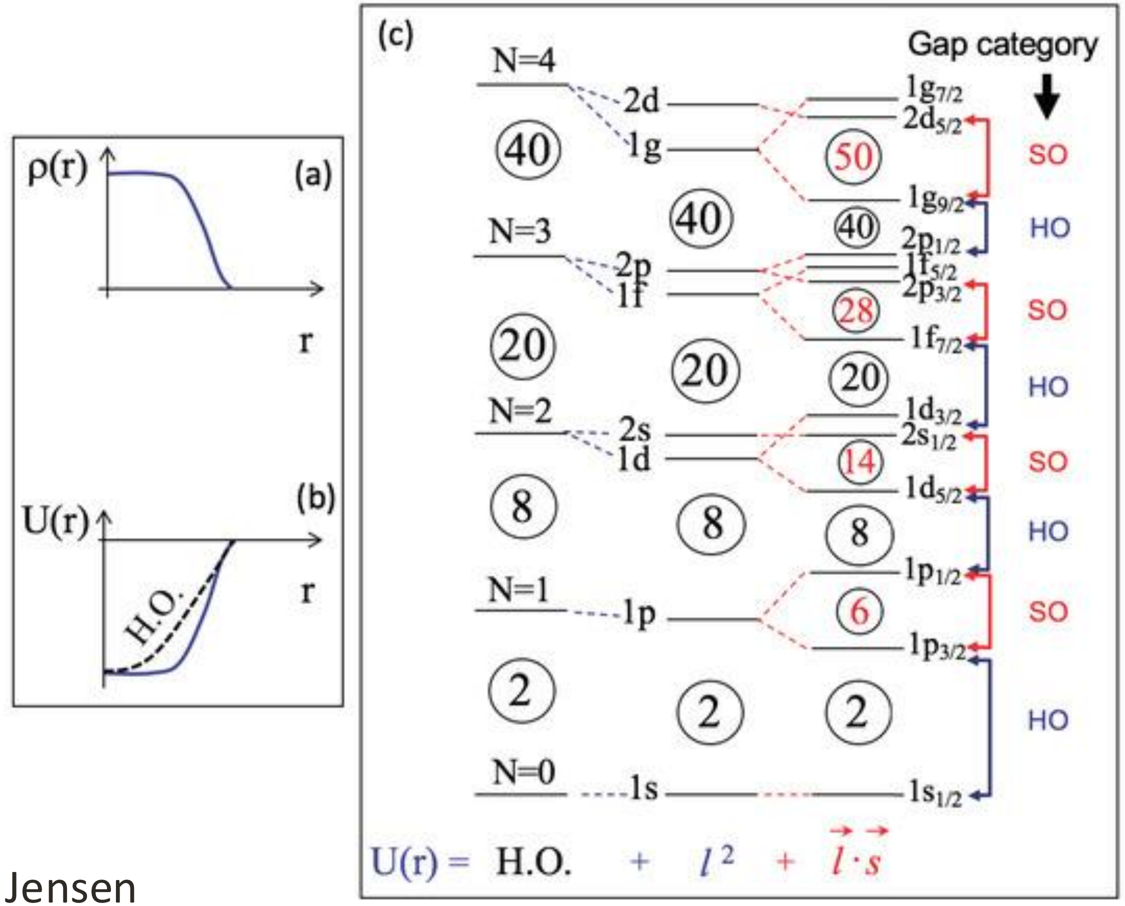


G. Mayer and J.H.D. Jensen

The collective (unified) model

Fig. 9

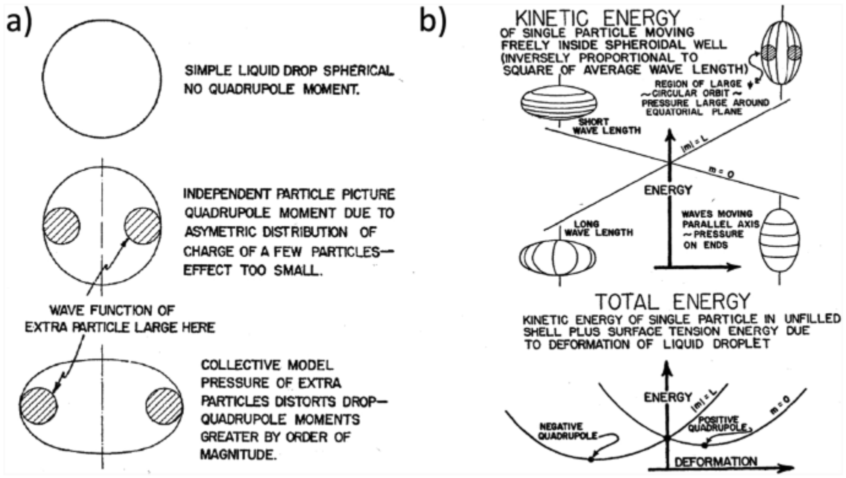

D.L. Hill and J.A. Wheeler, Phys. Rev. 89, 1102 (1953)

XVII

COLLECTIVE NUCLEAR MOTION AND THE UNIFIED MODEL

A. BOHR AND B. R. MOTTELSON

§ 1. Collective Oscillations of a Shell Structure

While a large body of empirical data has revealed the existence of a nuclear shell structure (cf. Ch. XV and XVI of this book), other features of the nuclear phenomena exhibit the influence of collective nuclear motion [1]. Indeed, it is to be expected from very general arguments that a system of particles held together by their mutual attraction can perform collective oscillations which resemble the degrees of freedom possessed by matter in bulk [2].

The generalization of shell models to include collective motion can be effected in a straightforward manner. In fact, the shell model operates with an average field in which the particles move and which is generated collectively by all the particles. In the usual shell models, this field is considered a static quantity, but a more complete description must take into account the variation of the field associated with collective oscillations.

In the atomic shell model, this aspect of the structure is of relatively minor significance due to the stabilizing influence of the heavy central nucleus. However, the lack of such an external stabilization of the nuclear field implies that the collective degrees of freedom are of fundamental significance for the nuclear dynamics.

Since the collective oscillations involve variations in the average nuclear field, they are strongly coupled to the motion of the individual nucleons. The unified model thus describes the nucleus in terms of a coupled system of particle and collective degrees of freedom. In many respects, the dynamics of such a system is similar to that of molecules, where one has a coupled system of electronic motion and collective rotations and vibrations of the structure as a whole.

The most important collective degrees of freedom for the low energy nuclear properties are expected to be those associated with oscillations in shape with approximate preservation of the nuclear volume. For a nucleus of constant density, these oscillations have the character of surface waves.

J. Rainwater, A. Bohr, and B. Mottelson

“Unexpected” nuclear properties in exotic nuclei

- The excitation energy of the first 2^+ state, $E(2^+)$, is a good indicator of nuclear collectivity
- Relatively large $E(2^+)$ (>=1 MeV) is expected for nuclei that are either semi or doubly magic, e.g., with N=20
- ^{32}Mg (Z=12, N=20) exhibits a low-lying 2^+ state (< 900 keV) even though N=20 is a magic number
  - Neutrons favor excitation across the N=20 shell gap to gain extra binding energies → N=20 shell is weak
- Exotic nuclei such as ^{32}Mg have been challenging nuclear models in the last few decades, advancing our understanding of nuclear evolution towards proton and neutron driplines

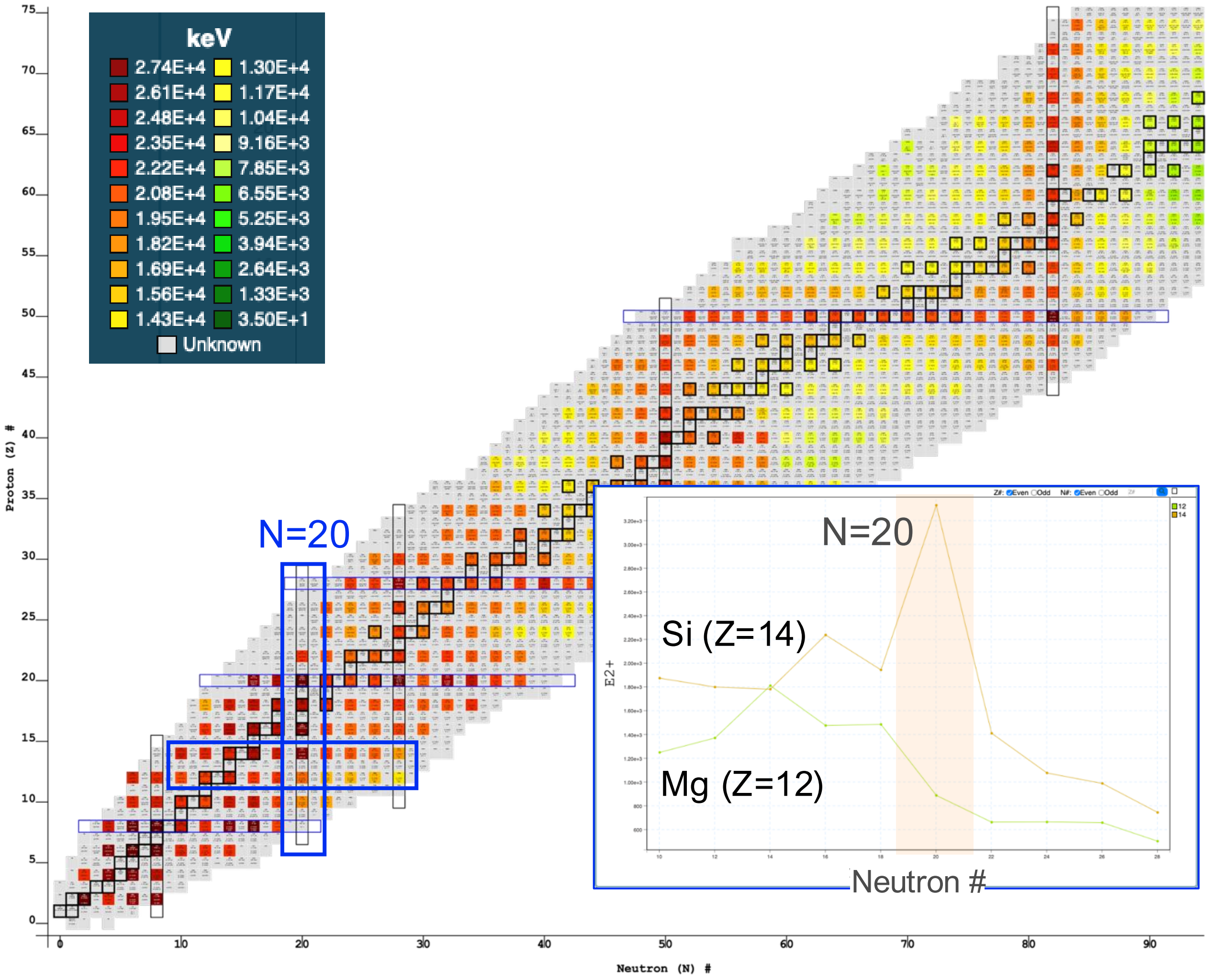

Studying exotic isotopes is an experimental challenge

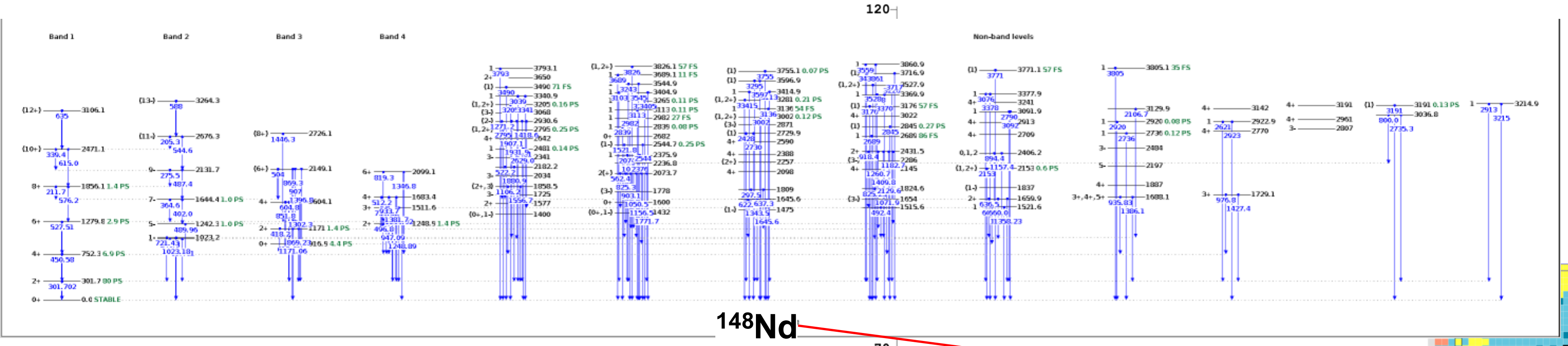

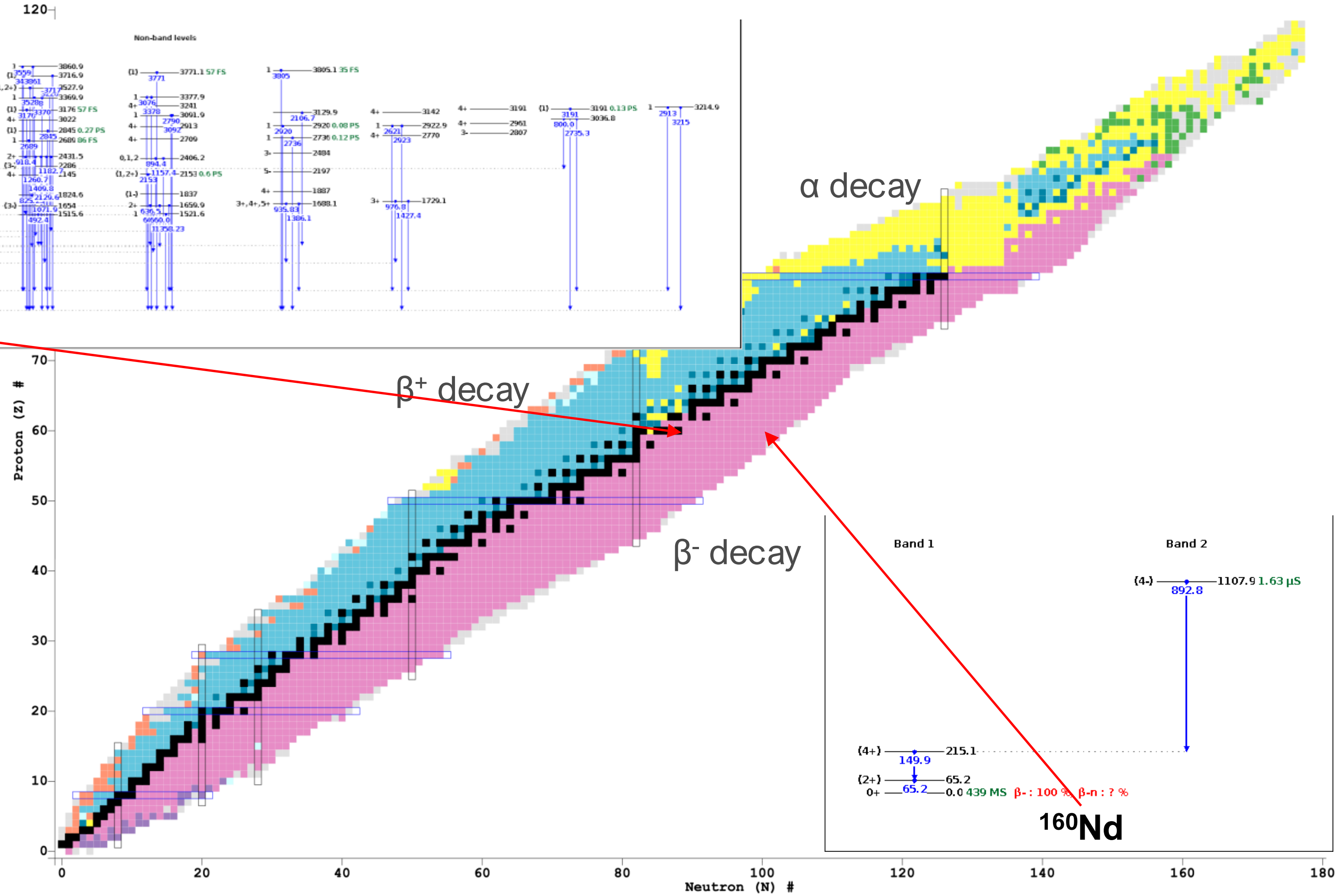

- Exotic nuclei don’t exist naturally (short-lived)
- They need to be produced before being studied in our laboratories
- How much we can produce them (statistics) makes the difference!

Radioactive ion-beam facilities

The radioactive ion-beam (RIB) facilities produces short-lived isotopes far from stability, via various nuclear reactions and delivers exotic beams for experimental measurements

- Two major types of methods to produce radioactive isotopes
  - Isotope Separation On-Line (ISOL): ISOLDE, IGISOL, TRIUMF, etc
  - In-flight Fragmentation: FRIB, RIBF, GSI, etc

ISOLDE at CERN

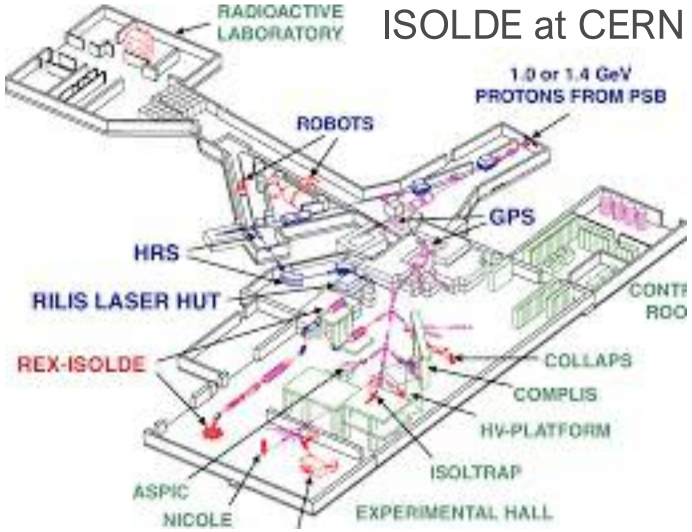

FRIB at MSU

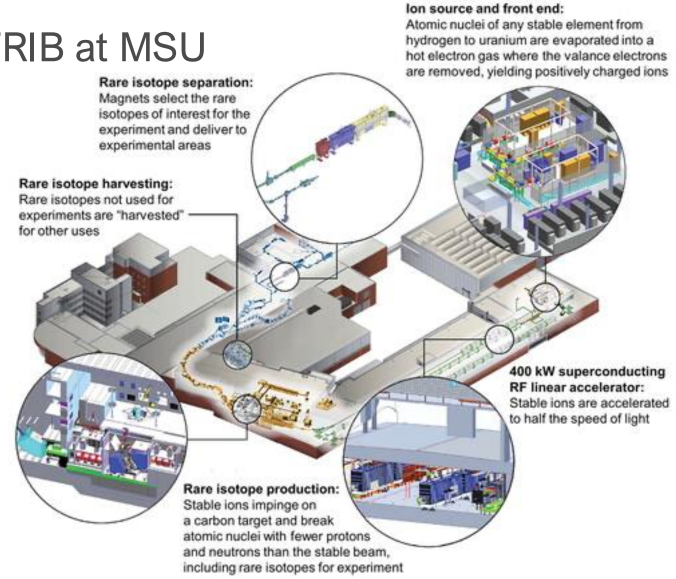

Isotope Separation On-Line

- A high-energy primary beam of light particles, e.g., protons, impinge on a thick target (a few centimeters) containing heavy elements, e.g., UCx
- The target is heated to high temperature so that the products diffuse into the ion sources, e.g., resonant ionization laser ion sources
- The ions of interest (mostly single charged) were selected by magnetic mass separators
- The beams can be directly delivered to low-energy experiments, or be reaccelerated for reaction experiments

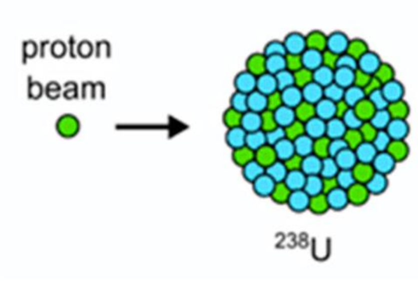

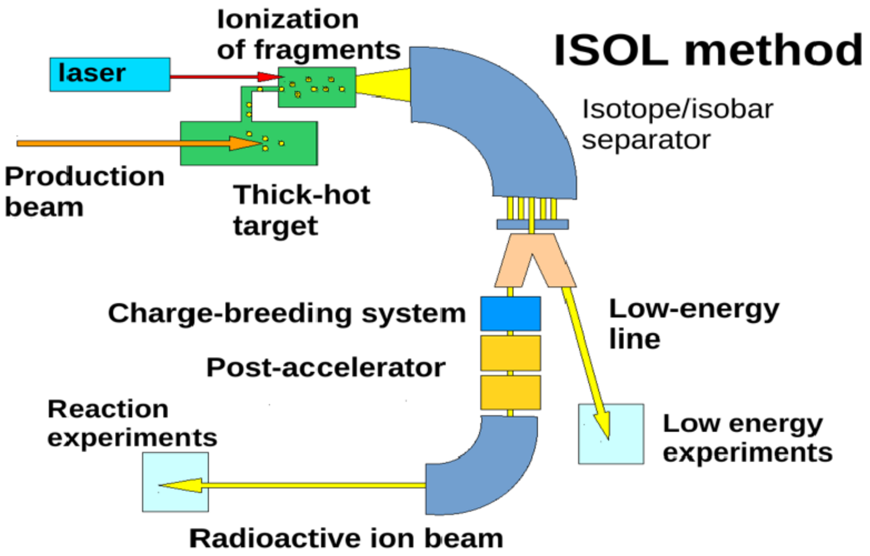

Courtesy of Maria J. G. Borge

In-flight fragmentation

- A high-energy primary beam of heavy particles, e.g., ^{238}U, impinges on a thin target (a few millimeters) of light element, e.g., carbon or beryllium

- The fragments are produced at large forward momentum, with a velocity similar to the primary beams, e.g., a fraction of the speed of light

- Isotopes of interest are selected by their magnetic rigidity (Bρ=*p*/*q*)

- After Bρ selection, the cocktail beams need to be tagged by their atomic numbers and mass-to-charge ratios (next slide)

- Beam can be delivered to the experimental setup (fast beam), or stopped in a gas catcher and reaccelerated to low kinetic energy (slow beam)

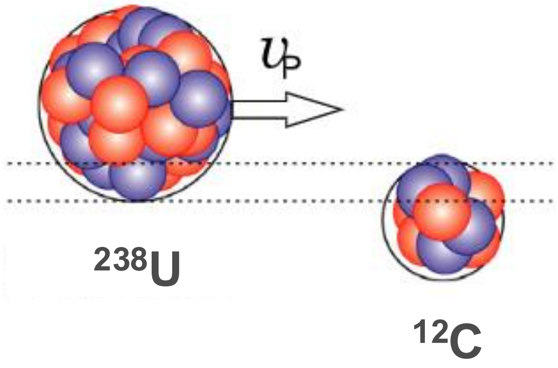

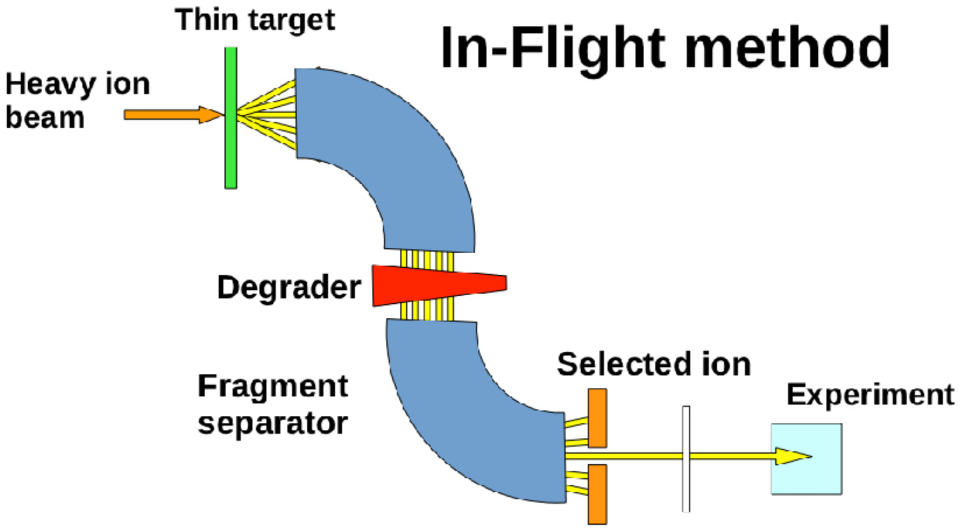

Courtesy of Maria J. G. Borge

Particle identification (PID) for cocktail beams

- Secondary beams from in-flight fragmentation facilities are usually cocktail beams
- We need to identify the ions on an event-by-event basis
- The goal is to reconstruct the atomic number (Z) and mass-to-charge ratio (A/Q) of the ions
  - Additionally, the charge (Q) if more than one charge state is transmitted (necessary in the heavy mass region)
- This is usually done in the so-called Bρ-TOF-ΔE approach
  - $A/Q \sim B\rho/\beta\gamma$ (β is velocity and γ is the Lorentz factor)
  - $Z \sim [\Delta E\ f(\beta)]^{1/2}$ (the Bethe-Bloch energy-loss formula)

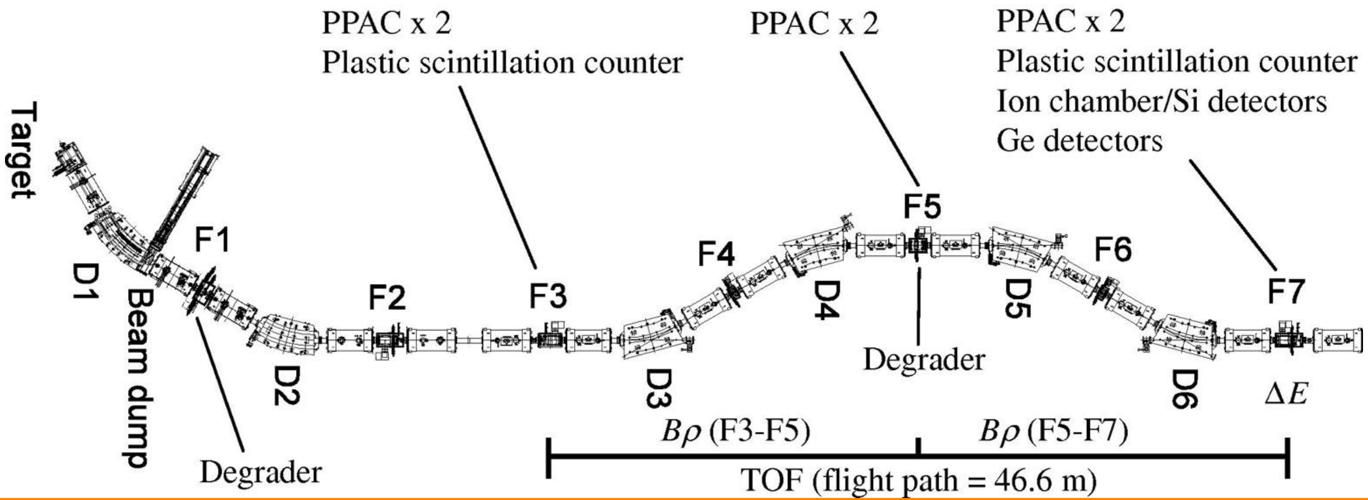

BigRIPS at RIBF, RIKEN

PID for the ^{238}U (345MeV/u) + Pb reaction

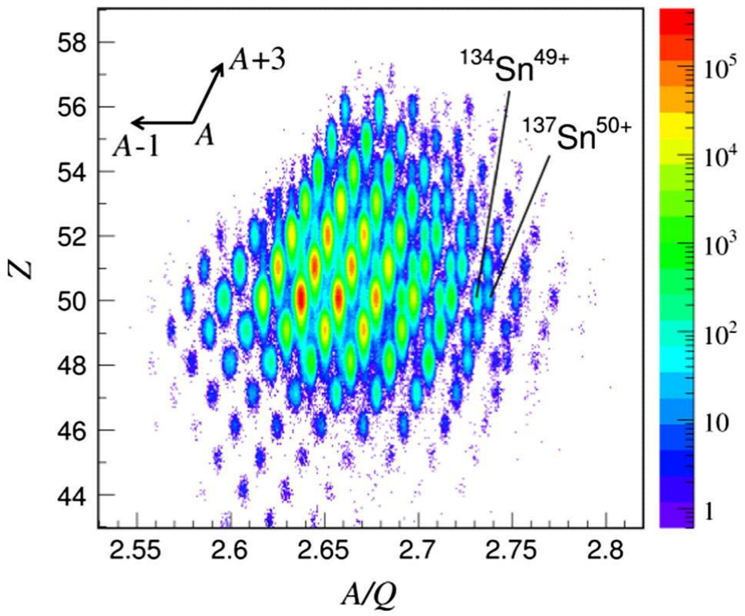

N.Fukuda et al., NIMB 317, 323 (2013)

THE UNIVERSITY OF TENNESSEE KNOXVILLE

Comparison between the two methods

	Isotope Separation On-Line	In-flight Fragmentation
Pros	• Usually very high beam rates • Usually excellent beam purities, low background • Well controlled beam energies allow for high-precision measurements	• Study multiple nuclei at the same time • Beam production doesn't depend on the chemical properties • Capable of studying nuclear states with sub-millisecond life times
Cons	• One isotope at a time • Beam extraction depends on their chemical properties • Hard to study nuclear states with sub-millisecond life times	• Beam purities are generally bad, especially for the most exotic species • Beam rates are usually not as high as the ISOL facilities • Particle identification becomes more challenging with increasing nuclear masses

β decay: definition

β decay is a weak process transforming a neutron into a proton, or vice versa (transitions between two neighboring isobars)

- β minus decay $\beta^-: n \rightarrow p + e^- + \tilde{\nu}$
- β plus decay $\beta^+: p \rightarrow n + e^+ + \nu$
- Electron capture $EC: p + e^- \rightarrow n + \nu$

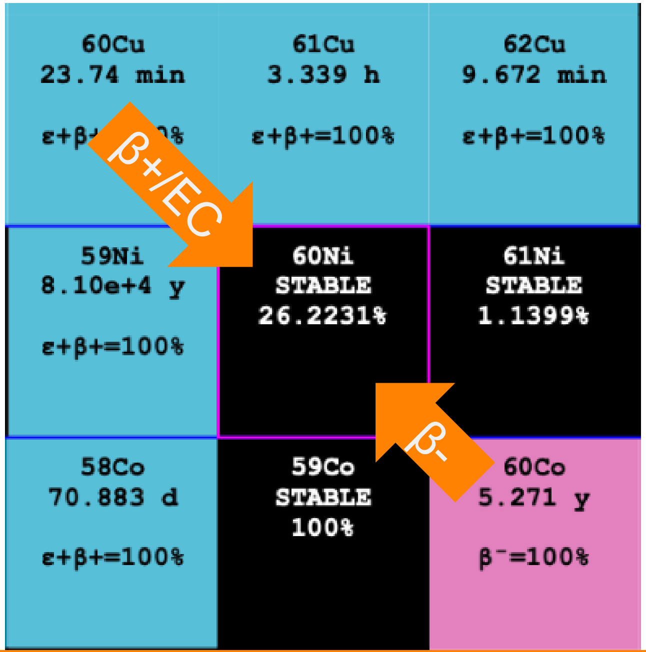

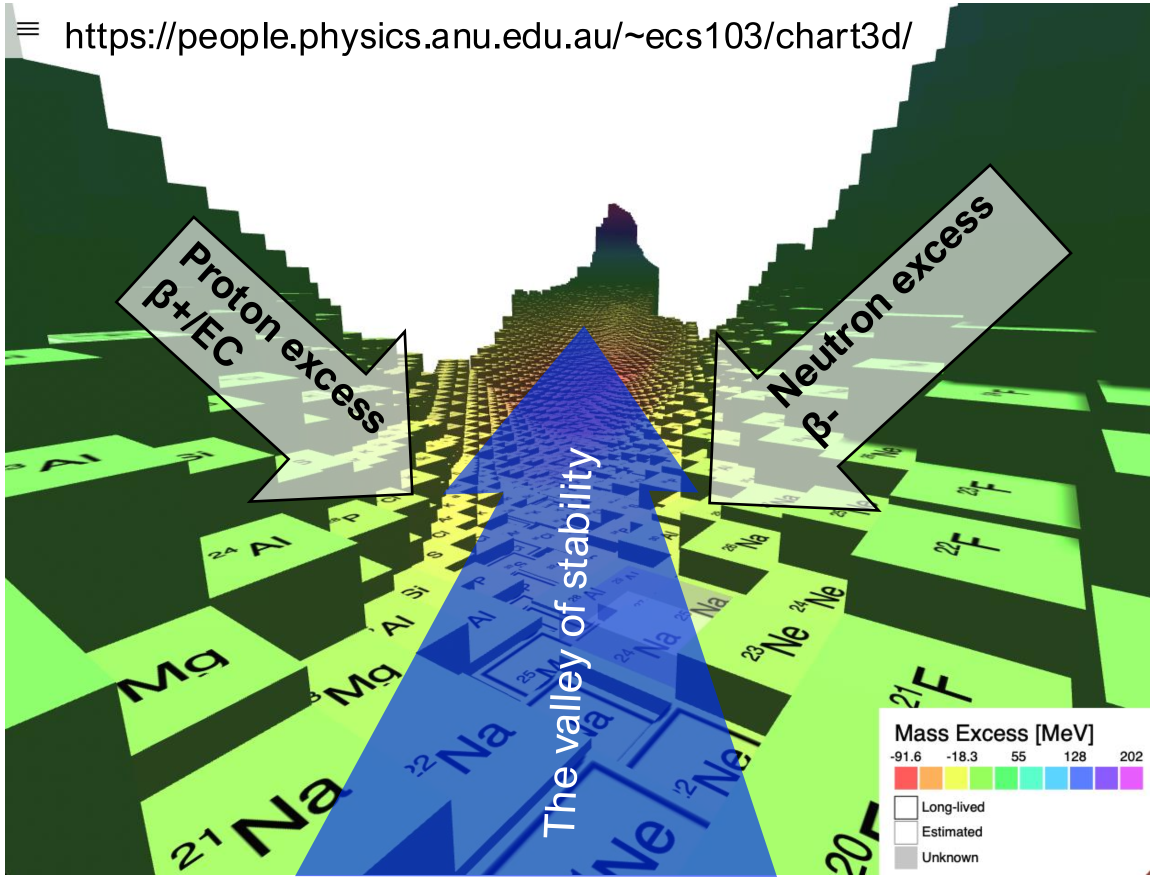

β decay energy window, Q_β

Q_β defines the maximum energy that can be released in the β decay (from parent ground state to daughter ground state)

- $Q_{\beta^-} = ME(Z, A) - ME(Z+1, A)$
- $Q_{\beta^+} = ME(Z, A) - ME(Z-1, A) - 2m_e$
- $Q_{EC} = ME(Z, A) - ME(Z-1, A)$

- β decay can only happen if $Q_\beta > 0$
- ME is atomic (not nuclear) mass excess
- The energy window of EC is about 1.022 MeV greater than that of β+ decay of the same nucleus
- The Q value of an actual β-decay transition depends on the excitation energy of the daughter nucleus (see next slide)

Classification of β-decay transition

- E_β is the total kinetic energy shared between leptons (β particle's energy is not discrete)
- $S_\beta = s_\beta + s_\nu$ = 0 or 1 (more details in the next slide)
- $L_\beta = l_\beta + l_\nu = n$ defines the degree of forbiddenness (n)
- Allowed β decay
  - $L_\beta = 0$ and $\pi_i = \pi_f$!! Populate a clean set of states
    - e.g., $g_{9/2} \rightarrow g_{7/2}$
- Forbidden β decay
  - $L_\beta = n > 0$ and $\pi_i \pi_f = (-1)^n$
    - $n = 1$ → First-forbidden transition
      - e.g., $g_{9/2} \rightarrow f_{7/2}$
    - $n = 2$ → Second-forbidden transition…
      - e.g., $g_{9/2} \rightarrow d_{5/2}$
- For the decay study of exotic isotopes, most of the observed transitions are (strong) allowed and (weak) first-forbidden β decay

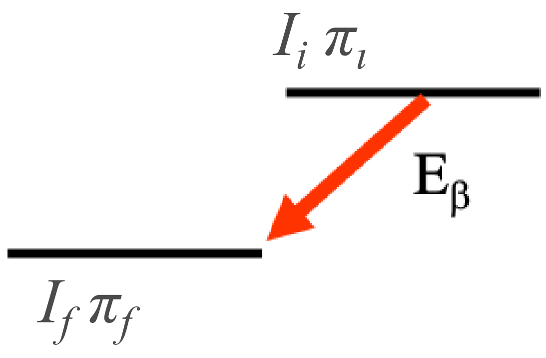

$$I_i = I_f + (L_\beta + S_\beta)$$
$$\pi_i = \pi_f (-1)^{L_\beta}$$

Classification of allowed transition

- With L_β = 0, an allowed transition can be either
  - Fermi transition: S_β = 0 (ΔI = 0)
    - Example: $0^+ \rightarrow 0^+$
  - Or Gamow-Teller transition: S_β = 1 (ΔI = 0 but not $0^+ \rightarrow 0^+$, -1 or 1)
    - Example: $0^+ \rightarrow 1^+$
- Only the Fermi transition allows a $0^+ \rightarrow 0^+$ decay
- A transition such as $1^+ \rightarrow 1^+$ can be a mixture of Fermi and Gamow-Teller transitions

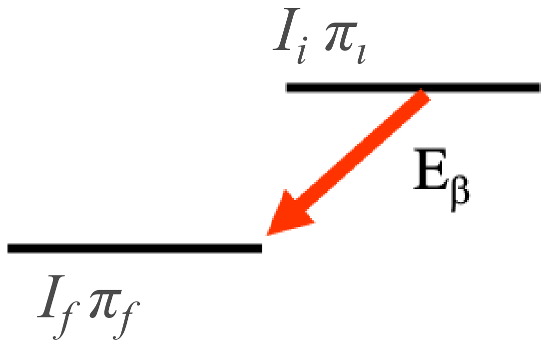

$$I_i = I_f + (L_\beta + S_\beta)$$
$$\pi_i = \pi_f (-1)^{L_\beta}$$

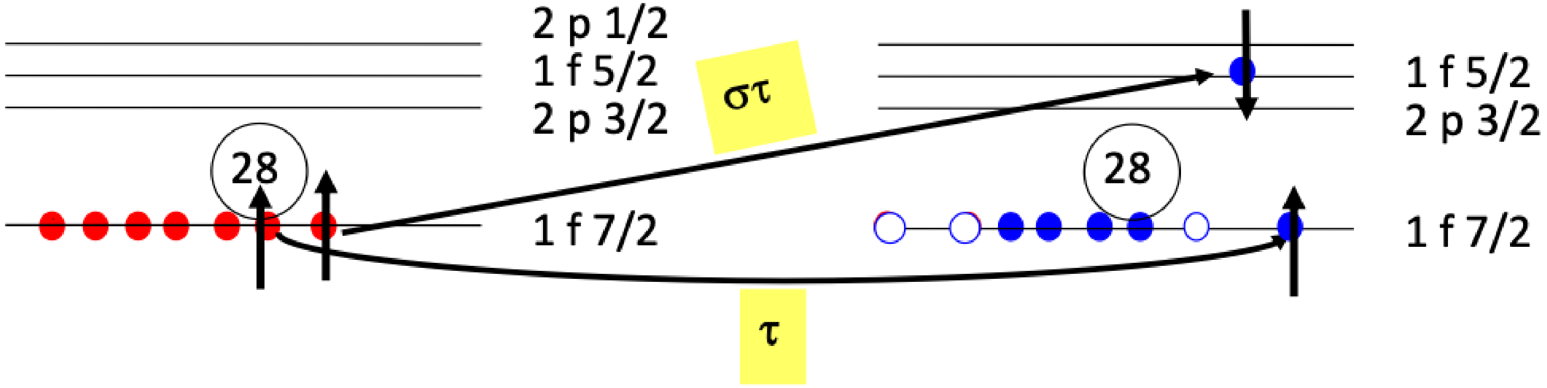

Selection rules of β decay transition

Class	ΔI	$\Delta\pi$	S	L_β
Allowed, Fermi	0	no	0	0
Allowed, Gamow-Teller	0, 1	no	1	0
First forbidden, Fermi	0, 1	yes	0	1
First forbidden, Gamow-Teller	0, 1, 2	yes	1	1
Second forbidden, Fermi	2	no	0	2
Second forbidden, Gamow-Teller	2, 3	no	1	2

β-decay rate, Fermi's Golden Rule

- The decay constant is given by Fermi's Golden Rule:

$$\lambda_\beta = \frac{2\pi}{\hbar}|M|^2 \rho(E_o); M = \int \psi_f V \psi_i dv$$

  - The transition matrix element *M* describes the strength of coupling between the initial and final states
  - The phase space factor ρ describes the volume of phase space available for outgoing leptons

- Measuring the β-decay rate (or the partial half-life) of a particular transition gives access to the wavefunctions of the initial (in parent) and final (in daughter) states!

Comparative half-lives, log*ft*

- The (partial) half-life of an allowed transition is

$$t_{1/2} = \frac{\kappa}{f_0(B_{\mathrm{F}} + B_{\mathrm{GT}})}$$

with $\kappa \equiv \frac{2\pi^3\hbar^7 \ln 2}{m_e^5 c^4 G_F^2} = 6147\,\mathrm{s}$ and $f_o = \int_1^{W_o} F(Z,W)W(W^2-1)^{1/2}(W_o - W)^2 dW$

  - f_0 is the phase space of leptons, corrected by the Coulomb interaction. It is a function of the atomic number Z of the daughter nucleus and the total kinetic energy W_0 of the leptons.

- $f_0 t$ is called the comparative half-life
  - It is the partial half-life corrected by the phase space
  - The $f_0 t$ value only depends on the strength of the transition matrix element
  - Because $f_0 t$ is usually enormously large, a more convenient number to use is

    logft = $\log_{10}(f_0 t)$

- Comparative half-life is an extremely important observable in β decay
  - $T_{1/2}$ (β-decay half-life) → I_β (decay probability of one particular transition) → $t_{1/2} = T_{1/2} / I_\beta$
  - Using Q_β from atomic mass evaluation [1] and Ex from experiment, f_0 can be either calculated with some approximations, e.g., in [2], or taken from tabulated values [3]
  - logft = $\log_{10} f_0 + \log_{10} t_{1/2}$

[1] M. Wang et al., CPC 45, 030003 (2021)
[2] Suhonen, From Nucleon to Nucleus (2007)
[3] N.B. Gove, M.J. Martin, Nucl. Data Tables 10, 205 (1971)

Comparative half-lives, log*ft*

- Although not decisive, the comparative half-life gives a quick estimate of the classification of the transition (allowed or forbidden), and thus the spin and parity of the final state if the spin and parity of the initial state are known, or vice versa.

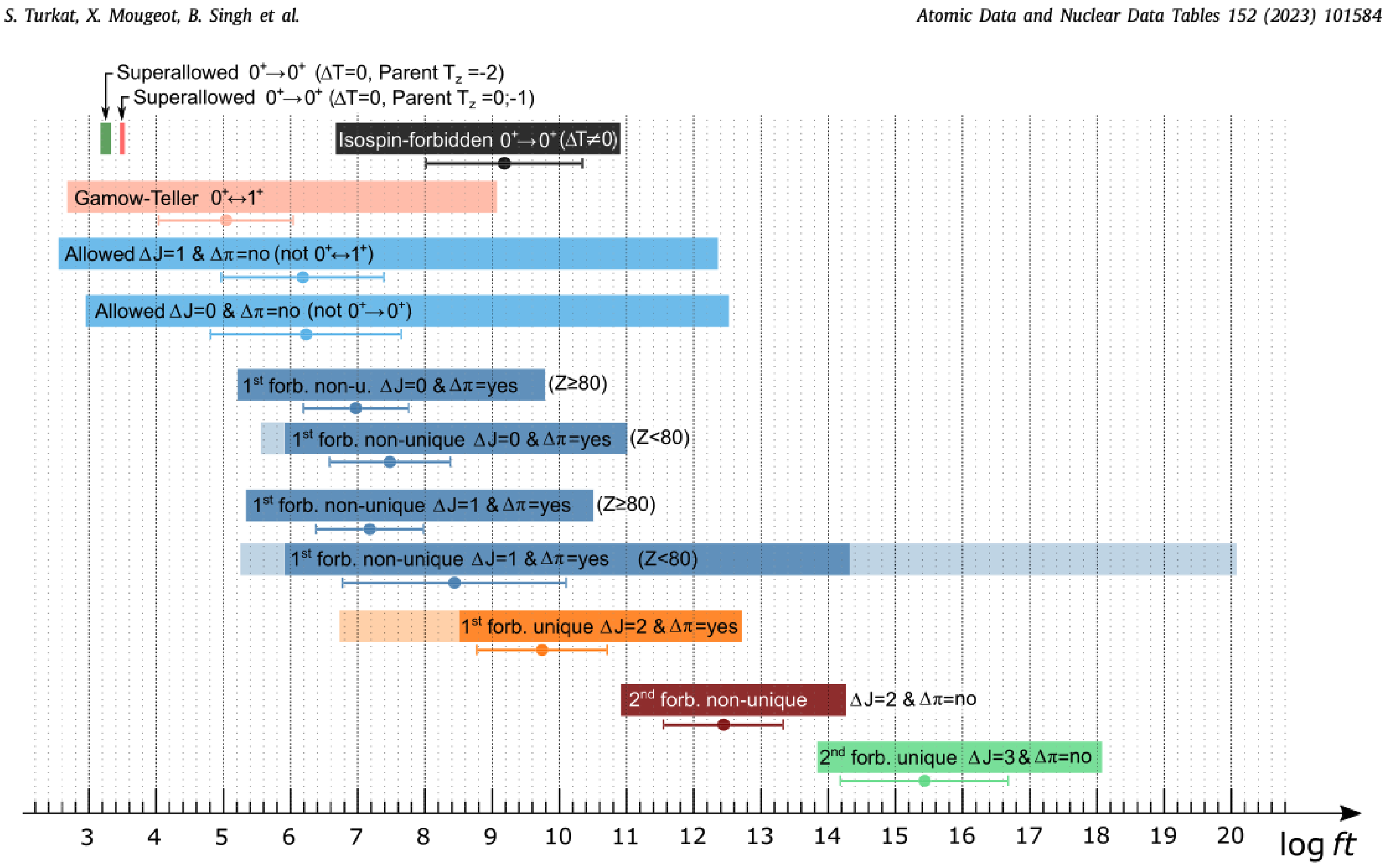

Example: β decay of ^{60}Co

Online log*ft* calculator: https://www.nndc.bnl.gov/logft/

Parent Information

Nucleus[a]	60Co	Decay Mode	B-		
E_{level} (keV) [b]	0	ΔE level			
$T_{1/2}$ [c]	1925.3	Units	d	$\Delta T_{1/2}$	
Q-Value (keV) [d]	2823	ΔQ-value			

Daughter Information

E_{level} (keV) [b]	2506	ΔE level			
Transition Intensity (%) [e]	99.88	ΔTI		Uniqueness	None

a: For Titanium-52 for instance, type "52TI"
b: Input should be a positive number, 0 for ground state
c: Input should be a positive number larger than 0
d: (Ground state to ground state)
Input should be a positive number larger than 0
e: Input should be a number larger than 0 and lower than or equal to 100

Output Uncertainty Format

○ Standard Style ◉ Nuclear Data Sheets (NDS) Style

Calculate

Log(FT)	7.51
Average decay energy	95.5

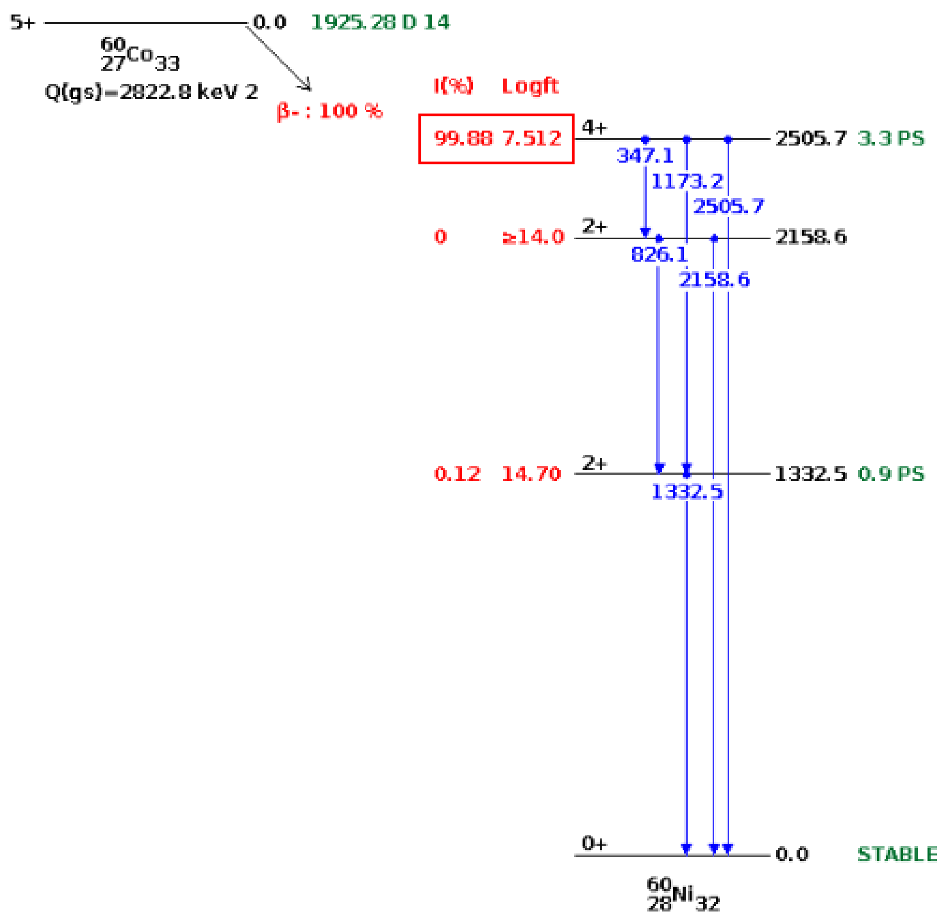

Decay station at radioactive ion-beam facilities

- The radioactive ion beams are stopped at the center of the decay stations
  - Active stopper, e.g., silicon strip detectors, inorganic scintillators, etc.
    - Measuring both implanted ions and their subsequent β decays
  - Passive stopper, e.g., tape station, surrounded by β trigger detectors (mainly for decay stations at ISOL facilities)
- Surrounding detectors for radiation following β decay
  - HPGe for high-resolution γ-ray energy
  - $LaBr_3$ for γ rays with finite lifetime (τ~100ps)
  - Plastic scintillators for neutrons

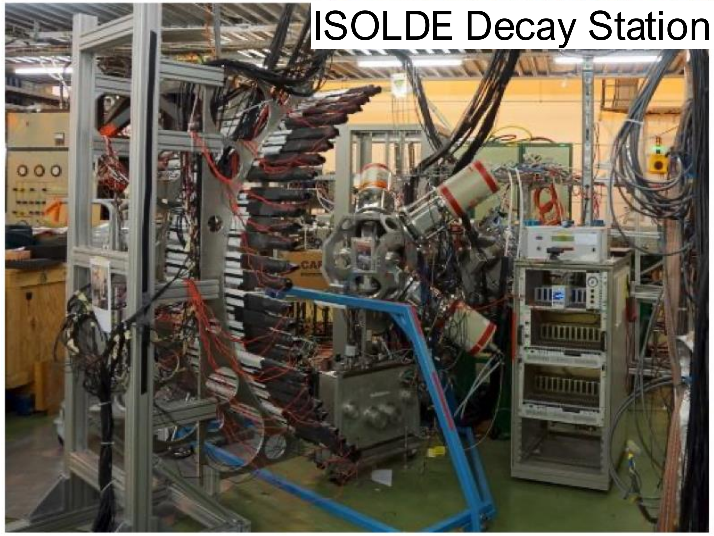
ISOLDE Decay Station

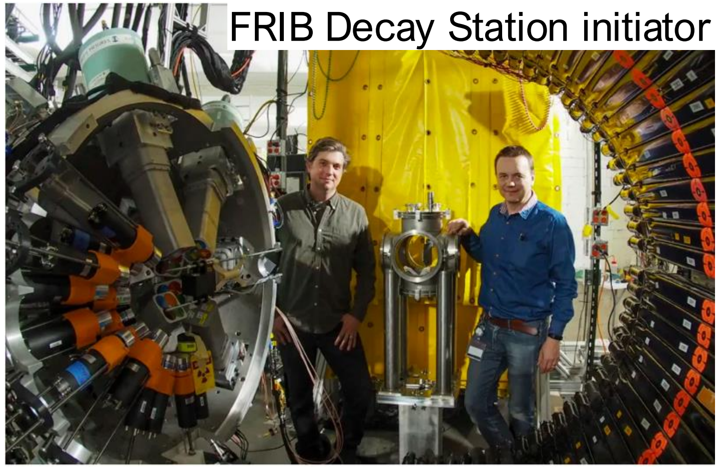
FRIB Decay Station initiator

A short detour: studying isomers using decay station

- Nuclear reaction produces exotic nuclei not only at the ground states but also at the excited states
- Most of the time, nuclei at excited states decay back to the ground state “immediately”
- Occasionally, the decay can be trapped in a metastable state (isomer), of which the half-life is long enough (>=10 ns) to survive the beam transmission to our decay station

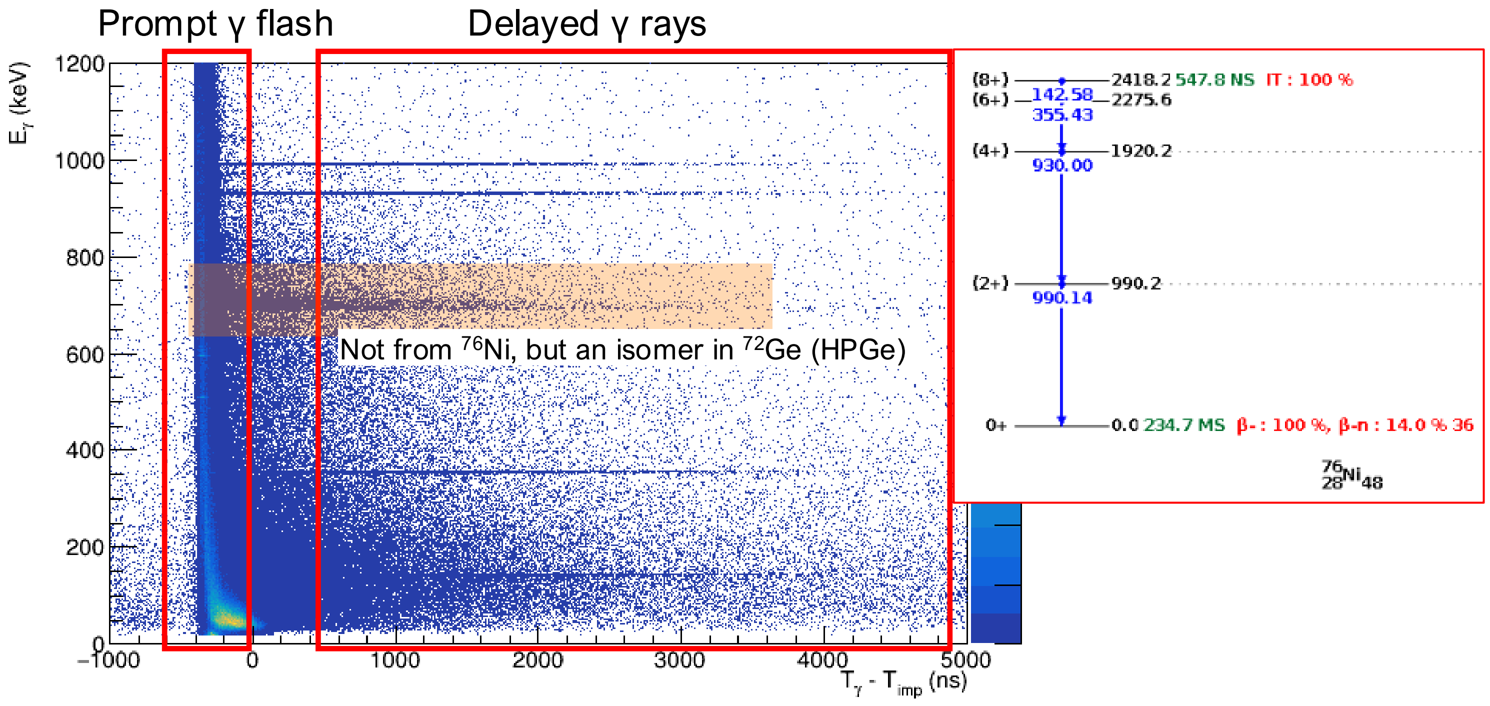

Example: the 8$^+$ isomer in ^{76}Ni

The 8$^+$ state in ^{76}Ni is a seniority isomer induced by the two neutron holes on the $g_{9/2}$ orbital below the N=50 shell gap

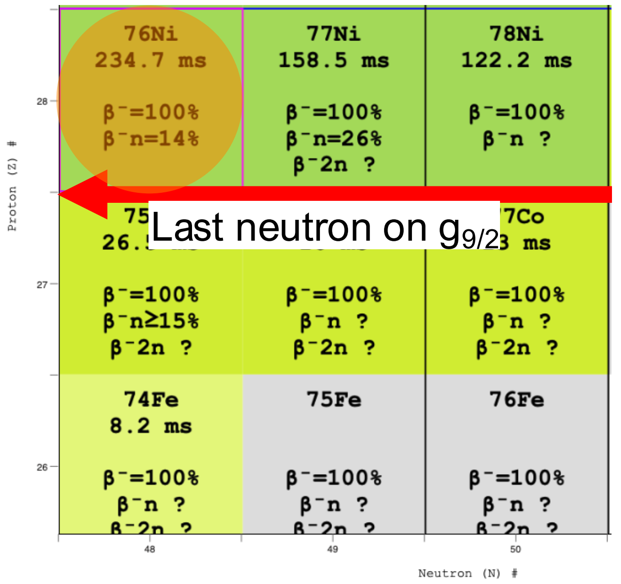

A short detour: studying isomers using decay station

- Nuclear reaction produces exotic nuclei not only at the ground states but also at the excited states
- Most of the time, nuclei at excited states decay back to the ground state "immediately"
- Occasionally, the decay can be trapped in a metastable state (isomer), of which the half-life is long enough (>=10 ns) to survive the beam transmission to our decay station
- The origin of the isomer is closely related to the nuclear structure

H. Watanabe et al., Phys. Rev. Lett. 111, 152501 (2013)

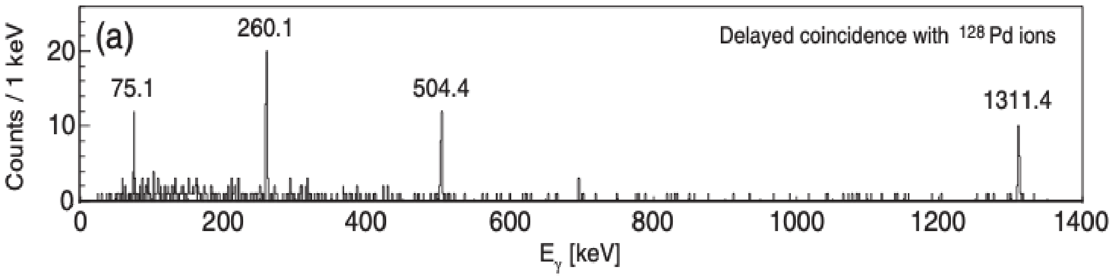

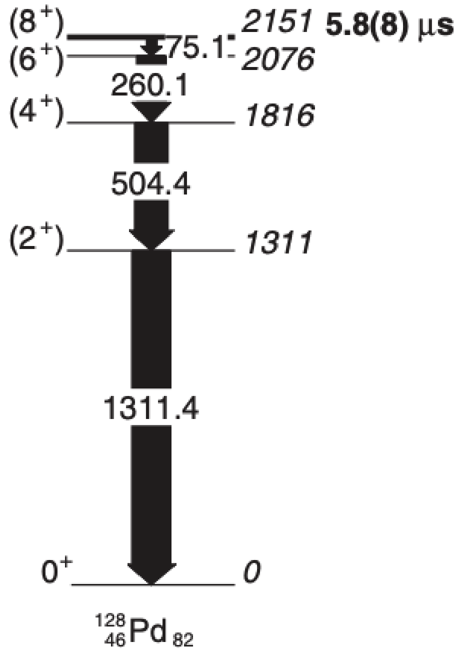

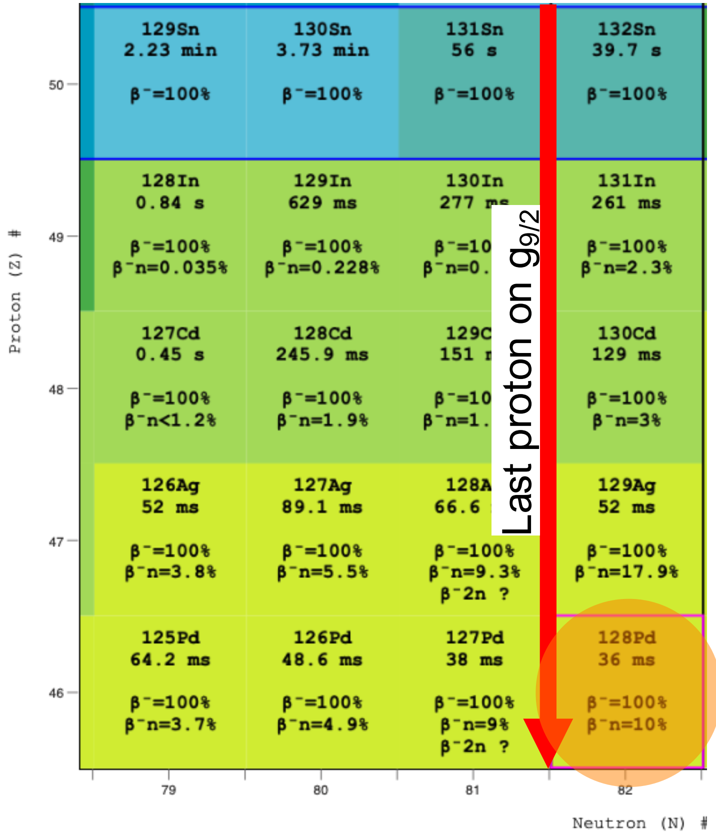

- The 8^+ seniority isomer in ^{128}Pd suggests robust neutron shell closure at N=82
- Very exotic and hard to access by other experimental approaches

A short detour: studying isomers using decay station

- Nuclear reaction produces exotic nuclei not only at the ground states but also at the excited states
- Most of the time, nuclei at excited states decay back to the ground state “immediately”
- Occasionally, the decay can be trapped in a metastable state (isomer), of which the half-life is long enough (>=10 ns) to survive the beam transmission to our decay station
- The origin of the isomer is closely related to the nuclear structure

A new FRIB experiment is coming in two weeks!

FRIB

Proposal 23064

Facility for Rare Isotope Beams

Proposal Form - PAC2

By submitting this proposal, the spokesperson certifies that all collaborators listed have read the proposal and have agreed to participate in the experiment.

Title

Seniority Isomers and Single-Particle Evolution in 218-222Pb Region: New Isotopes, Isomers, and Half Lives

Spokespeople

	Contact Spokesperson
Name	Mitch Allmond
Organization	Oak Ridge National Laboratory Physics Division Oak Ridge National Laboratory P.O. Box 2008 Building 6000, Mail Stop 6368 Oak Ridge

A short detour: studying isomers using decay station

- Nuclear reaction produces exotic nuclei not only at the ground states but also at the excited states
- Most of the time, nuclei at excited states decay back to the ground state “immediately”
- Occasionally, the decay can be trapped in a metastable state (isomer), of which the half-life is long enough (>=10 ns) to survive the beam transmission to our decay station
- The origin of the isomer is closely related to the nuclear structure

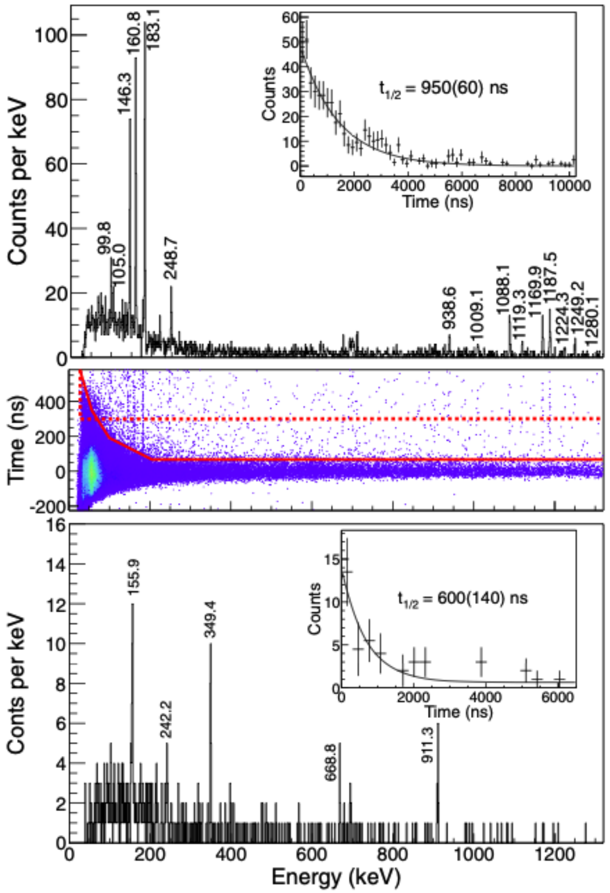

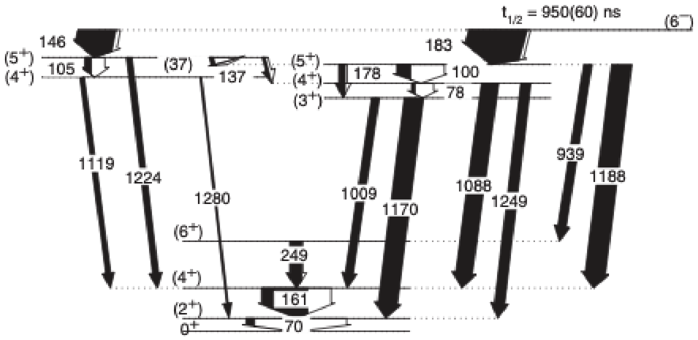

FIG. 2. Level scheme of ^{166}Gd obtained in this work.

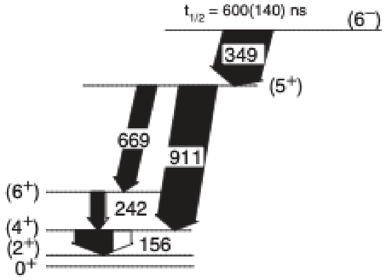

FIG. 3. Level scheme of ^{164}Sm obtained in this work.

- The isomers in ^{166}Gd and ^{164}Sm allowed us to access the low-lying states in these two exotic nuclei, extending the systematics to N=102
- The data resent evidence for the predicted deformed shell closure at N=100

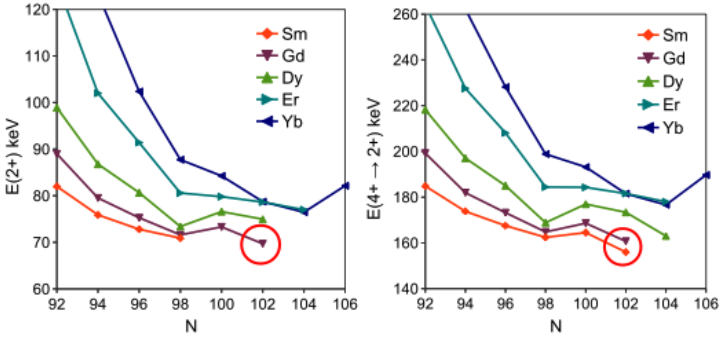

FIG. 4 (color online). Systematics of $E(2^+)$ and $E(4^+ \to 2^+)$ for Sm, Gd, Dy, Er, and Yb isotopes. All data points from [26] and this work.

Z. Patel et al., Phys. Rev. Lett. 113, 262502 (2014)

β-decay half-lives

- An important ground-state property of exotic nuclei
- Usually, the first quantity experimentally accessible after a new isotope is identified
- Provide benchmarks to nuclear models
- In astrophysics, half-lives are key ingredients to nucleosynthesis processes

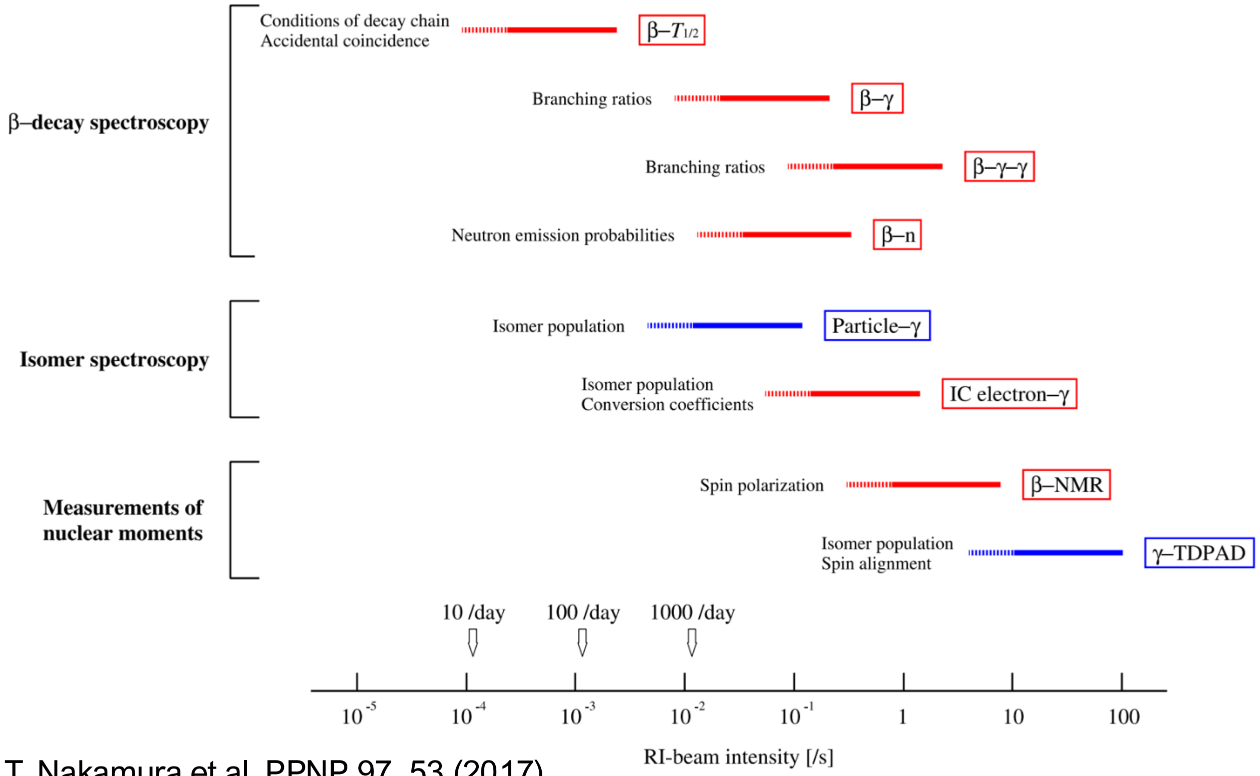

T. Nakamura et al. PPNP 97, 53 (2017)

Measuring β-decay half-lives using RI beams

- RI beams produced by in-flight fragmentation provide an ideal opportunity to measure half-lives efficiently
- Identify ions in the cocktail beams event-by-event, and find their implantation position in the detector
- Look for β decay around the implantation position within a reasonable time range (e.g., 5 s after the implantation)
- Count the number of β decays as a function of ion-β time difference
    - A simple exponential function won't fit such decay curves very well

Example: half-life measurement around ^{78}Ni at RIKEN

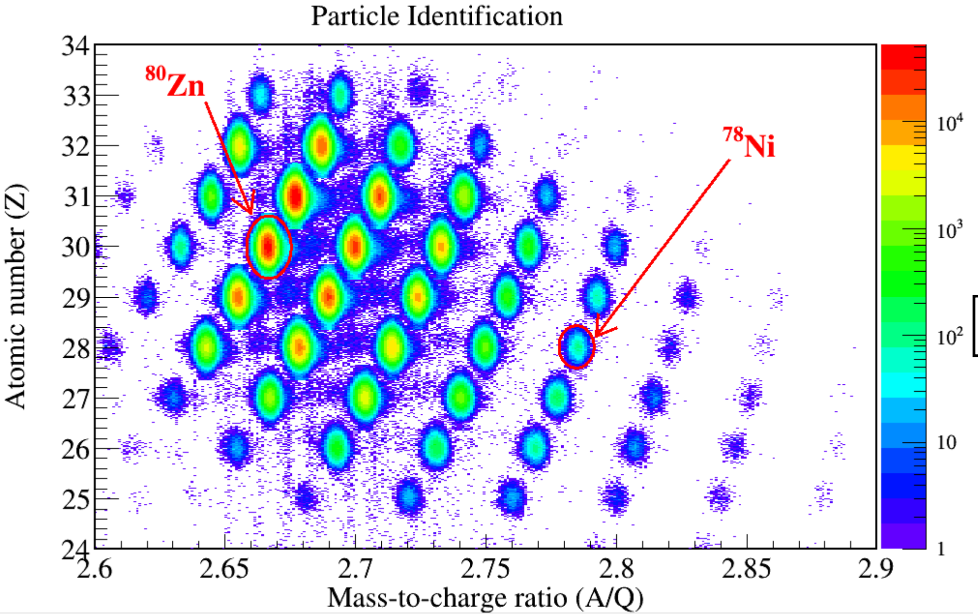

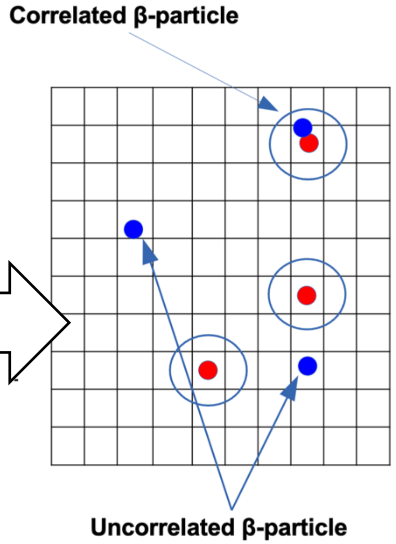

position correlation

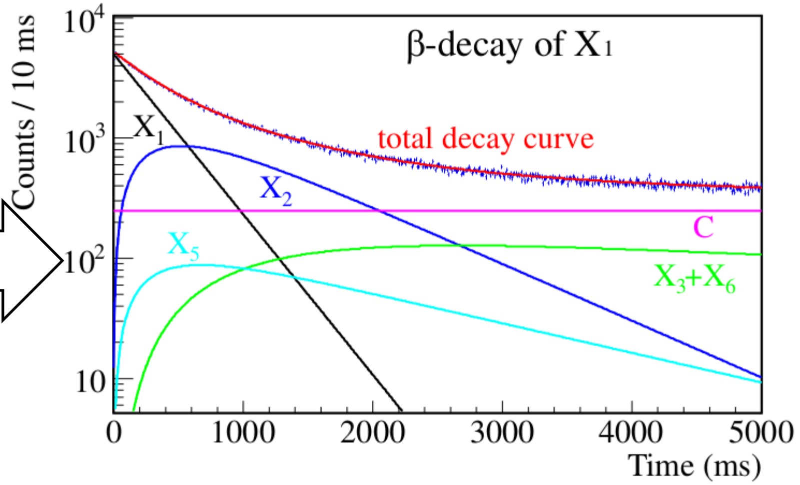

Measuring β-decay half-lives using RI beams

- RI beams produced by in-flight fragmentation provide an ideal opportunity to measure half-lives efficiently
- Identify ions in the cocktail beams event-by-event, and find their implantation position in the detector
- Look for β decay around the implantation position within a reasonable time range (e.g., 5 s after the implantation)
- Count the number of β decays as a function of ion-β time difference
    - A simple exponential function won’t fit such decay curves very well
    - The experimental decay curve includes activities from not only the parent nucleus X1 but also its descendants (X1 is extremely far from the stability line)

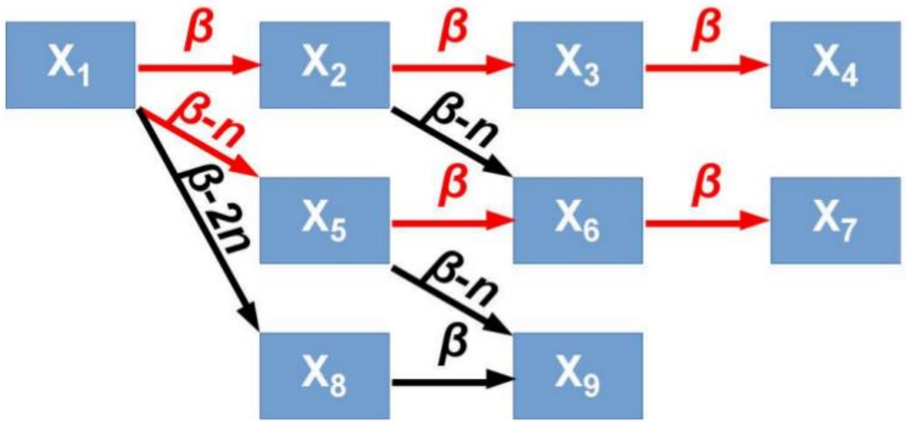

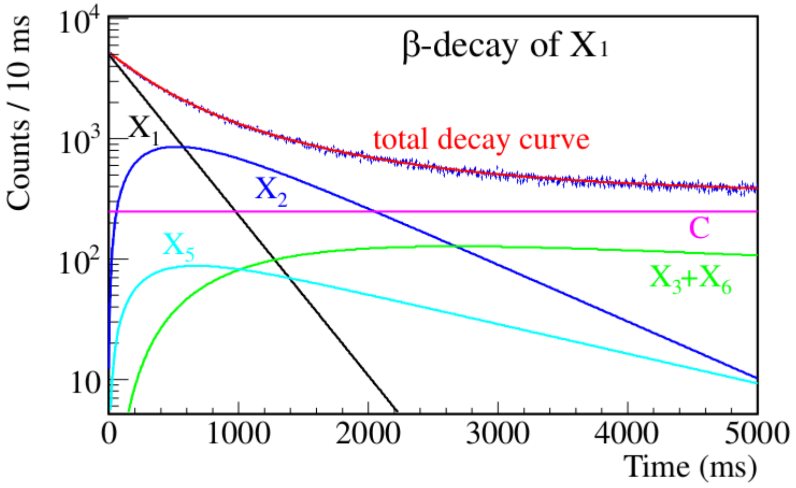

Deducing half-life using β-γ coincidence

- Many γ rays could be emitted “immediately” following β decays
- The activity of the parent nucleus X1 can be isolated from the rest by selecting β decays in coincidence with the unique γ emissions from X2
  - The single exponential decay function can describe the experimental histogram very well!
- However, such practice requires statistics (γ-detection efficiency is generally not very high)

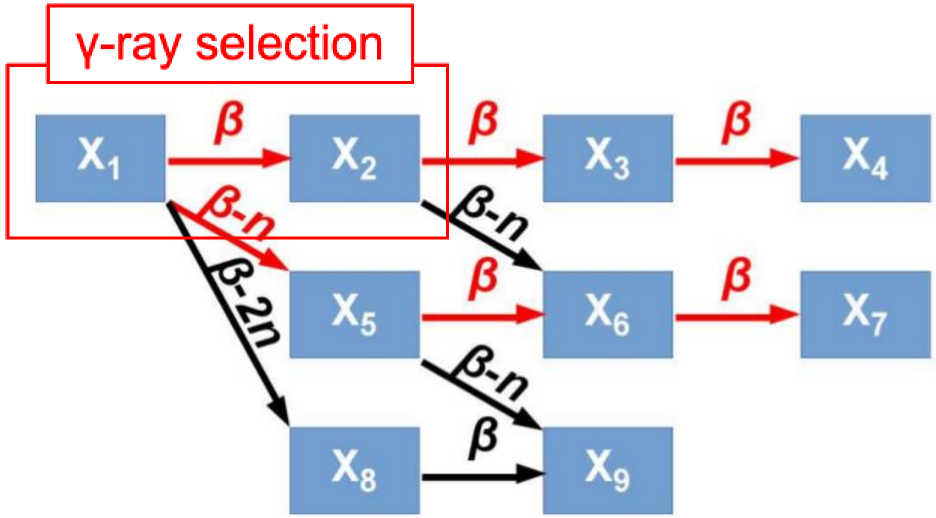

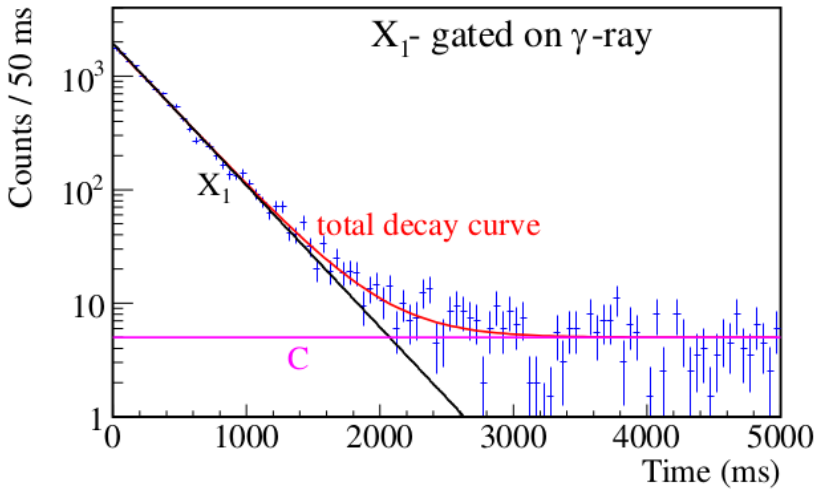

Deducing half-life using the Bateman equation

- For the most exotic species, γ detection is generally not possible
- To model the decay curve, the activities from descendants (daughter, granddaughter, etc.) need to be included
- The Bateman equation describes the activities of the *i*-th isotope in the decay chain
- Practically, the decay chain should be truncated at the *i*-th isotope if the half-life of the (*i*+1)-th isotope is too long to contribute to the total activity

$$\frac{dN_1(t)}{dt} = -\lambda_1 N_1(t)$$
$$\frac{dN_i(t)}{dt} = -\lambda_i N_i(t) + \lambda_{i-1} N_{i-1}(t)$$

$$\Rightarrow \quad N_n(t) = N_1(0) \times \left(\prod_{i=1}^{n-1} \lambda_i\right) \times \sum_{i=1}^{n} \frac{e^{-\lambda_i t}}{\prod_{j=1, j\neq i}^{n} (\lambda_j - \lambda_i)}$$

- Fitting the model that includes all activities to the experimental decay curve allows us to determine the half-life of the parent nucleus

Systematics of half-lives

- Empirical rule: for very exotic nuclei, the half-life $T_{1/2}$ is inversely proportional to the fifth power of Q_β
- Q_β is approximately a linear function of N in the mid-shell (if we ignore the odd-even staggering caused by the pairing)
- $\log T_{1/2}$ is a linear function of N

Around ^{78}Ni:
ZX et al., PRL 113, 032505 (2014)

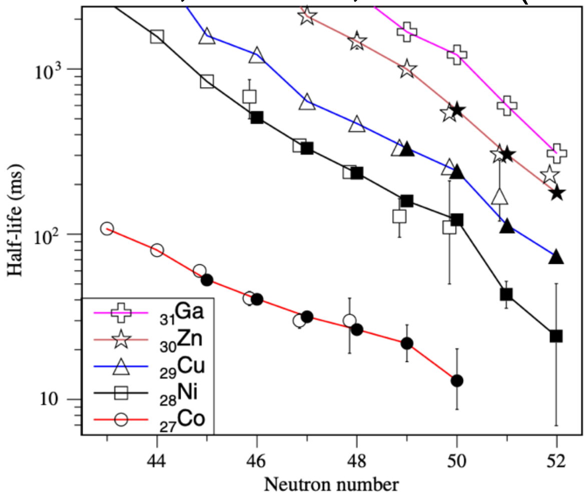

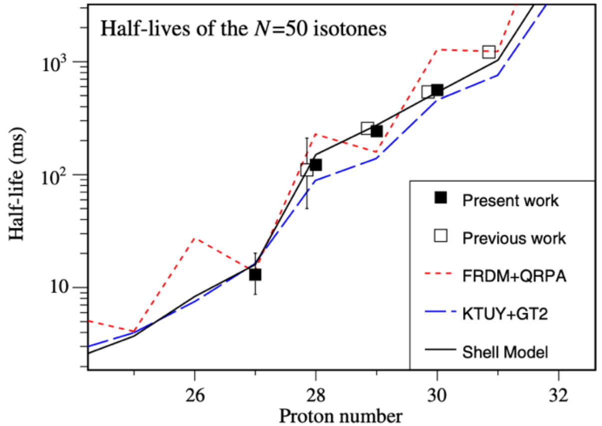

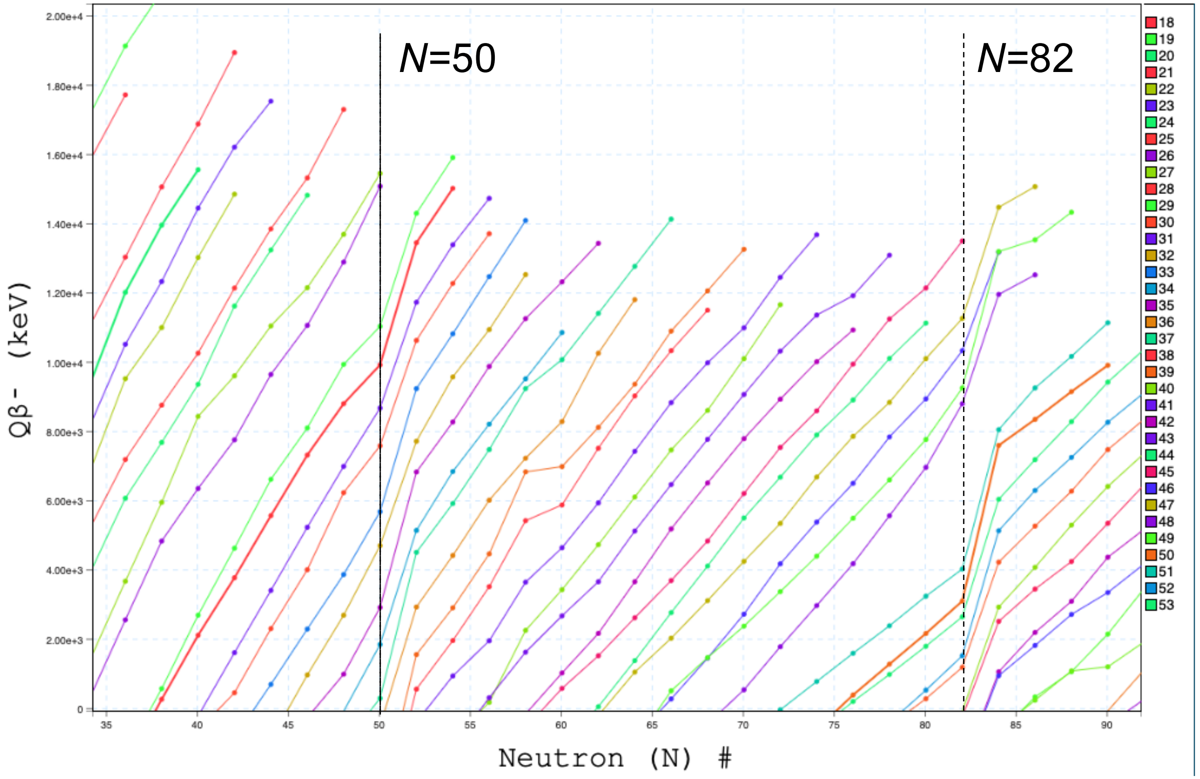

Systematics of half-lives

- Empirical rule: for very exotic nuclei, the half-life $T_{1/2}$ is inversely proportional to the fifth power of Q_β
- Q_β is approximately a linear function of N in the mid-shell (if we ignore the odd-even staggering caused by the pairing)
- $\log T_{1/2}$ is a linear function of N

Around ^{78}Ni:
ZX et al., PRL 113, 032505 (2014)

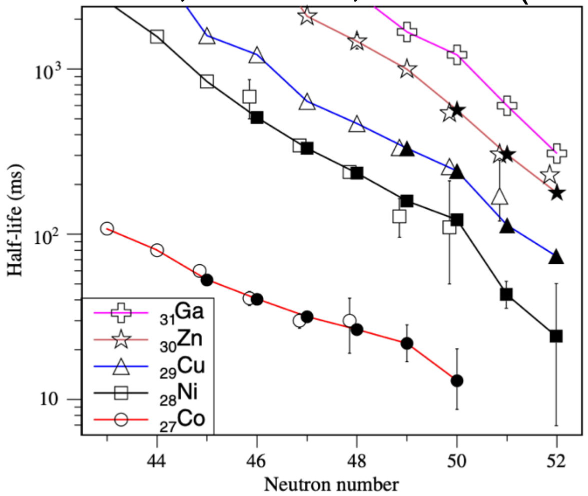

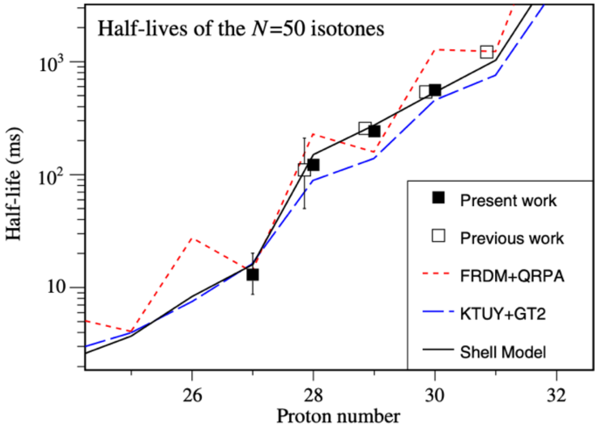

Around ^{42}Si (the first-ever FRIB experiment!):
H.L.Crawford et al., PRL 129, 212501 (2022)

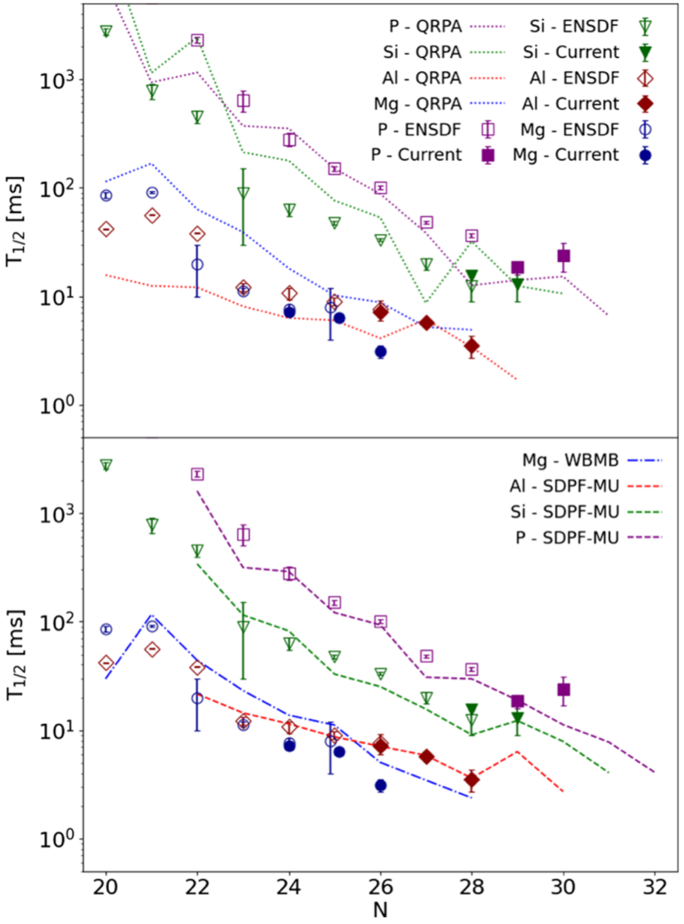

THE UNIVERSITY OF TENNESSEE KNOXVILLE

Systematics of half-lives

- Empirical rule: for very exotic nuclei, the half-life $T_{1/2}$ is inversely proportional to the fifth power of Q_β
- Q_β is approximately a linear function of N in the mid-shell (if we ignore the odd-even staggering caused by the pairing)
- $\log T_{1/2}$ is a linear function of N

Around and beyond ^{54}Ca:
W.-J. Ong et al., PRL 136, 092502 (2026)

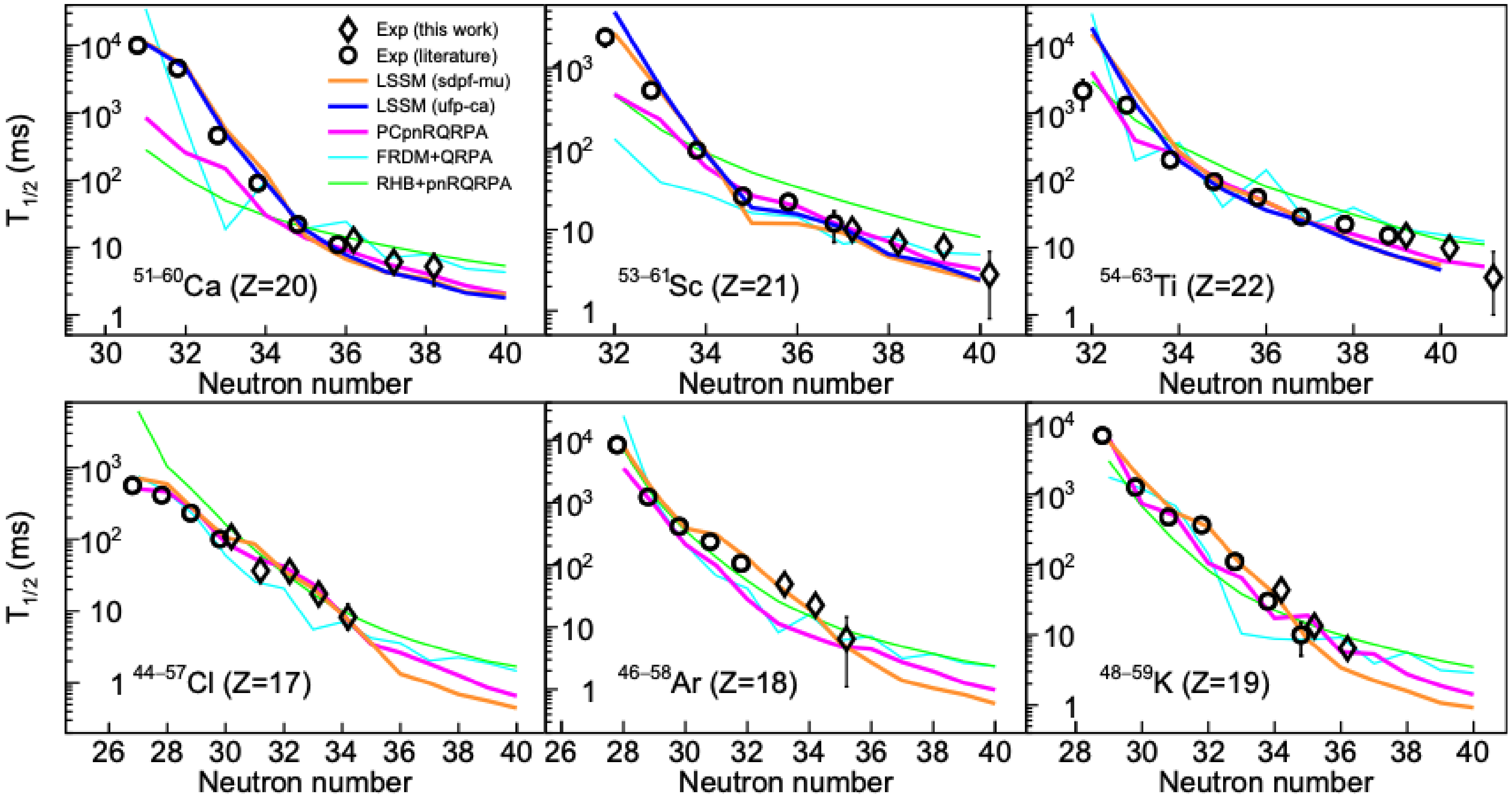

Systematics of half-lives

- The systematics of $T_{1/2}$ give the first benchmark to the theories in unexplored territories

- Since half-life is an aggregated quantity, the comparison with theories is not always conclusive:
  - Agreement → Is it accidental?
  - Discrepancy → How to reduce it?

- We need a probe that can provide more detailed and comprehensive tests of theories
  → β-strength function: β-decay strength as a function of excitation energy in the daughter nucleus

β strength function, $S_\beta(E)$

- The β decay strength is related to the *ft* value
  - $S_\beta = 1/ft$
- The $S_\beta(E)$ distribution determines all the essential β-decay properties
  - Half-lives
  - Probabilities of β-delayed particle emissions (proton, neutron, etc.)
- Experimentally, we measure the β-feeding probabilities as a function of excitation energy: $I_\beta(E)$
  - $I_\beta(E) \rightarrow S_\beta(E)$
- Theoretically, we calculated B(F) and B(GT) for allowed transitions
  - $S_\beta = [B(F)+B(GT)] / \kappa$, with $\kappa=6147$
- For first-forbidden transitions, there are multiple independent matrix elements
  - Calculate the decay constant λ summed over all the matrix elements
  - The partial half-life $t = \log(2)/\lambda$
  - Convert t to S_β using the f value of the allowed transitions
- A correct theoretical $S_\beta(E)$ leads to a consistent half-life prediction, but not vice versa! → more insights from comparing experimental and theoretical $S_\beta(E)$

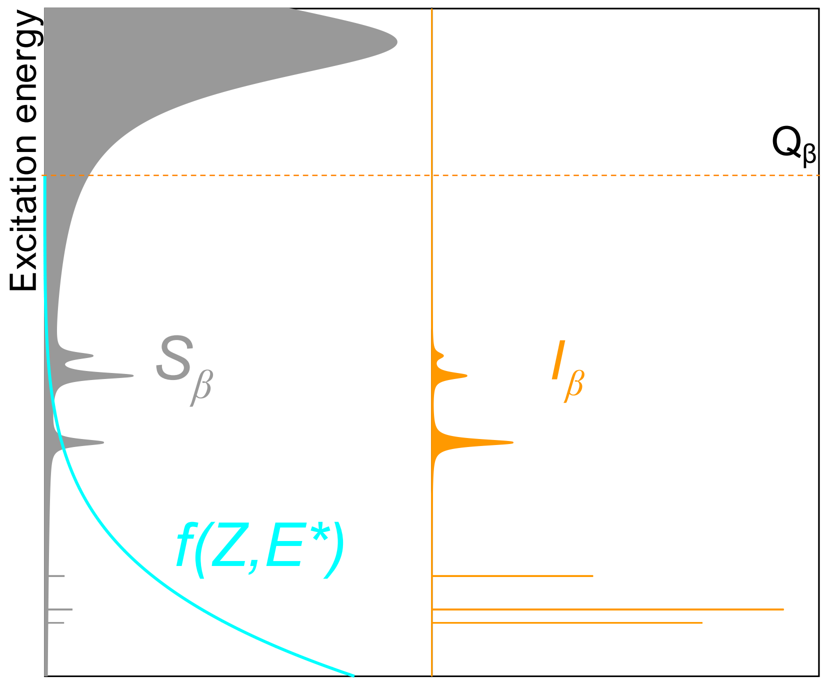

Extracting I_β below particle separation energy

- Electromagnetic transitions with γ emissions are the most common decay mode for the excited states below the particle separation energy
- Traditionally, we use HPGe detectors (superior energy resolution) to construct the level scheme populated in β decay
- If we measure the γ-ray intensities per 100 β decays, I_γ, we can extract β-feeding from the γ balance: $I_\beta = I_\gamma(\text{out}) - I_\gamma(\text{in})$
  - $I_{\beta 1} = I_{\gamma 1} - I_{\gamma 2}$
  - $I_{\beta 2} = I_{\gamma 2} + I_{\gamma 3}$
- After measuring I_β to all the excited states, I_β to the ground state can be deduced as
  - $I_\beta(\text{g.s.}) = 100\% - \Sigma I_\beta(\text{ex})$

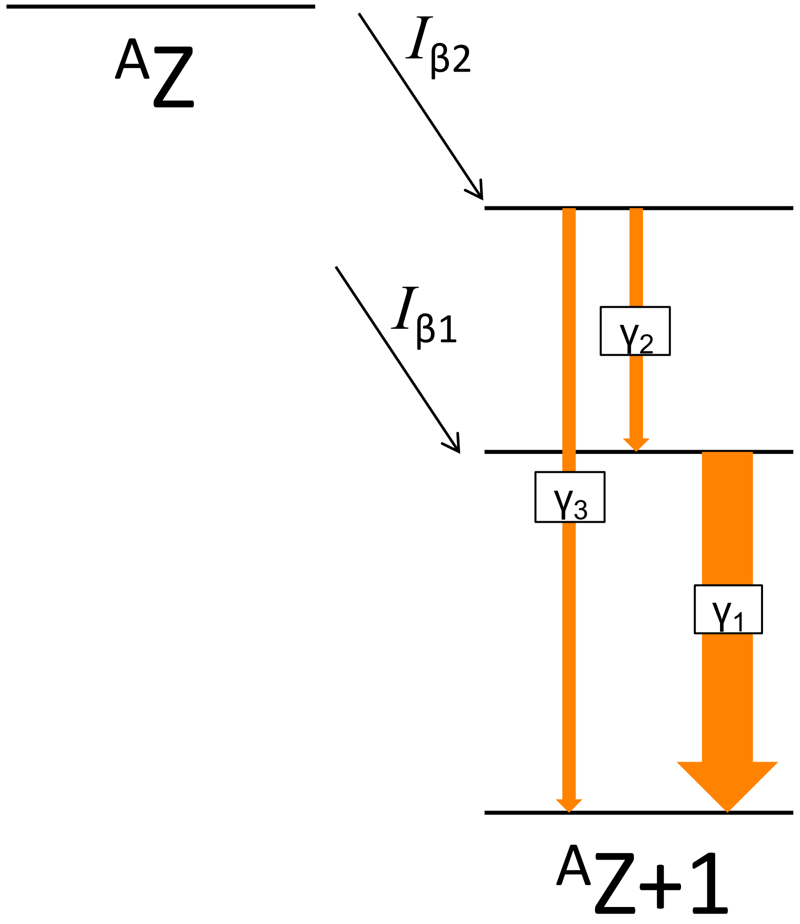

Extracting I_β below particle separation energy

- Electromagnetic transitions with γ emissions are the most common decay mode for the excited states below the particle separation energy
- Traditionally, we use HPGe detectors (superior energy resolution) to construct the level scheme populated in β decay
- If we measure the γ-ray intensities per 100 β decays, I_γ, we can extract β-feeding from the γ balance: $I_\beta = I_\gamma(\text{out}) - I_\gamma(\text{in})$
  - $I_{\beta 1} = I_{\gamma 1} - I_{\gamma 2}$
  - $I_{\beta 2} = I_{\gamma 2} + I_{\gamma 3}$
- After measuring I_β to all the excited states, I_β to the ground state can be deduced as
  - $I_\beta(\text{g.s.}) = 100\% - \Sigma I_\beta(\text{ex})$

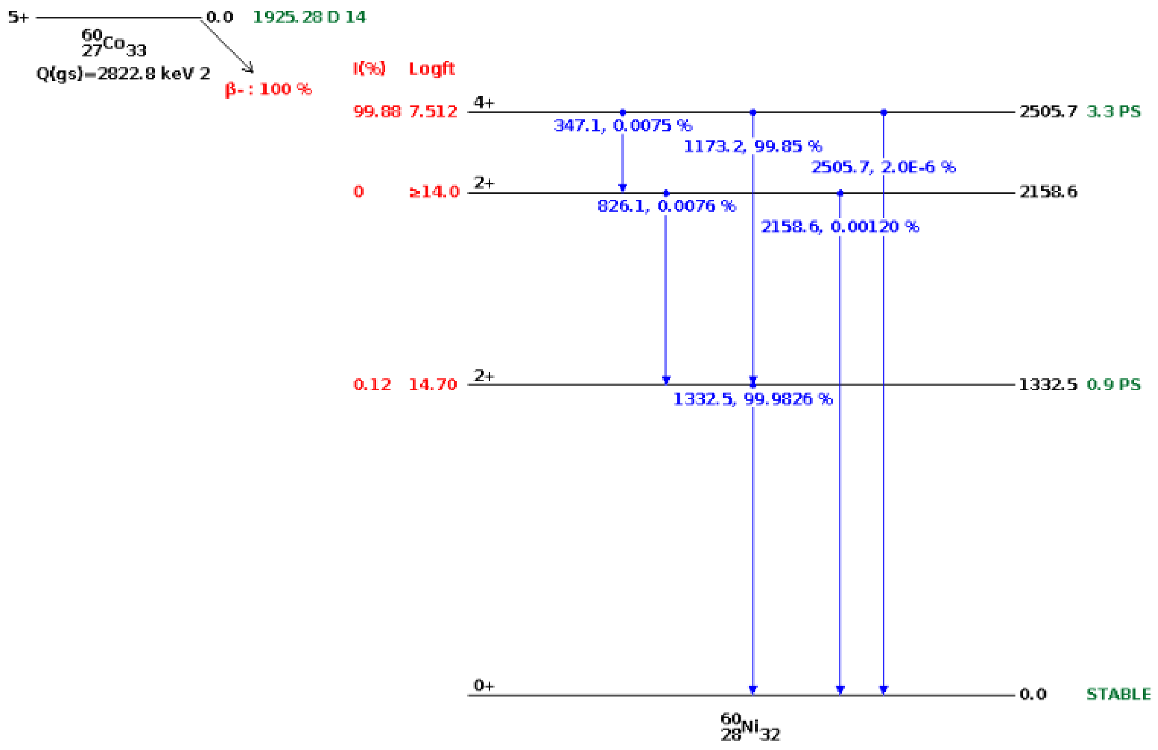

The pandemonium effect

- HPGe detectors have limited γ efficiency, in particular at higher energy
- If we fail to detect weak, high-energy γ rays emitted from highly excited states, the extracted β feeding probabilities from the γ-balance will be biased towards lower states
- The extracted β feeding does not correspond to the real β feeding anymore
- Solution: increasing the γ detection efficiency

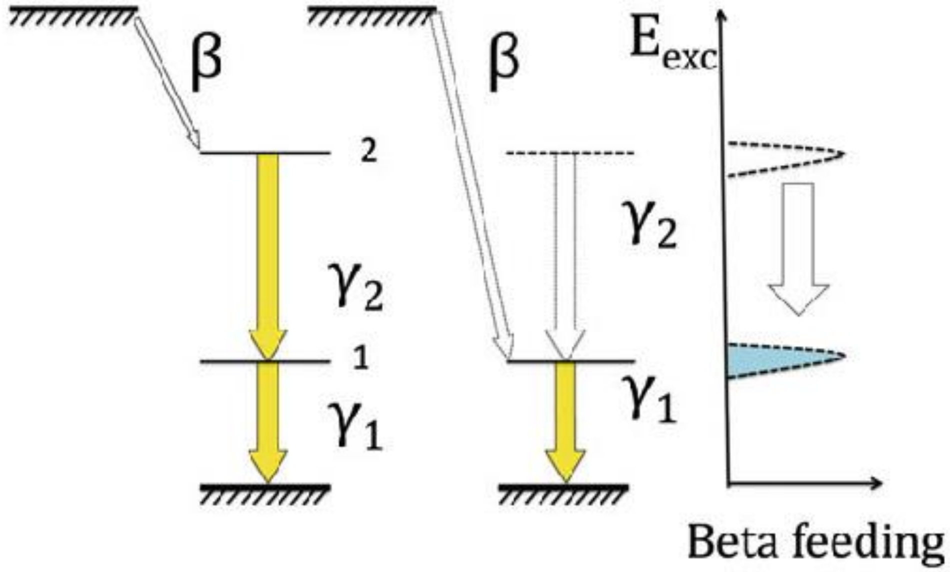

Algora, A., Rubio, B., Tain, J.L., Gelletly, W. (2024).

Total absorption spectroscopy (TAS)

- TAS is built of massive, large-size γ-ray calorimeters, e.g., NaI(Tl)
- Owing to its excellent detection efficiency, TAS is capable of measuring all the γ rays within a single cascade
- The sum of the γ-ray energies corresponds to the excitation energy of the initial state of the cascade
- With compromised energy resolution, TAS is an ideal approach to measure I_β with high precision
- Many TAS detectors are available around the world
  - Modular Total Absorption Spectrometer (MTAS)
  - The (upgraded) Summing NaI absorption spectrometer (SuN/SuN++)
  - Lucrecia
  - Decay Total Absorption Spectrometer (DTAS)

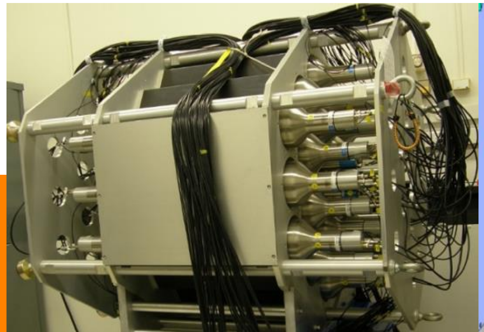

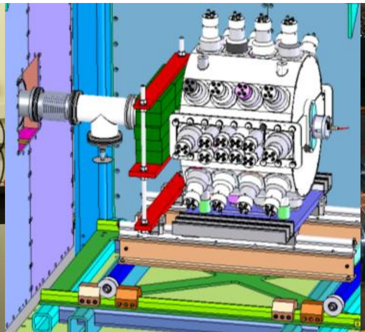

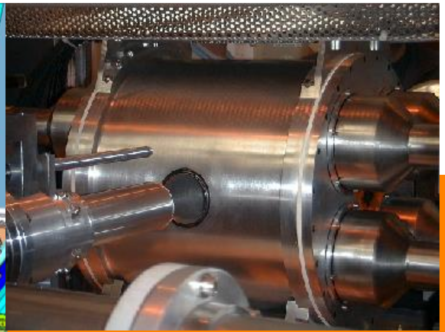

A. Algora et al., Nuclear Physics News, Vol. 28, No. 2, 2018

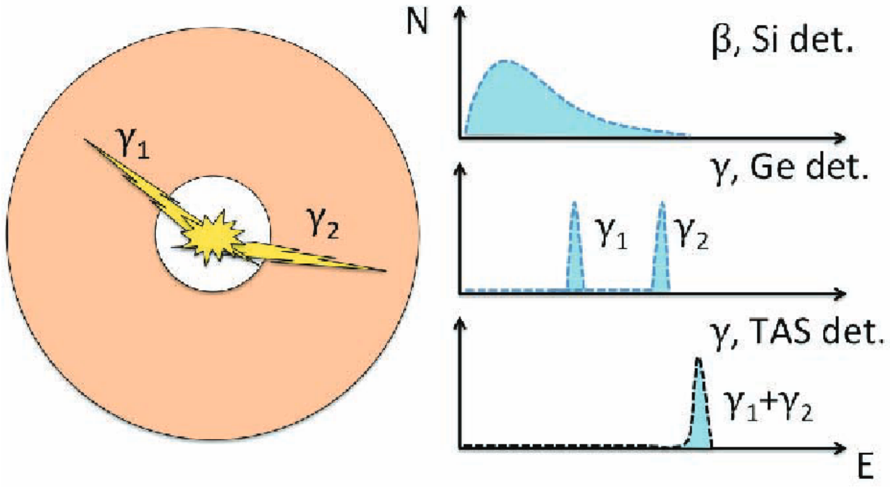

M. Karny et al., NIMA 836, 83 (2016)

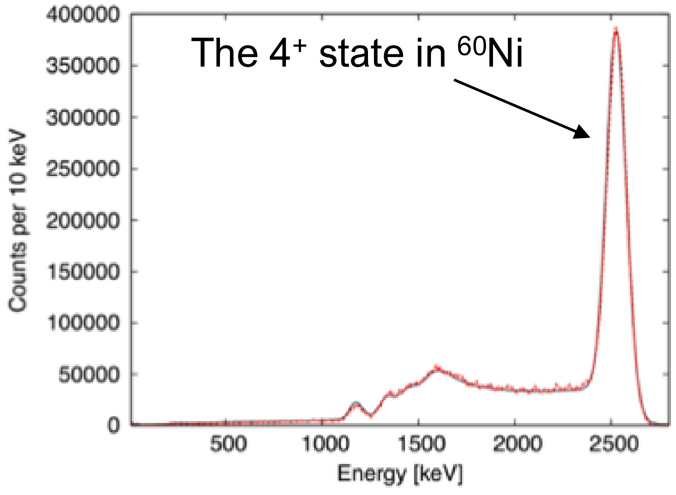

Fig. 5. ^{60}Co experimental spectrum as seen by MTAS (black) compared to the GEANT4 simulation (grey/red(on-line)). (For interpretation of the references to color in this figure caption, the reader is referred to the web version of this paper.)

Nuclear structure from S_β measured by TAS

^{74}Kr, shape admixture

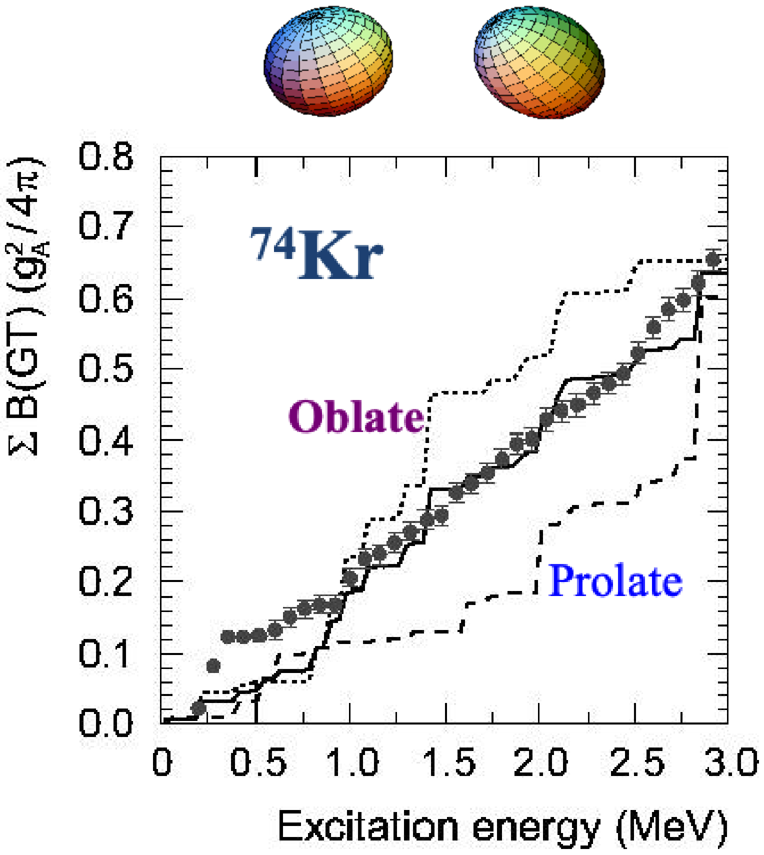

E. Poirier et al., PRC 69, 034307 (2004)

^{76}Sr, clearly prolate

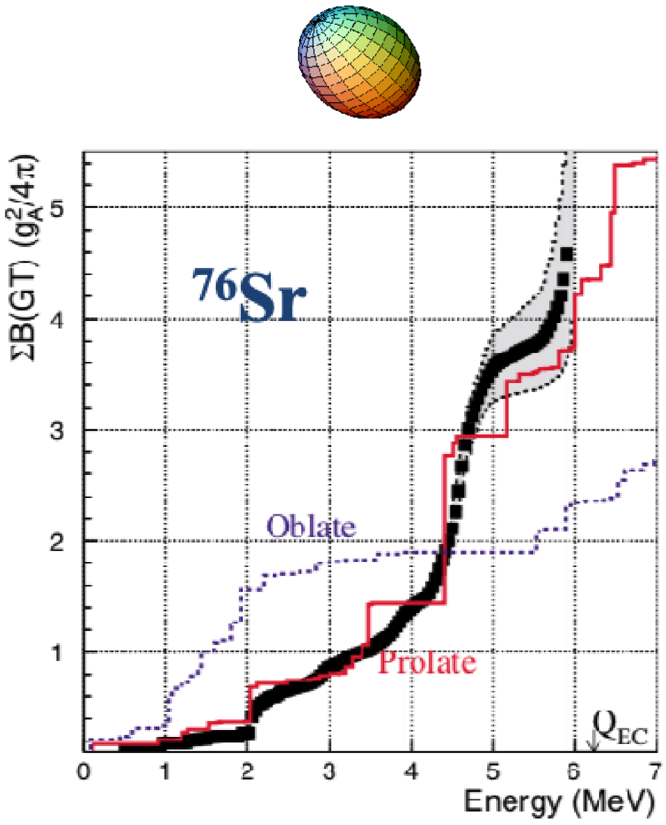

E. Nácher et al., PRL 92, 232501 (2004)

Extracting I_β above particle separation energy

- Above the particle separation energy, particle emissions become energetically possible and can be dominant over γ emission, e.g., neutron emission above S_n
- Measuring the energy of the emitted particles following β decay is necessary to reconstruct I_β above the particle separation energy
- Auxiliary detectors are needed in addition to the β and γ detectors, for example:
  - Si detectors for charged particles such as protons and alpha particles
  - Plastic scintillators for neutrons
- Complete decay spectroscopy → the full I_β distribution from ground state all the way to Q_β

FRIB Decay Station initiator

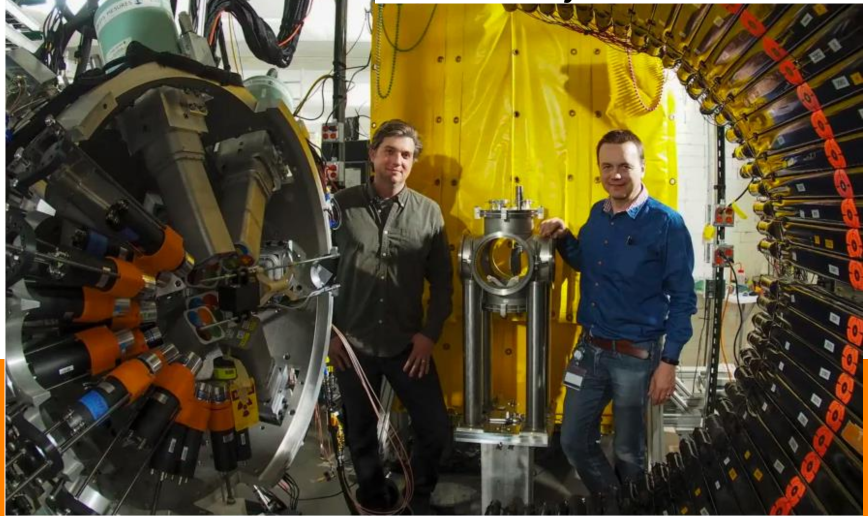

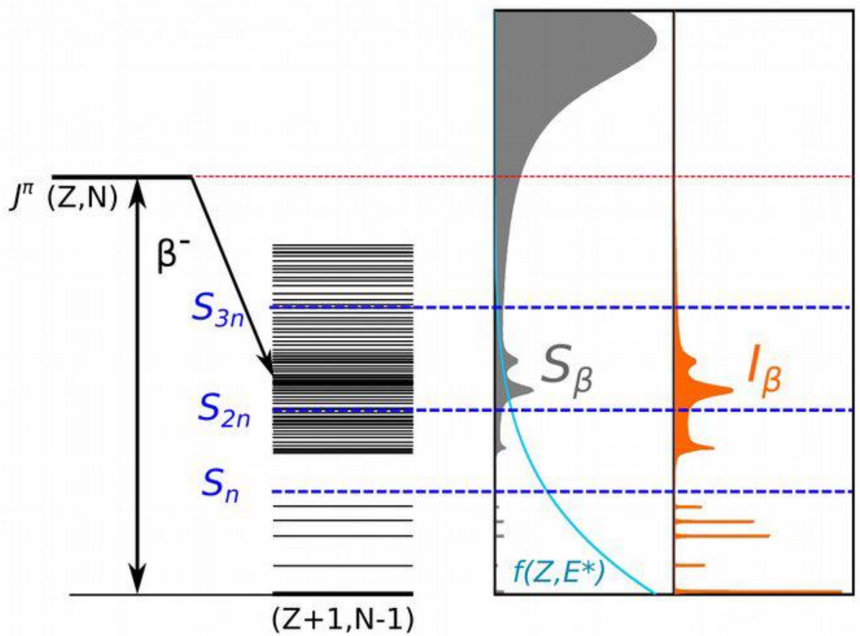

Example: β-delayed neutron emission

Measuring βn for neutron-rich nuclei

- β-delayed neutron (βn) emission is energetically possible if $Q_\beta > S_n$
- More neutron-rich nuclei: Q_β↑ and S_n↓ → Most decay strength is located above S_n, e.g., many nuclei to the northeast of ^{78}Ni have a significant P_n value
- To reconstruct the I_β of those neutron-rich nuclei, we need to measure both neutrons and γ rays following their β decay
- Many neutron time-of-flight arrays have been constructed for decay studies
  - TONneau pour NEutRons REtardes (TONNERRE)
  - Versatile Array for Neutron Detection at Low Energy (VANDLE)
  - Neutron dEtector with Xn Tracking (NEXT)

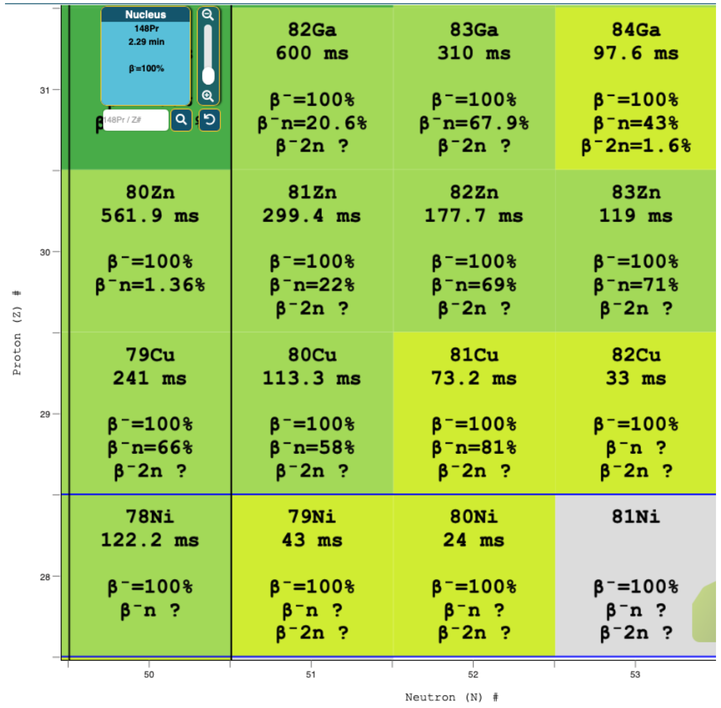

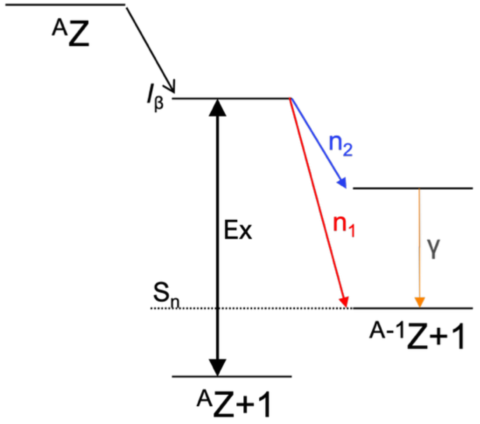

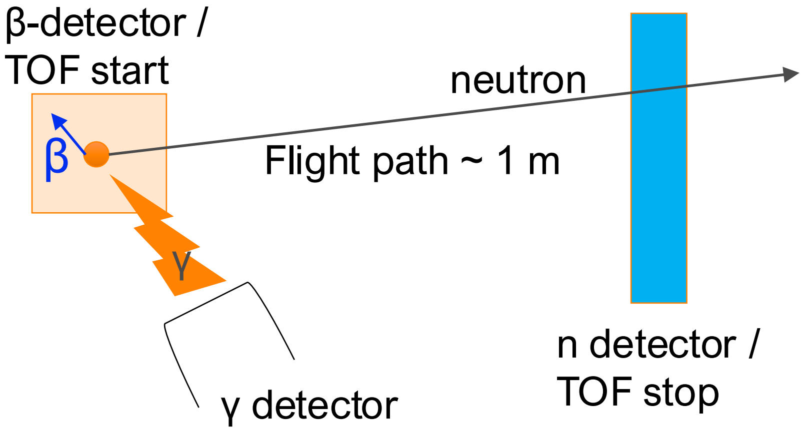

A little bit more about neutron TOF measurement

- For nTOF measurement, the energy resolution is given by

$$\frac{\Delta E}{E} = \sqrt{\left(\frac{2\Delta T}{T}\right)^2 + \left(\frac{2\Delta L}{L}\right)^2}$$

- The uncertainty of the flight path, ΔL, is usually determined by the thickness of the neutron detectors
  - Thin detector (small ΔL): good energy resolution, poor efficiency
  - Thick detector (large ΔL): poor energy resolution, good efficiency

- Can we have both good energy resolution and good efficiency?
  - Solution: NEXT, a thick neutron detector with optical isolation/segmentation along the neutron flight path
  - ΔL is now the thickness of each segment, instead of the whole detector

* J. Heideman et al., NIMA 946, 162528 (2019); S. Neupane et al., PRC 106, 044320 (2022)

Nuclear structure from S_β above S_n

- Neutron-rich gallium isotopes $^{83,84}Ga$ were produced at HRIBF at ORNL, and their β-delayed neutron emissions were investigated by the Versatile Array of Neutron Detection at Low Energy (VANDLE)
- The neutron time-of-flight spectra were dominated by fast neutrons, indicating strong population to the states far above the neutron separation energy
- The main Gamow-Teller transition was interpreted as transforming a neutron in the 50-82 shell ($f_{5/2}, p_{1/2,3/2}, g_{9/2}$) to a proton in the 50-82 shell ($f_{5/2}, p_{1/2,3/2}, g_{9/2}$)
- GT transitions populate highly excited states due to the neutron shell gap at N=50 (i.e., neutron 3p-1h configuration)
- The measured strength distribution (mostly above S_n) agree very well with the theory predictions (shell-model calculations)

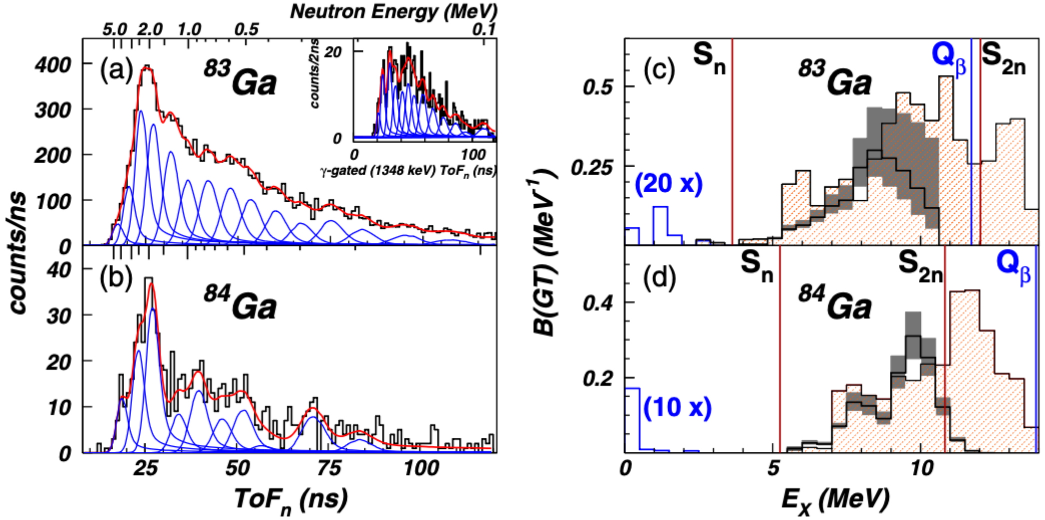

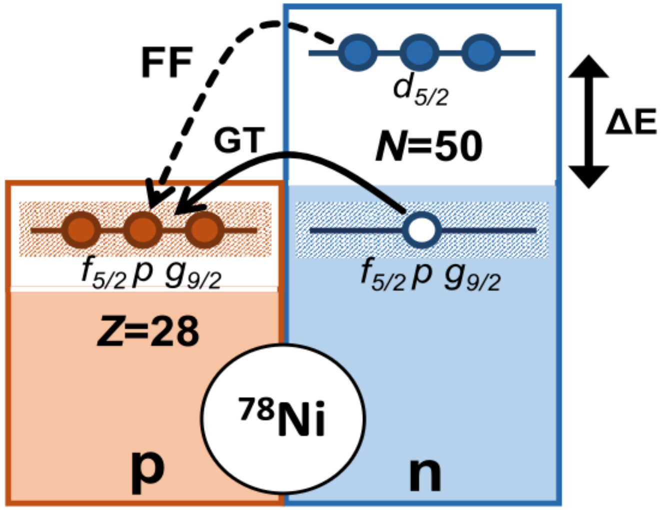

M. Madurga et al., PRL 117, 092502 (2016)

Nuclear structure from S_β above S_n

- The complete β-decay strength of ^{45}Cl was measured at FRIB Decay Station initiator (DEGAi + MTAS + VANDLE)

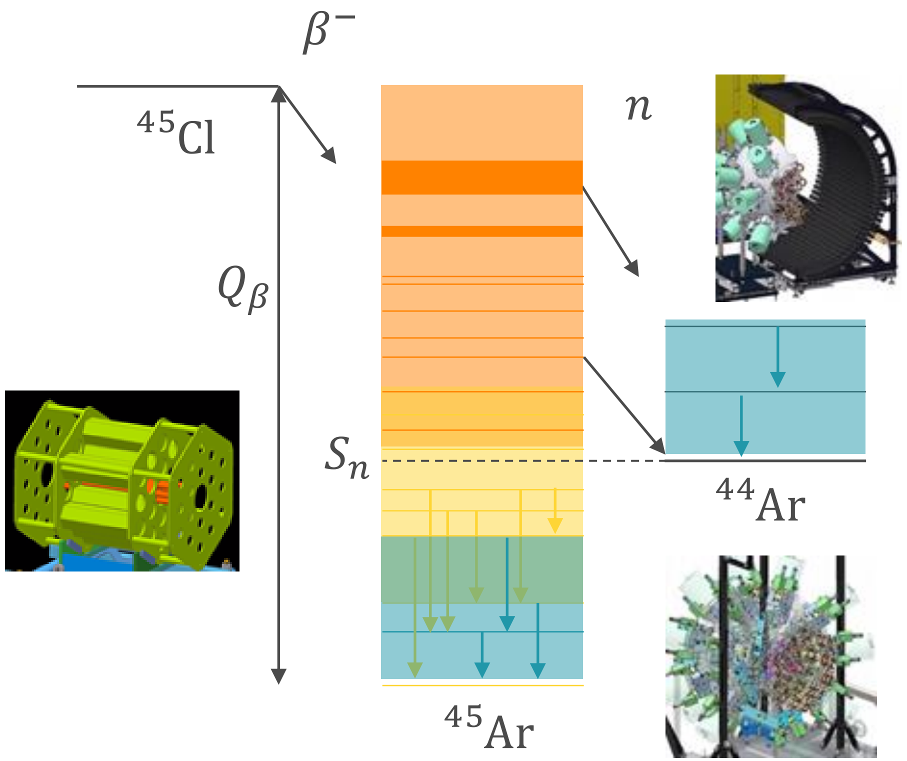

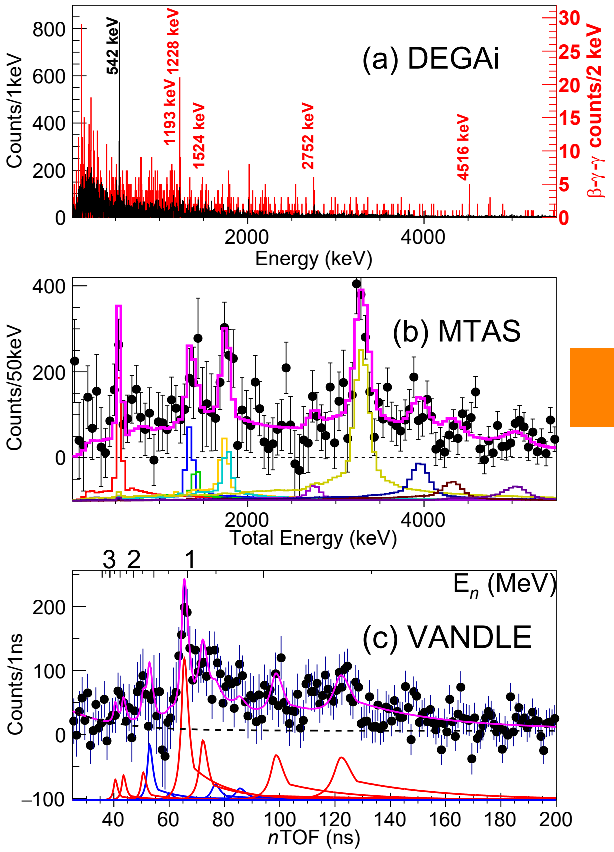

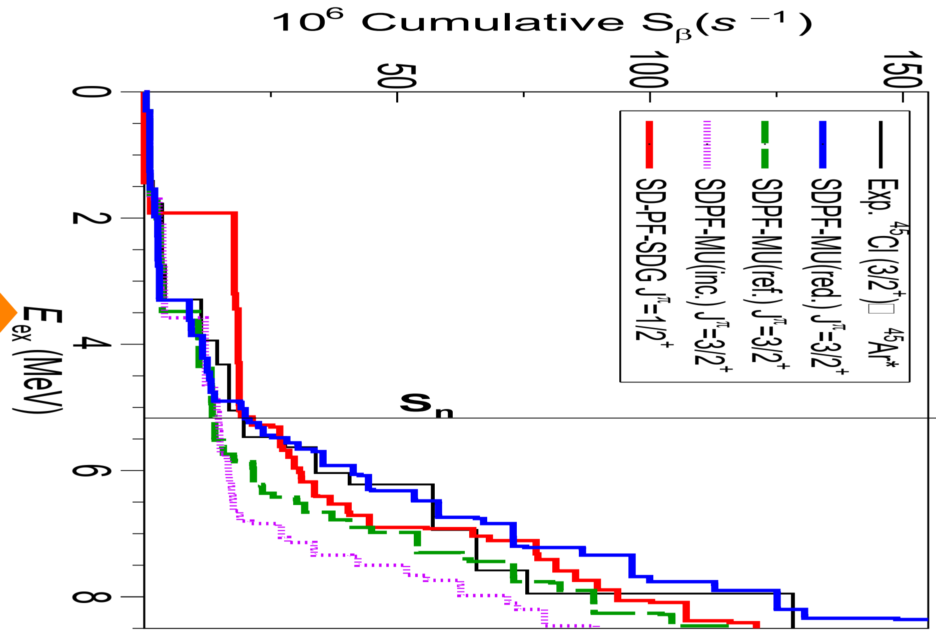

Courtesy of I. Cox

I. Cox et al., PRL 132, 152503 (2024)

Nuclear structure from S_β above S_n

- The complete β-decay strength of ^{45}Cl was measured at FRIB Decay Station initiator (DEGAi + MTAS + VANDLE)
- The ground-state J^π of ^{45}Cl is $3/2^+$ (Bhattacharya2023)
- The large-scale shell-model calculation with the nominal sdpf-mu interaction is consistent with the experimental S_β below S_n, but underestimates the strength above S_n
- According to the wavefunctions: ν(sd)→π(sd) at low Ex; ν(pf)→π(pf) at high Ex (above S_n)

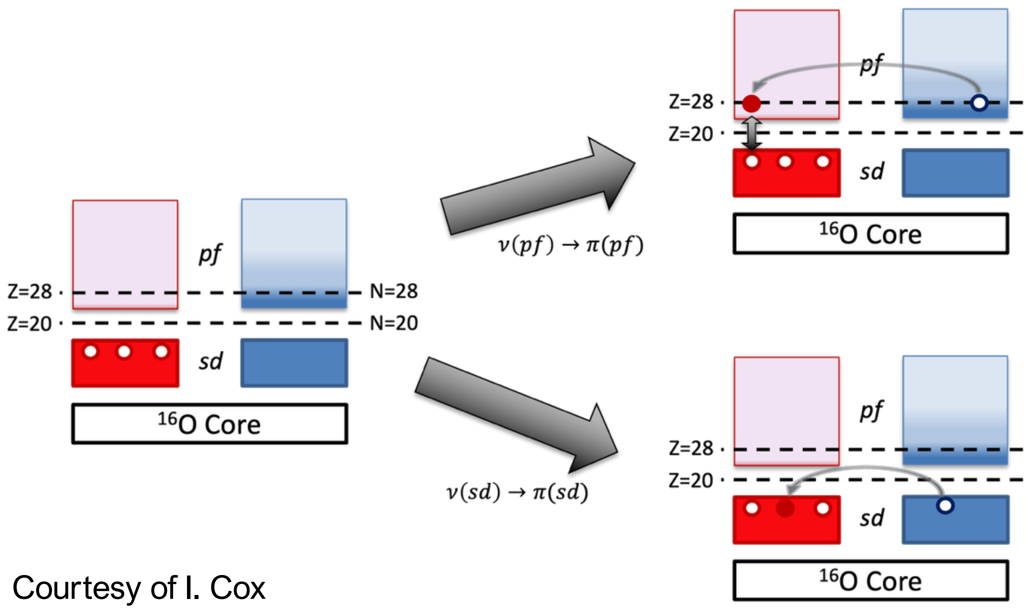

Courtesy of I. Cox

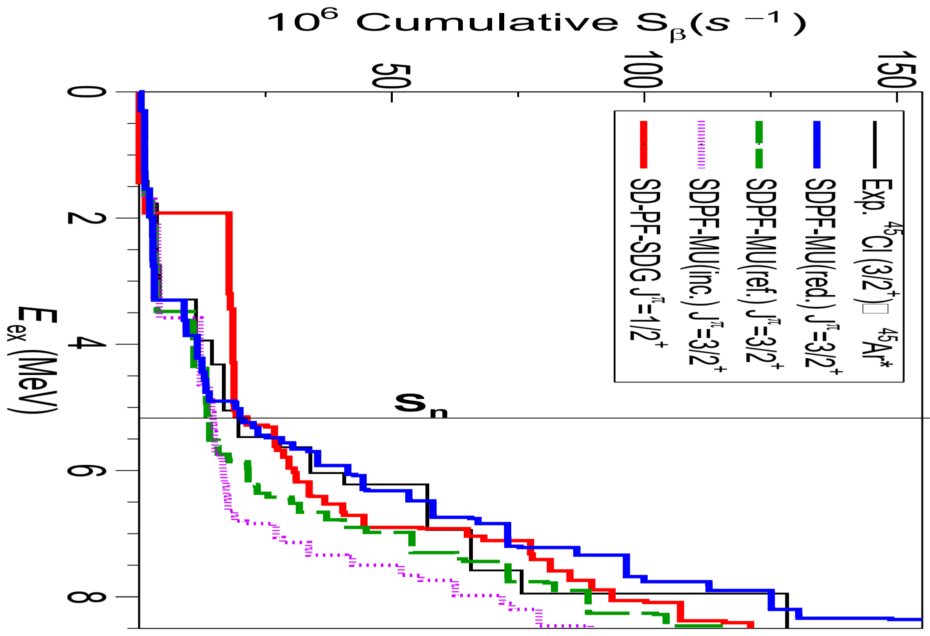

I. Cox et al., PRL 132, 152503 (2024)

Nuclear structure from S_β above S_n

- The complete β-decay strength of ^{45}Cl was measured at FRIB Decay Station initiator (DEGAi + MTAS + VANDLE)
- The ground-state J^π of ^{45}Cl is $3/2^+$ (Bhattacharya2023)
- The large-scale shell-model calculation with the nominal sdpf-mu interaction is consistent with the experimental S_β below S_n, but underestimates the strength above S_n
- According to the wavefunctions: ν(sd)→π(sd) at low Ex; ν(pf)→π(pf) at high Ex (above S_n)
- Reducing the Z=20 shell gap improves the strength above S_n while having little effect at low Ex
- Decay strength from ^{45}Cl to the highly excited states of ^{45}Ar sheds light on the Z=20 shell gap (difficult in other experimental approaches)

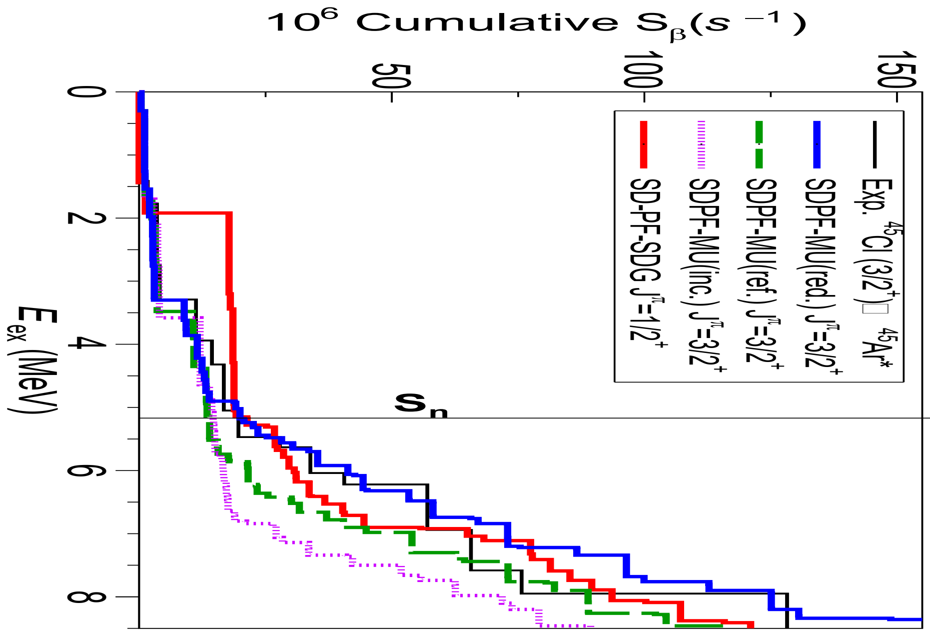

I. Cox et al., PRL 132, 152503 (2024)

Other β-related measurements worth mentioning

- Studying the level scheme of daughter nuclei following β decay
  - The energy and lifetime (with fast-timing detectors) of low-lying states

  V. Tripathi et al., Phys. Rev. Lett. 94, 162501 (2005)
  M. Piersa-Siłkowska et al., Phys. Rev. C 104, 044328 (2021)

- β decay with spin-polarized nuclei (unambiguous spin assignment)

Y. Hirayama et al., Phys. Lett. B 611, 239 (2005)

- β-NMR (β-detection nuclear magnetic resonance) to determine the nuclear magnetic moment and quadrupole moment

G. Neyens et al., Phys. Rev. Lett. 94, 022501 (2005)

- Measuring the inclusive β-delayed neutron emission probability, Pn, using, e.g., ^{3}He neutron counters

V. H. Phong et al., Phys. Rev. Lett. 129, 172701 (2022)

Pros and cons for β-decay studies of nuclear structure

Pros

- Mechanism under control
- Don't need massive statistics for essential quantities
- The further from stability, the more states can be studied within the Q_β window (benchmarking theoretical S_β over a broad range of excitation energy)
- May give access to study the mechanism of particle emission

Cons

- Accessible states are limited by Q_β
- Can only study the states of which the spins and parities follow the selection rules
- Spin assignment might be ambiguous

Experimental approaches to study nuclear structure far from the stability: part 2

THE UNIVERSITY OF TENNESSEE KNOXVILLE

Exotic beam summer school 2026

Part 1

- Nuclear structure in exotic nuclei
- Radioactive ion-beam facilities
- Access nuclear structure via β decay

Part 2

- Techniques for studying nuclear ground states
- Nuclear excitations and related measurements

Nuclear ground-state properties: binding energies, spins, electromagnetic moments, and charge radii

Nuclear masses and shell structure

- The mass of a nucleus, $M(N, Z)$, with N neutrons and Z protons, is less than the sum of the masses of N free neutrons and Z free protons, with the energy difference referred to as the binding energy: $B(N, Z) = \{N M_n + Z M_p - M(N, Z)\} c^2$
- The binding energy reflects how strongly the nucleons are bound together, and is directly related to the nucleon-nucleon interaction of the many-body quantum system
- Mass measurement played an important role in establishing the shell model (see part I)
- Using binding energies, one can establish the systematics of two-neutron (proton) separation energy, which manifests sudden drops at neutron (proton) shell closures:
  $S_{2n}(N, Z) = B(N, Z) - B(N\text{-}2, Z)$ or $S_{2p}(N, Z) = B(N, Z) - B(N, Z\text{-}2)$
- Furthermore, one can plot the derivative of S_{2n} (S_{2p}), to see the strength of the shell gaps:
  $\Delta_n(N_0, Z) = S_{2n}(N_0, Z) - S_{2n}(N_0+2, Z)$
  or $\Delta_p(N, Z_0) = S_{2p}(N, Z_0) - S_{2p}(N, Z_0+2)$

D. Lunney et al., RMP 75, 1021 (2003)

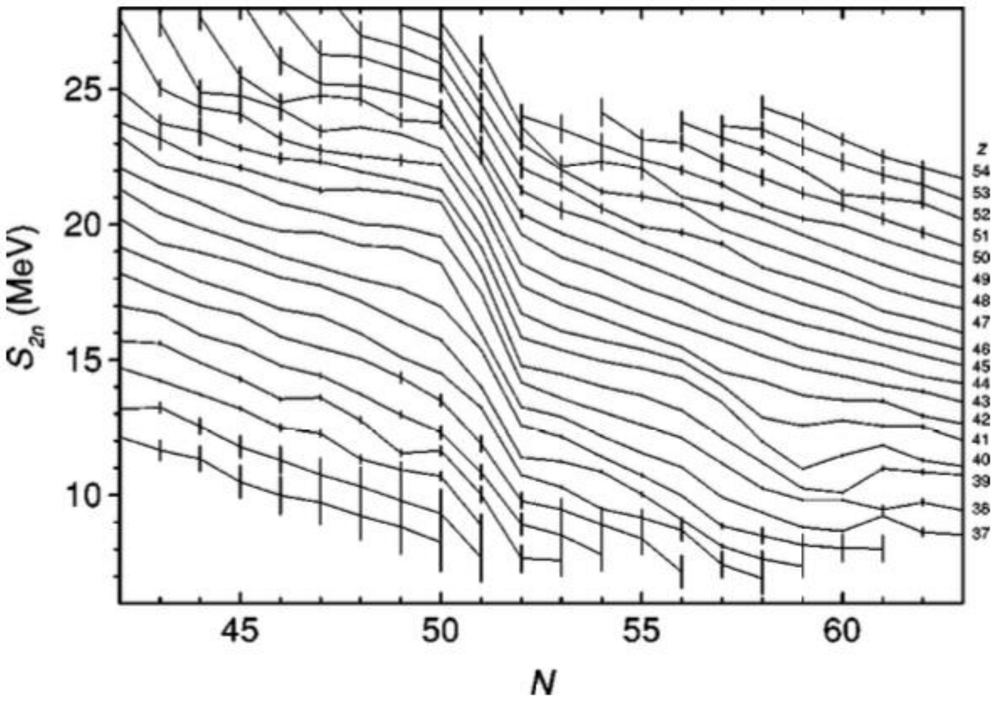

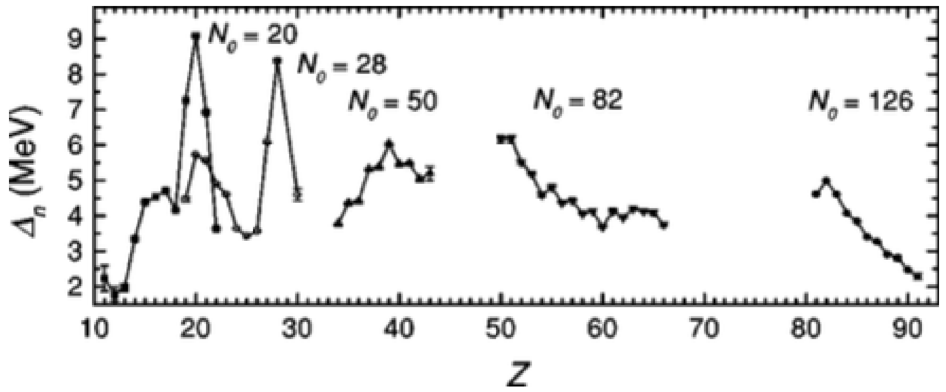

Direct mass spectrometry techniques (I)

- Penning trap spectrometer
  - Confining (low-energy) ions with magnetic (uniform) and electric (quadrupole) fields
  - The cyclotron motion of ions is composed of three eigenmotions: the axial (ω_z), magnetron (ω_-), and modified cyclotron (ω_+) motion
  - The cyclotron frequency $\omega_c = Bq/m$ (relative to nuclei with known q/m)
  - Brown-Gabrielse invariance theorem: $\omega_c^2 = \omega_z^2 + \omega_+^2 + \omega_-^2$

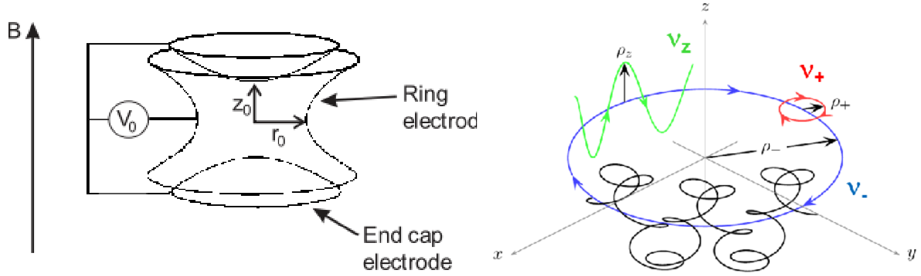

K. Blaum et al., Phys. Scr. T 152, 014017 (2013)

- Storage ring mass spectrometry
  - A storage ring stores and accumulates high-energy ions by setting the centrifugal and Lorentz forces acting on the stored ions equal
  - The relative differences in revolution frequencies of the ions are

$$\frac{\Delta f}{f} = -\frac{1}{\gamma_T^2}\frac{\Delta(m/q)}{m/q} + \left(1 - \frac{\gamma^2}{\gamma_T^2}\right)\frac{\Delta v}{v}$$

  - To eliminate the second term (velocity spread), one can do either
    - Schottky mass spectrometry: electron cooling of the ions to reduce $\Delta v/v$ down to10^{-6}, which takes a few seconds
    - Isochronous mass spectrometry: operating the ring in the Isochronous mode so that $\gamma = \gamma_T$

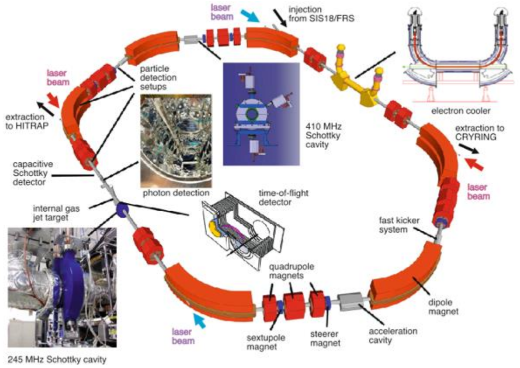

Y.A. Litvinov et al., Eur. Phys. J. Spec. Top. 233, 1191 (2024)

Direct mass spectrometry techniques (II)

- Time-of-flight mass spectroscopy
  - The time-of-flight t for an ion, with a fixed magnetic rigidity Bρ, to travel a known flight path of length L is related to m/q

$$t = \frac{L}{B\rho}\frac{m}{q} \qquad \text{(nonrelativistic)}$$

$$t^2 = \left(\frac{L}{B\rho}\right)^2\left[\left(\frac{m_0}{q}\right)^2 + \left(\frac{B\rho}{c}\right)^2\right] \qquad \text{(relativistic)}$$

  - Bρ needs to be measured at a dispersive focal plane event by event
  - With a typical flight path ~60 m (NSCL), the energy resolution is ~200 keV for nuclei with A~70

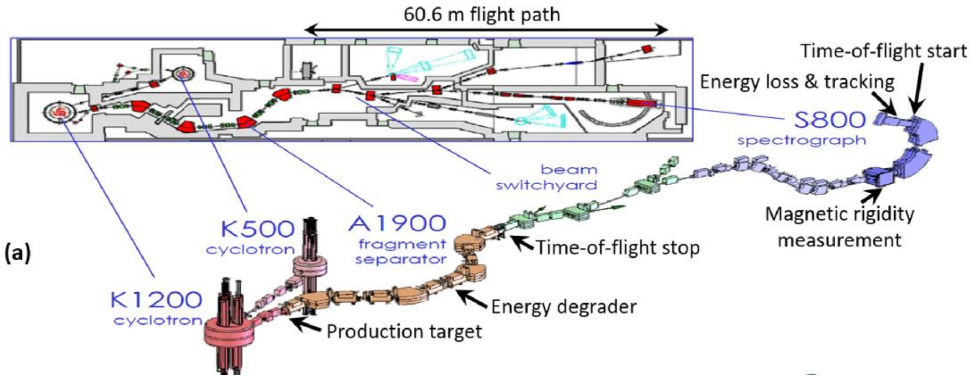

Z. Meisel et al., Phys. Rev. C 93, 035805 (2016)

- Multi-reflection time-of-flight mass spectrometer (MRTOF-MS)
  - To increase the flight path, MRTOF-MS traps ions between a pair of electrostatic mirrors
  - The extended flight path can be > 1 km
  - For ions with fixed kinetic energy (accelerated over the same potential difference)

$$t = a\sqrt{\frac{m}{q}} + b,$$

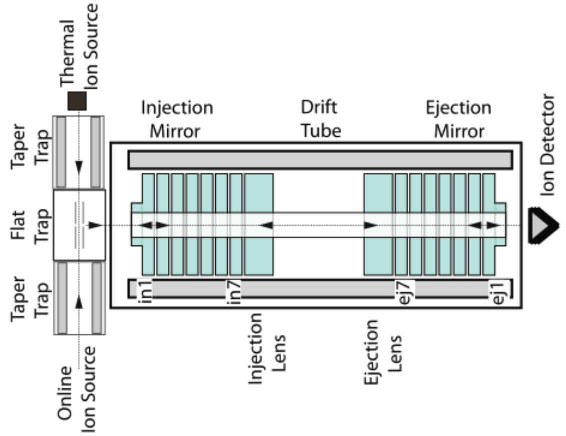

P. Schury et al., NIMB 335, 39 (2014)

Empirical neutron shell gaps at N=32, 34

- The attractive $\pi f_{7/2}\ \nu f_{5/2}$ interaction makes the $\nu f_{5/2}$ orbital go higher when protons are removed from $\pi f_{7/2}$, leading to the N=32 and 34 subshell closure in the calcium isotopes (no valence protons on $\pi f_{7/2}$)

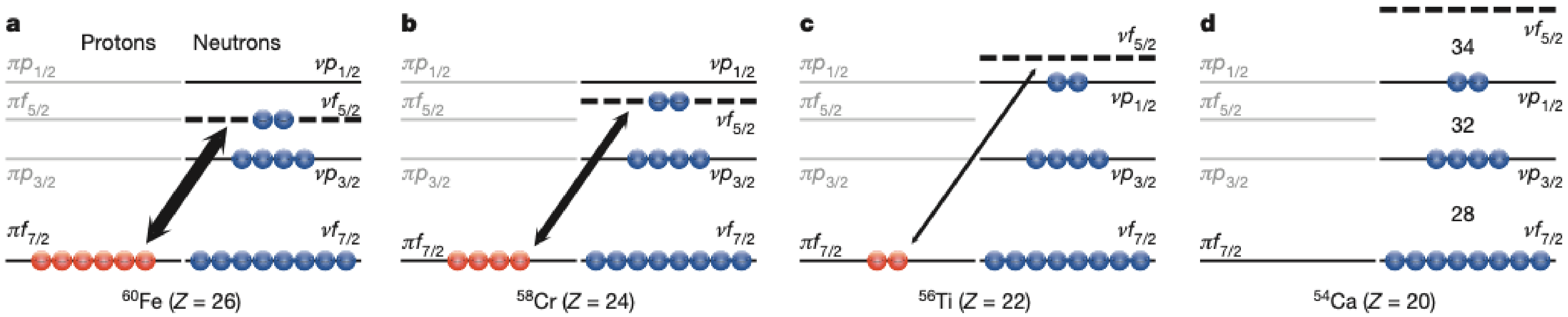

D. Steppenbeck et al., Nature 502, 207 (2013)

Empirical neutron shell gaps at N=32, 34

- The attractive $\pi f_{7/2}\ \nu f_{5/2}$ interaction makes the $\nu f_{5/2}$ orbital go higher when protons are removed from $\pi f_{7/2}$, leading to the N=32 and 34 subshell closure in the calcium isotopes (no valence protons on $\pi f_{7/2}$)

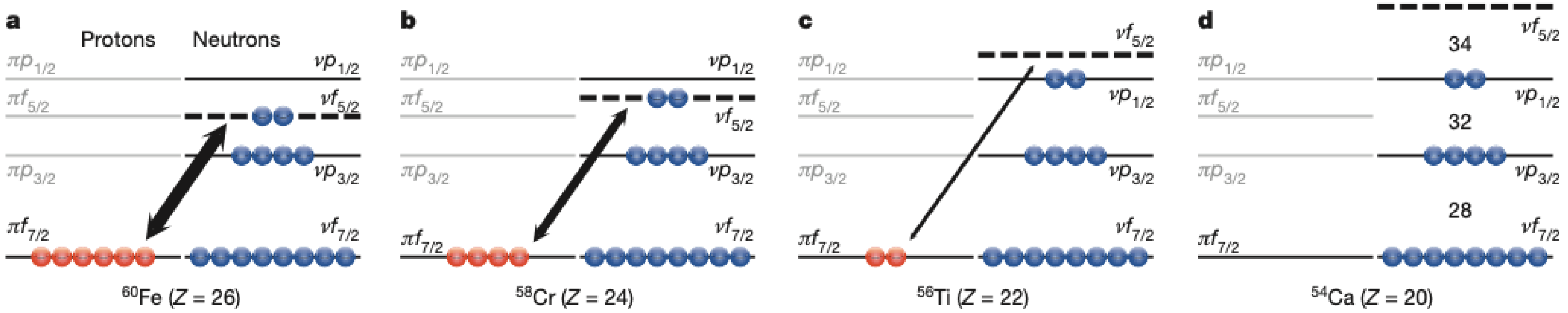

D. Steppenbeck et al., Nature 502, 207 (2013)

- The first direct mass measurements of ^{51,52}Ca were done at the Los Alamos Meson Physics Facility using the time-of-flight technique [X.L. Tu et al., Z. Phys. A 337, 31 (1990)], and then improved significantly by the Penning Trap at TRIUMF (TITAN) [A.T. Gallant et al., Phys. Rev. Lett. 109, 032506 (2012)]

- However, to identify the magicity at N=32, we need to measure nuclear masses beyond N=32, to see if there is a significant drop in two-neutron separation energies

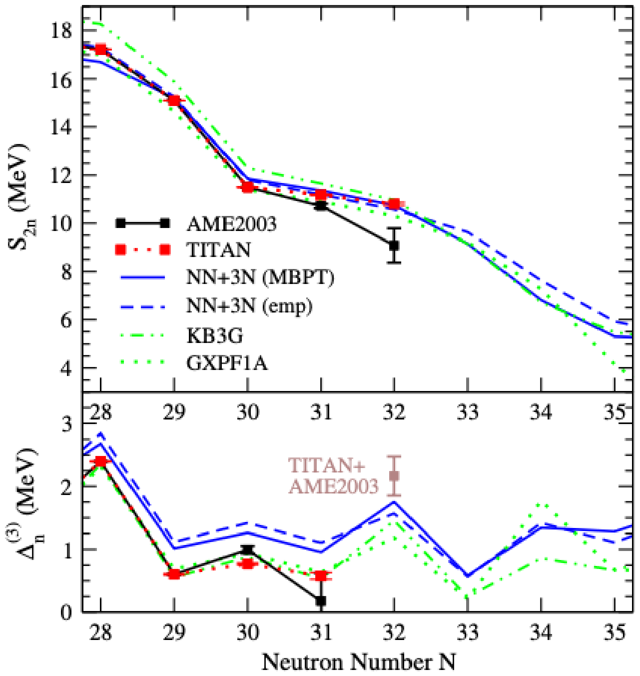

A.T. Gallant et al., Phys. Rev. Lett. 109, 032506 (2012)

Empirical neutron shell gaps at N=32, 34

- The masses of ^{53,54}Ca were measured by the MRTOF mass spectrometer of ISOLTRAP at ISOLDE [F. Wienholtz et al., Nature 498, 346 (2013)]
- During the same experiment, the masses of ^{51,52}Ca were remeasured using the Penning trap with improved precision
- The neutron N=32 shell gap can be seen at Z=20

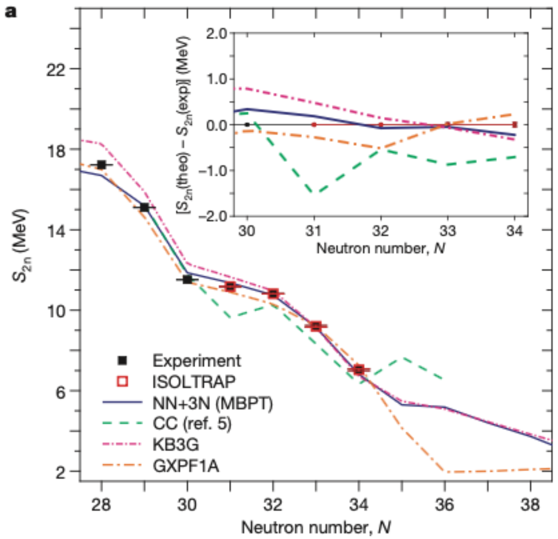

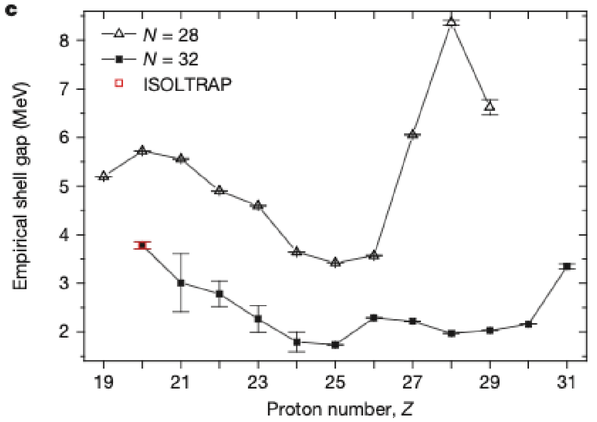

F. Wienholtz et al., Nature 498, 346 (2013)

- The masses of $^{55\text{-}57}$Ca were measured at RIBF, RIKEN using the time-of-flight technique [S. Michimasa et al., Phys. Rev. Lett. 121, 022506 (2018)]
- Their masses provide experimental evidence for the emergence of neutron magicity at N=34

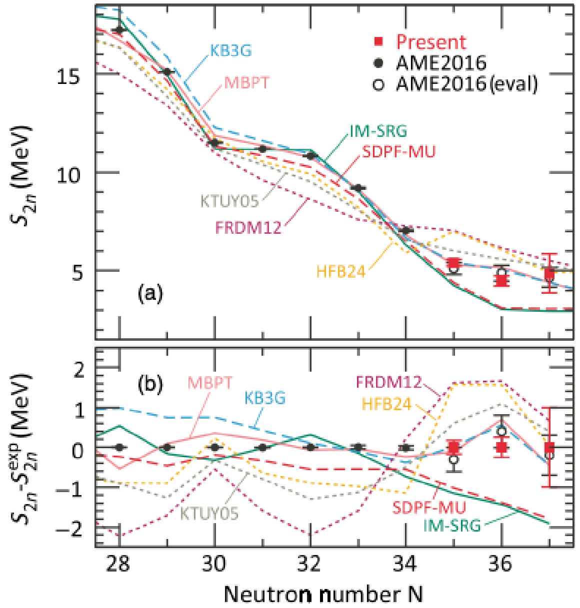

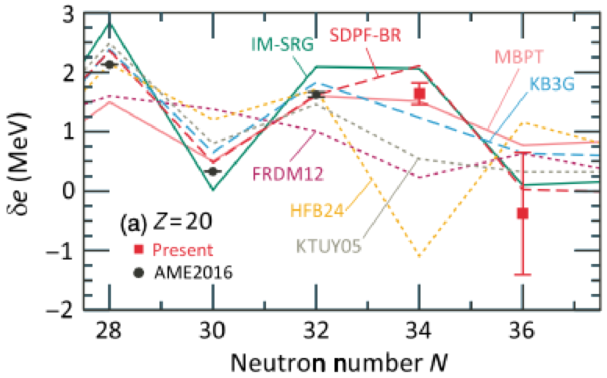

S. Michimasa et al., Phys. Rev. Lett. 121, 022506 (2018)

Ground-state properties from hyperfine structure

- The hyperfine structure results from the interaction between the nucleus and the electromagnetic field generated by the surrounding electrons
- Measuring the transition energies (usually in terms of frequency) between the electronic hyperfine levels gives access to the nuclear properties, including nuclear spins, charge radii, magnetic dipole moments, and electric quadrupole moments
- The isotope shift is the difference in the frequency of an atomic transition between two isotopes of the same element

$$\delta\nu_{\mathrm{IS}}^{AA'} = \nu^{A'} - \nu^{A} = K_{\mathrm{MS}} \frac{M_{A'} - M_A}{M_A M_{A'}} + F\,\delta\langle r_c^2\rangle^{AA'}$$

change in mean-square charge radii

  - Isotope shift can be approximately decomposed into mass shift and field shift
  - The change in mean-square charge radii can be deduced from the isotope shift, if the constants K_{MS} and F are known (they need to be either calculated or calibrated)
- The energy shift for an atomic hyperfine level with respect to the fine-structure level is

$$\Delta E_{HFS} = \Delta E_{dipole} + \Delta E_{quadrupole}$$
$$= \frac{A}{2}C + \frac{B}{4}\frac{\frac{3}{2}C(C+1) - 2IJ(I+1)(J+1)}{IJ(2I-1)(2J-1)}$$

with $C = F(F+1) - J(J+1) - I(I+1)$

  - A and B (hyperfine coefficients) depend on both nuclear and atomic structure parameters

$$A = \frac{\mu_I B_e(0)}{hIJ} \quad \text{and} \quad B = \frac{eQ_s}{h}\left.\frac{\partial^2 V}{\partial z^2}\right|_{r=0}$$

μ_I and Q_s are the nuclear magnetic dipole and electric quadrupole moments we want to measure

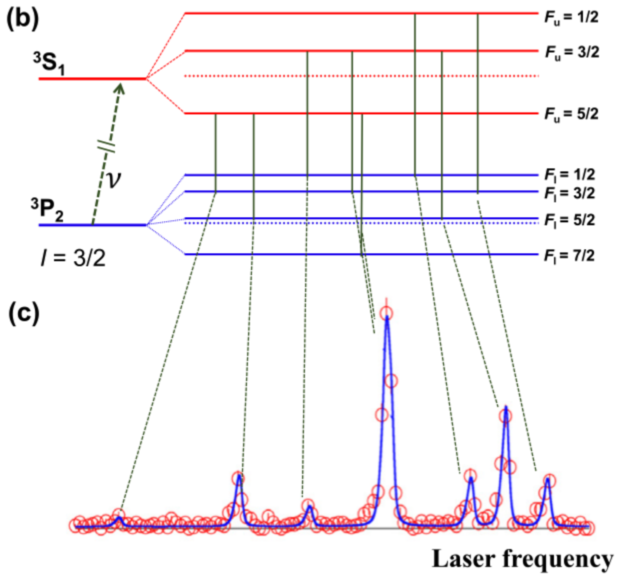

X.F. Yang et al., PPNP 129, 104005 (2023)

THE UNIVERSITY OF TENNESSEE KNOXVILLE

Collinear laser spectroscopy

- Since the energy shifts caused by hyperfine interaction is extremely tiny, we need high-resolution techniques such as laser spectroscopy

- To reduce the Doppler broadening of the experimental linewidth, laser light collinearly overlaps with accelerated ion beams that experience a velocity compression along the axis of their motion
    - The acceleration to a well-defined energy *E* preserves the energy spread δE but reduces the velocity spread of the beam to

$$\delta \upsilon = \frac{\delta E}{m\upsilon} = \frac{\delta E}{\sqrt{2meU}}$$

- Collinear laser spectroscopy with laser-induced fluorescence detection
    - Atoms or ions that are resonantly excited by laser photons will spontaneously decay. By detecting the fluorescent photons as a function of laser frequency, the hyperfine structure can be obtained

- Collinear resonance ionization spectroscopy
    - After the resonant excitation, the atoms can be subsequently ionized by using multiple laser lights simultaneously. The hyperfine spectrum can be obtained by detecting the number of resulted ions (or their decays) as a function of the (first) laser frequency

X.F. Yang et al., PPNP 129, 104005 (2023)

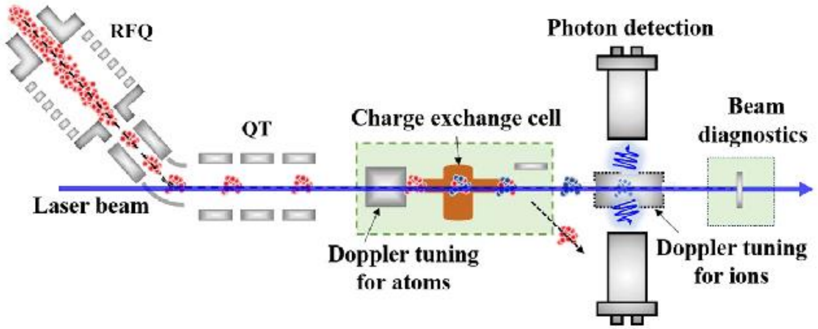

A typical schematic of a collinear laser spectroscopy setup based on detecting laser-induced fluorescence

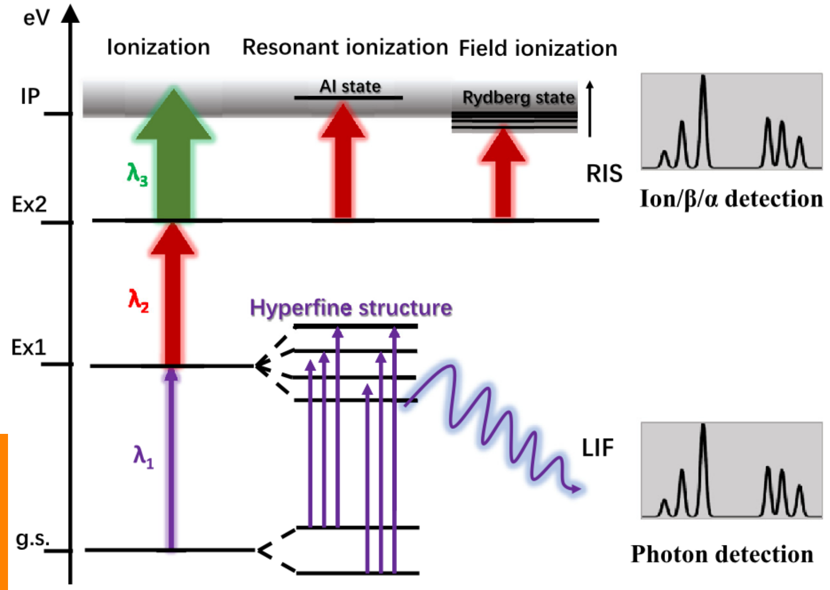

Spin and magnetic moments of $^{49,51}K$

- For the neutron-rich nuclei below ^{48}Ca ($Z<20$, $N\sim28$), protons occupy the *sd* shell and neutrons occupy the *pf* shell
- In theory, due to the proton-neutron residual interaction, the proton $s_{1/2}$ and $d_{3/2}$ orbitals come close and invert at $N=28$
- Measuring the ground-state spins and magnetic moments in neutron-rich potassium ($Z=19$) isotopes provides critical constraints to the theories
- CLS on $^{49,51}K$ was carried out at ISOLDE with induced fluorescence detection
- From the hyperfine structure and magnetic moment, the ground-state spin and parity of ^{51}K were deduced as $3/2^+$, with a dominant proton $d_{3/2}$ hole configuration

Effective SP energy for potassium (SDPF-MU)

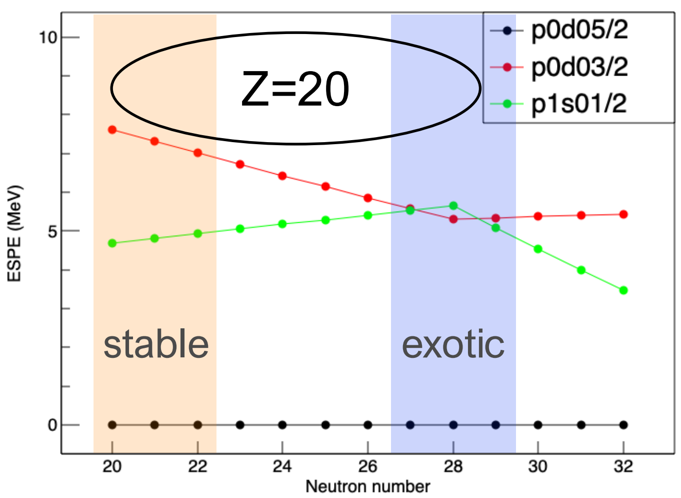

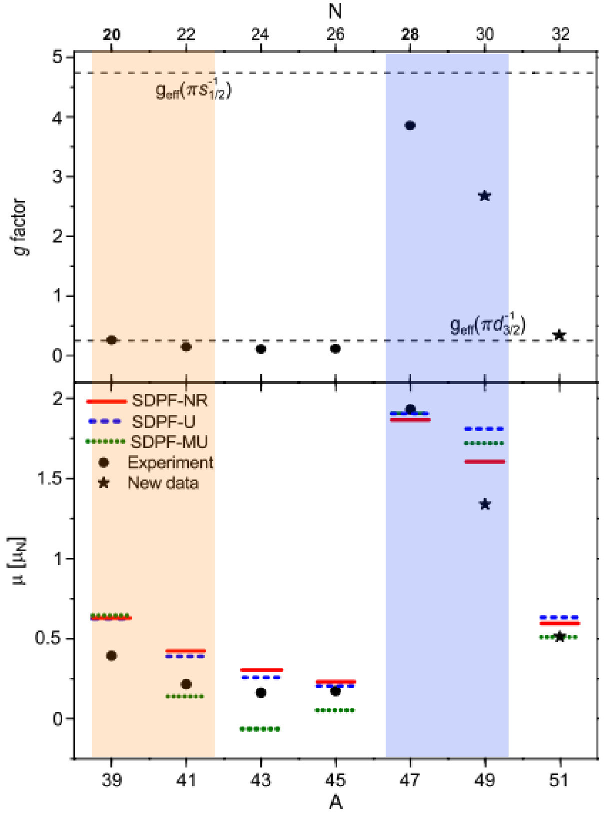

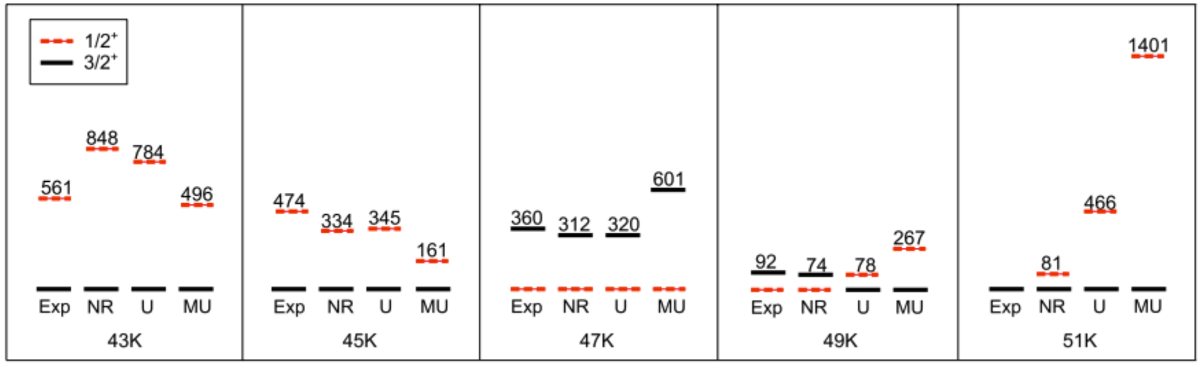

J. Papuga et al., PRL 110, 172503 (2013)

Charge radii of exotic potassium isotopes from CLS

- At neutron magic numbers *N*=28, 50, 82, and 126, the nuclear charge radii feature a kink along isotopic chains
- To investigate whether such a kink exist at *N*=32 along the potassium isotopic chain, the charge radii of neutron-rich potassium isotopes were measured at ISODLE-CERN with the Collinear Resonance Ionization Spectroscopy
- The new data point at ^{52}K shows no kink at *N*=32, similar to the manganese isotopic chain, where no subshell closure at *N*=32 was reported
- Coupled-cluster calculations reproduced the odd-even variations in the charge radii, but not the notable increase beyond *N*=28
- The Fayans nuclear density functional theory captures the increase in charge radii beyond *N*=28, but overestimates the odd-even staggering along the chain

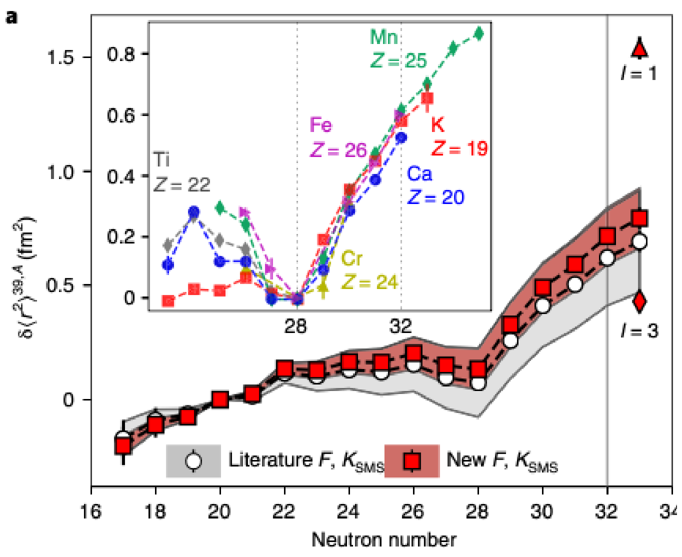

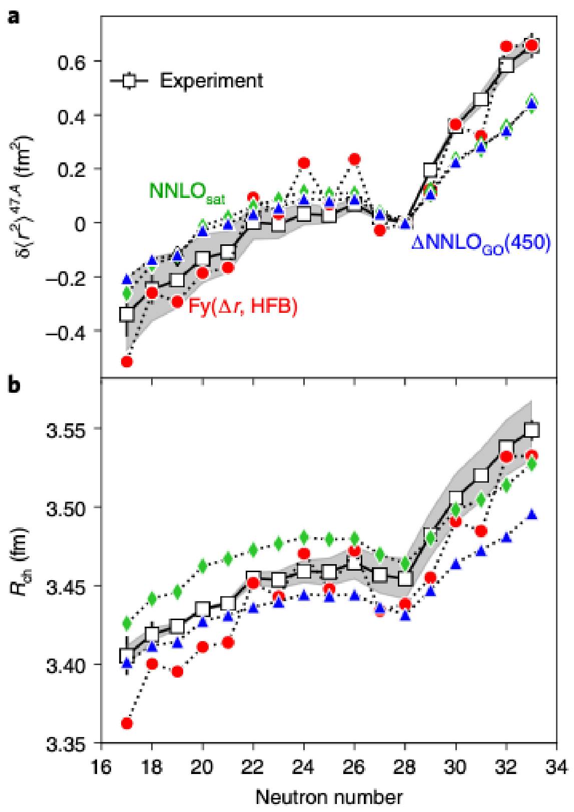

A. Koszorus et al., Nat. Phys. 17, 439 (2021)

Coulomb excitations, nucleon transfer and knockout reactions

Coulomb excitation and nuclear collectivity

- Coulomb excitation is a process of inelastic scattering caused by the time-dependent electromagnetic field between two colliding nuclei
- Because the process selectively populates low-lying collective states, it is ideally suited to study nuclear collectivity and nuclear shape
- The nucleus of interest is excited purely by the electromagnetic interaction from state | i〉 to | j 〉 and then decay to the lower state via emitting γ ray
- Since the electromagnetic interaction is well known, the process allows for nuclear-model-independent interpretation of the observed data
- The matrix elements 〈j | M(E2) | i 〉, which describe the excitation and decay pattern, can be determined by the γ-ray intensities observed in the experiment
- The matrix elements are related to the deformation parameters in the intrinsic frame of the nucleus (strong or weak deformation, prolate or oblate shape, etc)

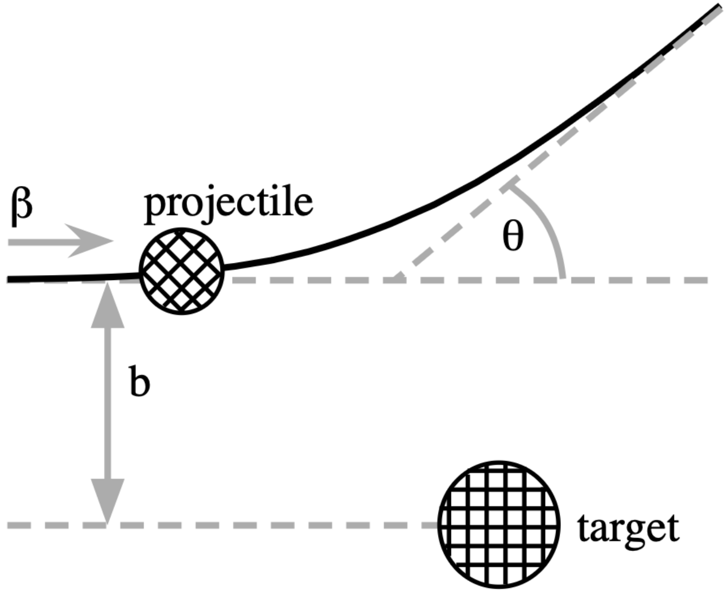

T. Glasmacher, Annu. Rev. Nucl. Part. Sci. 48, 1 (1998)

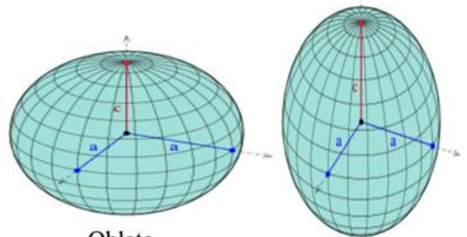

Coulomb excitation with radioactive ion beams

- Low-energy Coulomb excitation
  - Radioactive ion beams from ISOL facilities were accelerated to an energy of 2~5 MeV/u, below the Coulomb barrier
  - Multi-step Coulomb excitation is possible depending on the beam energy and atomic numbers of the collision partners
  - Scattered projectile and target recoil are detected by position-sensitive detectors (e.g., DSSD) to derive their scattering angles
  - Additional selection on the scattering angles of the projectile is possible to ensure that the distance of closest approach, D_{min}, is at least 5 fm
  - The γ rays deexciting the nuclei after Coulomb excitation are measured by γ detectors in the laboratory frame, and then their Doppler shifts are corrected event-by-event (lab frame → nucleus frame)
  - Use the Coulomb excitation analysis code, such as GOSIA, to determine the EM matrix elements with the obtained γ-ray yields and other experimental inputs (level schemes, detector geometry, etc)

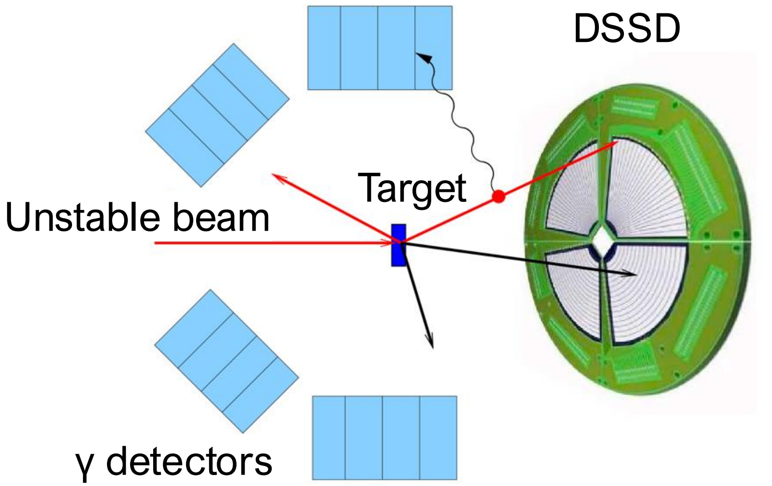

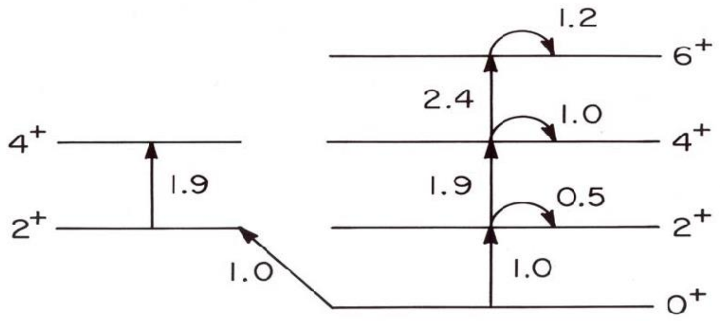

GOSIA's manual, 2006

Coulomb excitation with radioactive ion beams

- Intermediate-energy Coulomb excitation
  - In-flight fragmentation facilities deliver unstable beams at energies around 30-300 MeV/u, allowing for the use of a thick target to increase the luminosity
  - At such a high energy, the reaction is limited to single-step Coulomb excitation
  - Since the beam energy is much higher than the Coulomb barrier, the nuclear contribution to the excitation process needs to be properly accounted for
    - Select events with very forward projectile scattering angles in the laboratory
    - Make reference measurements with a low-Z target, e.g., ^{12}C
  - To select the Coulomb excitation channel of the nuclei of interest, incoming and outgoing beam particles need to be identified event-by-event (see particle identification in part 1)
  - The Doppler-corrected γ-ray spectrum is constructed by measuring the emitting angle of the γ ray and the beam velocity event-by-event
  - After subtracting the contribution from the feeding from higher-lying states, the Coulomb excitation cross section can be determined, which is used to extract the transition matrix elements

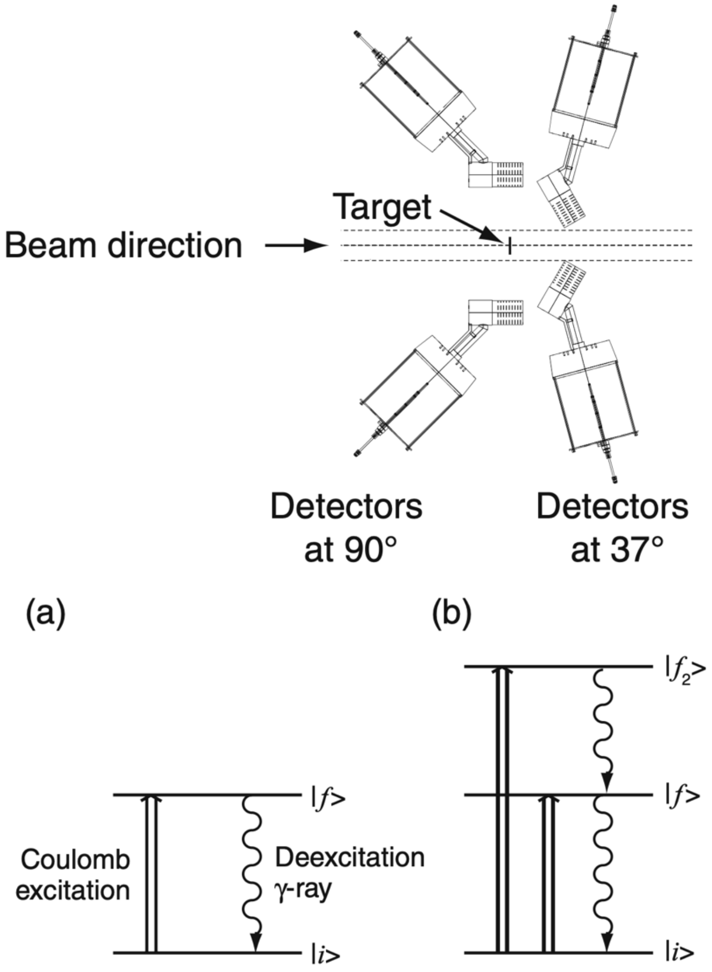

T. Glasmacher, Lect. Notes Phys. 764, 27 (2009)

Intermediate-energy Coulomb excitation of ^{104}Sn

- Tin (Z=50) has a long isotopic chain crossing two doubly magic nuclei far from stability: ^{132}Sn and ^{100}Sn
  - While the doubly magic nature of ^{132}Sn has been experimentally verified, that of ^{100}Sn still remains a theoretical suggestion
- The systematics of B(E2) in the proton-rich, even-A tin isotopes show discrepancies with the theory predictions
  - Theory → gradually decreases from mid-shell ^{112}Sn down to ^{106}Sn
  - Experiment → almost constant B(E2) from ^{112}Sn down to ^{106}Sn
- To reveal the B(E2) systematics approaching ^{100}Sn, three Coulomb excitation experiments of ^{104}Sn have been performed at intermediate energy
  - At GSI, the B(E2) of ^{104}Sn was measured with respect to ^{112}Sn, showing a huge decrease relative to ^{106}Sn [G. Guastalla et al., PRL 110, 172501 (2013)]
  - At NSCL, it was remeasured with respect to ^{102}Cd, disagreeing with the previous measurement and theory prediction [V. Bader et al., PRC 88, 051301 (2013)]
  - At RIBF, it was measured from the absolute cross section of inelastic scattering of ^{104}Sn on a Pb target [P. Doornenbal et al., PRC 90, 061302 (2014)]
- At that time, the B(E2) results in proton-rich tin imposed a serious challenge to the theories, in particular, the shell-model calculations

P. Doornenbal et al., PRC 90, 061302(R) (2014)

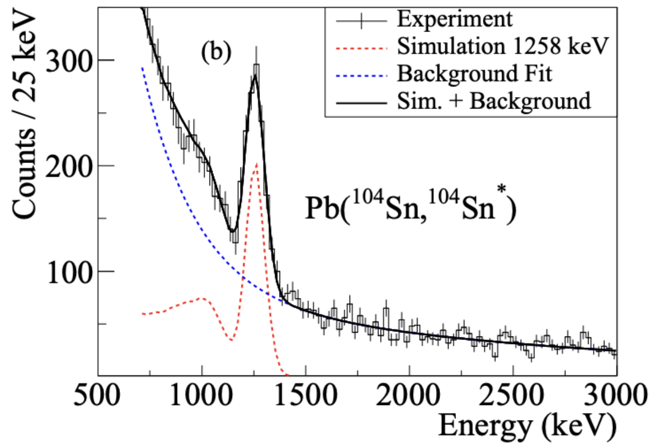

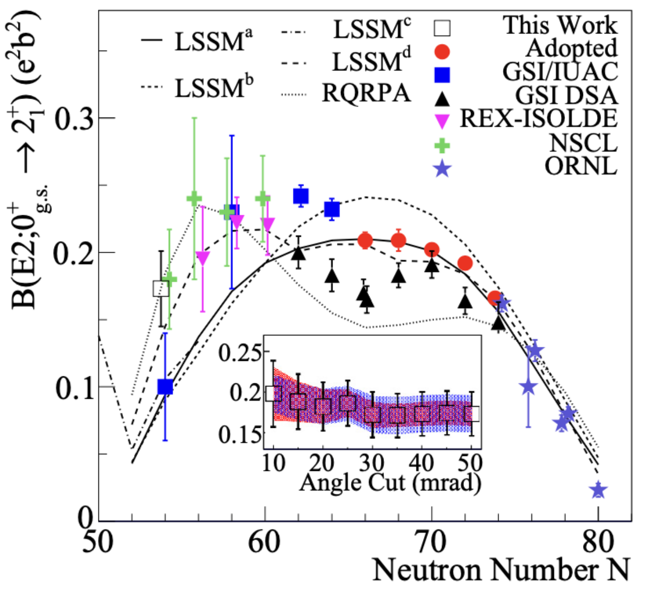

Coulomb excitation of ^{136}Te

- Atomic nuclei with a few valence protons and neutrons outside of double shell closures are ideal laboratories for exploring the emergence of collectivity and nucleon-nucleon interactions.

- ^{136}Te is such an example with two valence protons and two valence neutrons outside ^{132}Sn

- The first B(E2, $0^+ \rightarrow 2^+$) of ^{136}Te was measured at HRIBF at ORNL, using a ^{136}Te beam and a carbon target; the result is exceptionally small compared with systematics and model predictions [D. C. Radford et al., PRL 88, 222501 (2002)]

- It was remeasured at HRIBF at ORNL with a ^{136}Te beam and a titanium target [J.M. Allmond et al., PRL 118, 092503 (2017)]
    - The new result of B(E2) was about 50% greater than the previous measurement, and indicated the emergence of prolate-deformed quadrupole collectivity
    - Shell-model calculations with different effective interactions and effective charges can well reproduce the experimental data

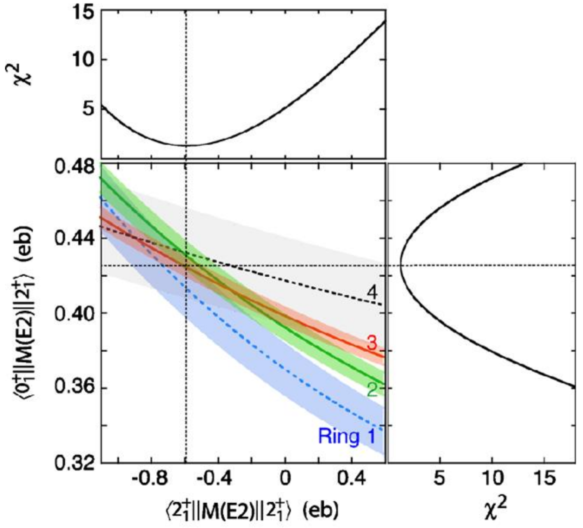

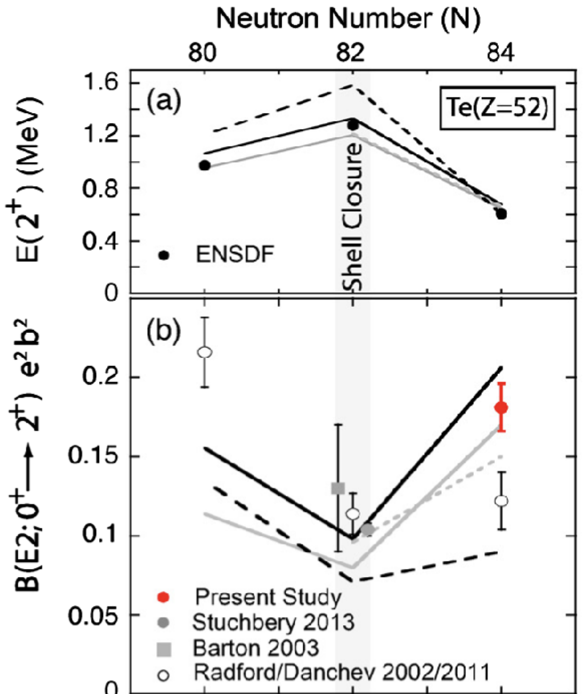

J.M. Allmond et al., PRL 118, 092503 (2017)

Studying nuclear structure with transfer reactions

- Transfer reactions are one of the most important types of direct reaction (fast, peripheral) to probe the single-particle structure in atomic nuclei
- Transfer reactions are highly selective because the reaction probability depends on matching conditions and structural overlap, e.g.,
  - One-neutron-adding reactions, or (d,p) reactions → single-particle states
  - One-neutron-removal reactions, or (p,d) reactions → single-hole states
- For a typical (d,p) reaction, we want to measure the angle and energy of the outgoing fragments, e.g., the protons, so that we can extract
  - The Q-value of the reaction → Excitation energies of the residual
  - The total angular momentum transfer of the reaction → Spin assignment of the final states in the residual
  - Spectroscopic factors → Information (model dependent) on the microscopic wavefunctions
- Traditionally, transfer reactions were performed in normal kinematics, i.e., with a heavy target and a light ion beam
- When using a radioactive ion beam, it is necessary to perform the reaction in inverse kinematics, i.e., with a heavy beam and a light target

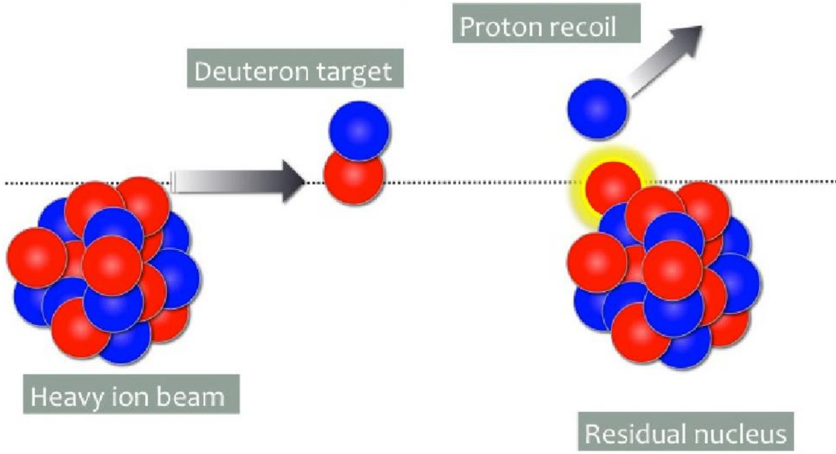

K. L. Jones, Phys. Scr. T 152, 014020 (2013)

The Oak Ridge Rutgers University Barrel Array

- ORRUBA is a high-solid-angle silicon detector array designed for measuring light ions from transfer reactions in inverse kinematics
  - Twelve-sided barrel of silicon detectors, covering angle from ~45° to ~135°, with approximately 1° resolution in polar angle
  - If particle identification is needed at forward angles (to distinguish protons, deuterons, etc.), a thin layer of ΔE detector can be added in front of the thick Si detector, creating a telescope that can distinguish light particles with the ΔE-E method
- Because it is very compact, the ORRUBA detector array can be coupled with the large γ-ray detector array, such as Gammasphere and GRETINA/GRETA → GODDESS
  - Detecting γ rays in coincidence with charged particles is highly advantageous
    - Separating closely-spaced states populated in the reactions
    - Providing additional information on the states populated directly in the reactions (decay path, angular distribution, lifetimes, etc.)
    - Giving access to the state not directly populated in the reactions

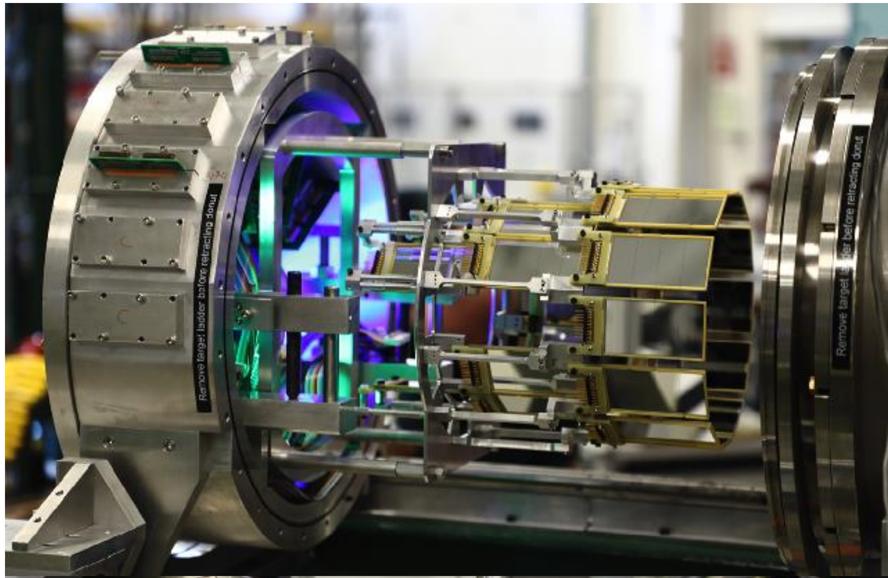

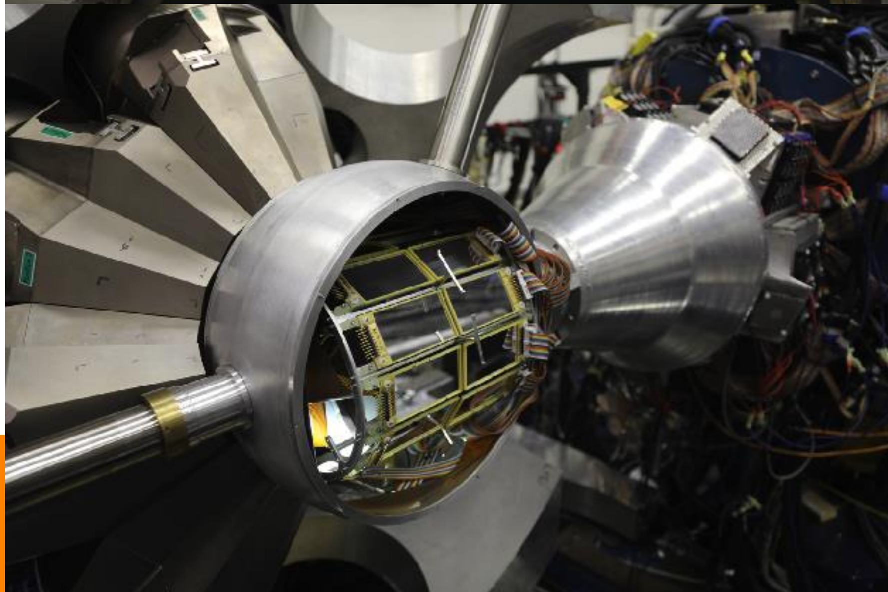

S.D. Pain, Front. Phys. 13, 1537984 (2025)

Solenoidal spectrometers for transfer reactions

- When transferring the measurements made in the laboratory to the center-of-mass frame, to reconstruct Q values for the residual nucleus, it shows that the energy (in laboratory) of outgoing particles populating a particular state (Q value) varies with angle (in laboratory) → the kinematic shift
  - The variation with angle is different for different ion energies
  - It leads to a severe compression in energy when transforming to the *Q*-value spectrum at the forward center-of-mass angles

- A different method for measuring changed particles emitted from transfer reactions uses a large-bore superconducting solenoid magnet
  - In a homogeneous magnetic field, a charged particle performs helical motion with a radius *r* independent of the longitudinal velocity
  - After one orbital motion, the charged particle returns to the beam axis, and the cyclotron period (T_{cyc}) is only a function of the magnetic field *B* and the particle's mass-to-charge ratio
  - A position-sensitive silicon detector array (hollow) is placed around the beam axis to detect the energy, travel distance (along the beam direction), and time-of-flight of the charged particle
  - The particle's energy and emitting angle in the center-of-mass frame are

$$E_{\mathrm{cm}} = E_{\mathrm{lab}} + \frac{m}{2} V_{\mathrm{cm}}^2 - \frac{m V_{\mathrm{cm}} z}{T_{\mathrm{cyc}}} \quad \text{and} \quad \cos\theta_{\mathrm{cm}} = \frac{v_{\mathrm{lab}}^2 - V_{\mathrm{cm}}^2 - v_0^2}{2 v_0 V_{\mathrm{cm}}}$$

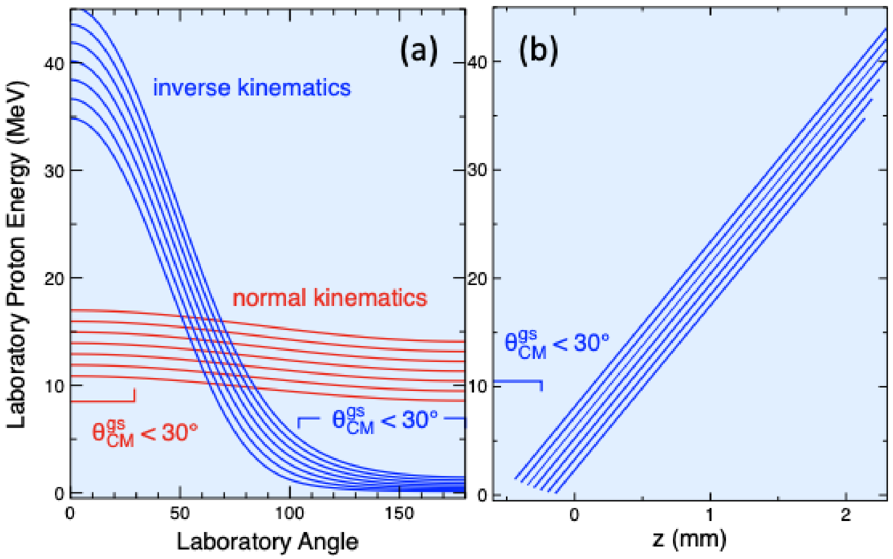

S.J. Freeman, Acta Phys. Pol. B Proc. Suppl. 16, 4-A19 (2023)

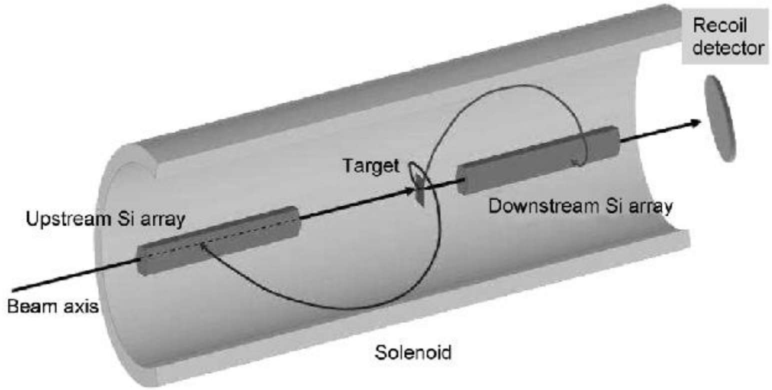

A.H. Wuosmaa et al., NIMA 580, 1290 (2007)

THE UNIVERSITY OF TENNESSEE KNOXVILLE

Active-target time projection chamber

- A time projection chamber (TPC) is a gas detector that tracks the traces of changed particles
    - Ionized electrons drift towards the anode and get multiplied (avalanche) near the sensor plane, which is segmented into readout pads
    - The *x*-*y* information can be obtained from the signals induced in the position-sensitive pads
    - The *z* information can be obtained from the signal's time difference in the pads, caused by different electron drifting time

- A new detector concept is to operate TPC in the Active Target mode (AT-TPC), in which the gas medium in TPC is used as a reaction target (containing, e.g., protons, deuterium, α, etc.) as well
    - It is well suited for the transfer reaction study with radioactive ion beams in inverse kinematics
    - The 3D position reconstruction of the charged particles before and after reactions allow for determining the position of reaction vertex and reaction kinematics
    - Operating the AT-TPC inside a solenoidal magnetic field will enable the measurement of the magnetic rigidity of the charged particles based on the curvatures of their tracks

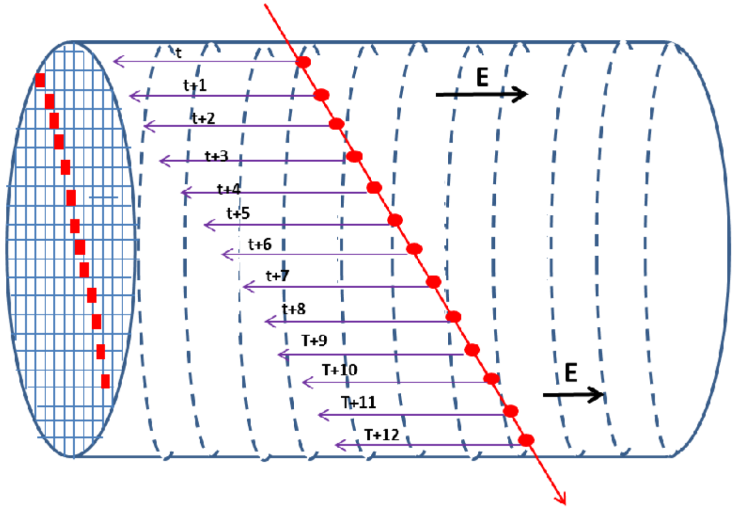

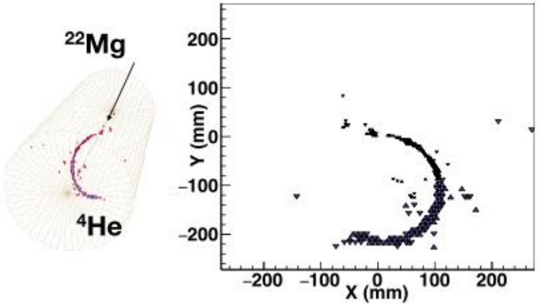

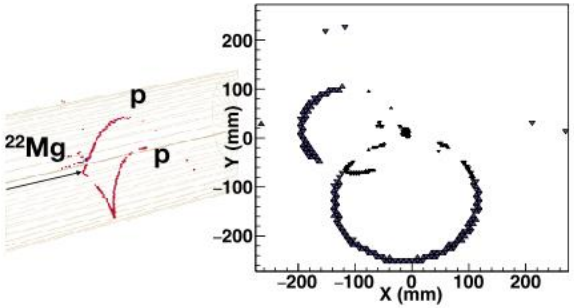

Y. Ayyad et al., NIMA 954, 161341 (2020)

The magic nature of ^{132}Sn from (d, p) reaction

- For ^{132}Sn, a critical question is: how good the approximation is to treat the low-lying states in ^{133}Sn as a single-particle neutron outside the ^{132}Sn core
  - The propriate reaction would be ^{132}Sn(d, p)^{133}Sn, in which a single neutron from a deuteron is transferred to the ^{132}Sn nucleus, creating a low-lying state in ^{133}Sn and emitting a proton
  - Because ^{132}Sn is unstable ($T_{1/2}$ ~ 40s), the measurement must be done in inverse kinematics

- The first such experiment was done by K.L. Jones et al at HRIBF at ORNL, with a ^{132}Sn beam and a deuterated polyethylene target (CD_2)
  - The outgoing protons were measured by ORRUBA
  - Four peaks were clearly visible in the reconstructed Q-value spectrum, including a newly observed state at 1363 keV ($1/2^-$)
  - The differential cross sections $d\sigma/d\Omega$ were compared with the reaction theory assuming single-particle natures, and the scaling factors were close to unity (indeed single-particle states)

- A new measurement, lead by Ben Kay from ANL, was done at ISOLDE in 2024 using the same reaction (slightly higher beam energy) but with the ISOLDE Solenoidal Spectrometer (ISS)
  - The neutron $i_{13/2}$ state missing from the previous experiment was firmly located

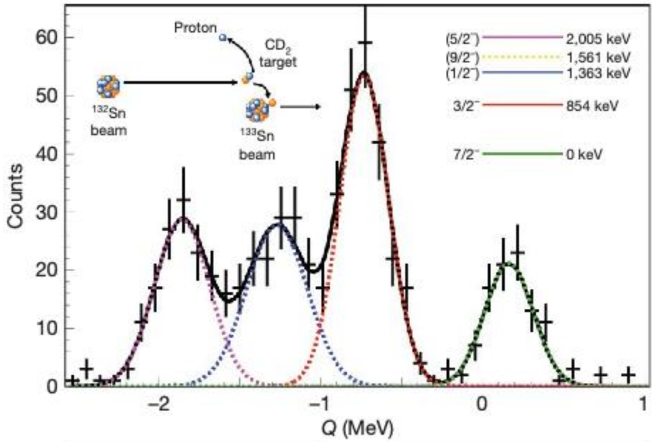

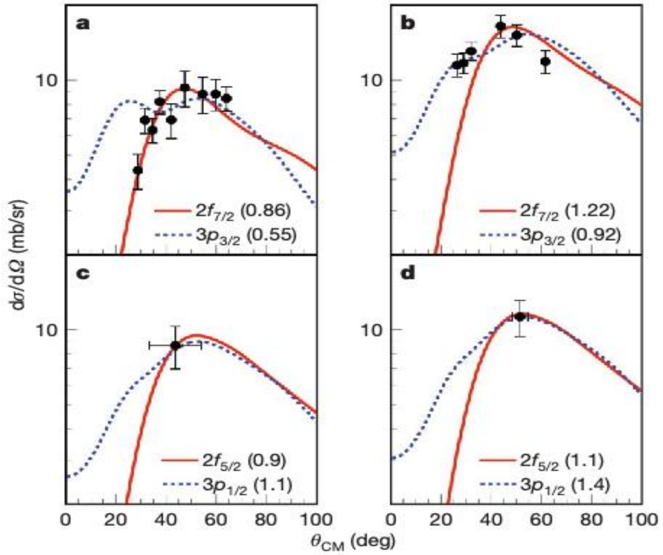

K.L. Jones et al., Nature 465, 454 (2010)

Knockout reactions with fast RI beams

- Nucleon knockout reactions with fast beam provide an efficient tool to excite nuclei extremely far from the stability and study their decay (in-flight)
  - At intermediate beam energy, a thick target (~g/cm^2) can be used to improve the luminosity
  - The secondary beam can be less exotic than the nuclei of interest, e.g.,
    - ^{70}Zn (stable) → ^{55}Sc or ^{56}Ti (2nd beam) → ^{54}Ca (interest)
    - ^{238}U (stable) → ^{79}Cu or ^{80}Zn (2nd beam) → ^{78}Ni (interest)

- Coupled with a large γ-ray detector array around the secondary reaction target, valuable information can be obtained, such as the energy of the first excited state in the residue nucleus
  - In even-even nuclei, the excitation energy of the first 2$^+$ state is very sensitive to the shell structure near the Fermi surface

- The parallel and transverse momentum distributions of the residue are sensitive to the angular momentum of the removed nucleon(s), constraining the spin-parity assignment to the populated excited states

- Comparing the measured partial cross sections to a particular excited state with single-particle cross sections calculated using reaction theory leads to the spectroscopic factors ($C^2S = \sigma_{exp}/\sigma_{sp}$) (again, it is model dependent)

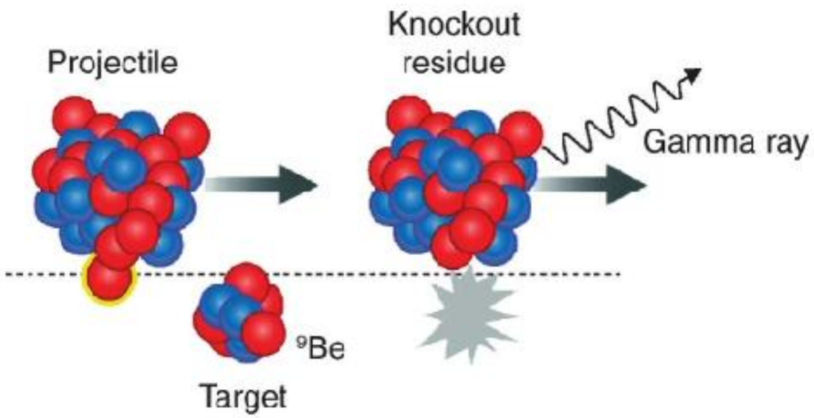

A. Gade et al., Phys. News 20:1, 11 (2010)

Proton-knockout reactions with a LH_2 target

- The energies of the prompt γ rays emitted from the reaction residue are Doppler shifted when detected by the γ detectors (E_γ) in the laboratory frame

$$E_0 = E_\gamma \frac{1 - \beta\cos(\theta)}{\sqrt{1-\beta^2}}$$

- The Doppler correction to obtain the transition energy E_0 in the nucleus frame requires
  - The angle of the emitted photon (θ) relative to the residue's velocity
  - The velocity of the residue (β) when emitting the photon

- Modern γ-ray tracking arrays (e.g., GRETINA/GRETA, AGATA, etc) have a large granularity to determine the photon-interaction positions precisely
  - The target thickness becomes the limiting factor
    - Thick → good luminosity and thus statistics, limited Doppler correction
    - Thin → good sensitivity for Doppler correction, limited luminosity

- A new technique was developed to install a thick liquid hydrogen target (10~15 cm) inside a time projection chamber (TPC)
  - Tracking the scattered protons (e.g., in *p*,2*p* reactions) allows for reconstructing the reaction-vertex position event-by-event
  - β (related to z) and θ (related to z) can be determined precisely for the Doppler correction, without compromising the luminosity

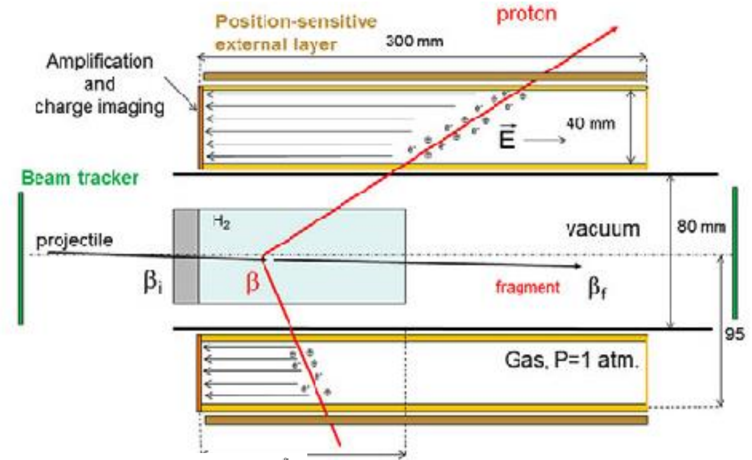

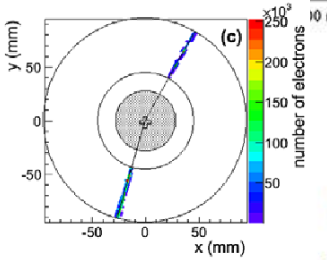

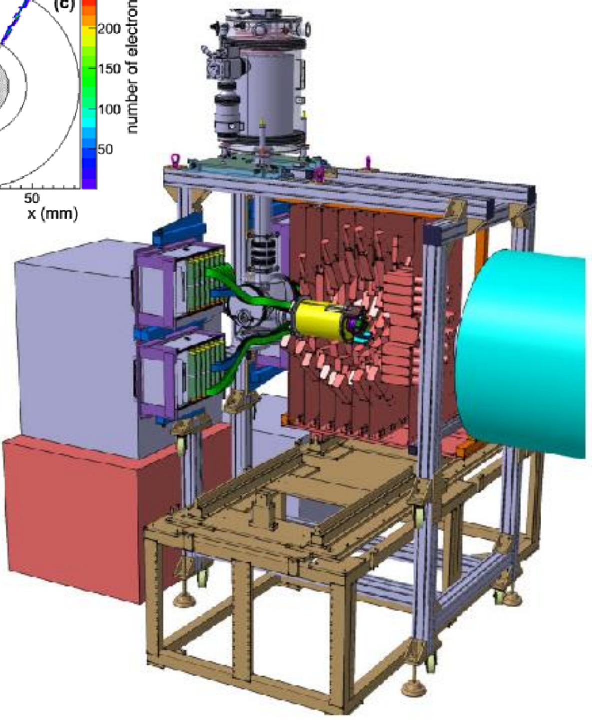

A. Obertelli et al., Eur. Phys. J. A 50, 8 (2014)

Measuring the excited states in ^{78}Ni

- According to the traditional shell model, ^{78}Ni is a doubly magic nucleus (Z=28, N=50)

- Those magic numbers have been suggested to shift at extreme neutron-to-proton ratios
  - Some previous works suggested Z=28 and N=50 persist, some said otherwise
  - A direct measurement on the first 2^+ state energy in ^{78}Ni is extremely critical

- The measurement was done at RIBF, RIKEN with the in-beam γ-ray spectroscopy using an array of NaI(Tl) scintillators (DALI2) in coincidence with ^{79}Cu(p, 2p) and ^{80}Zn(p, 3p) reactions
  - ^{79}Cu and ^{80}Zn were produced by the in-flight fission of 238U on a beryllium target
  - The use of the a LH_2 target (coupled with a TPC) made the measurement possible

- The first 2^+ state was revealed at 2.6 MeV, the first direct evidence for its doubly magic nature
  - Theoretical calculations were mostly consistent with the new results, and predicted a competing, deformed 0^+ excited state around 2.5 MeV (remains experimentally unknown)

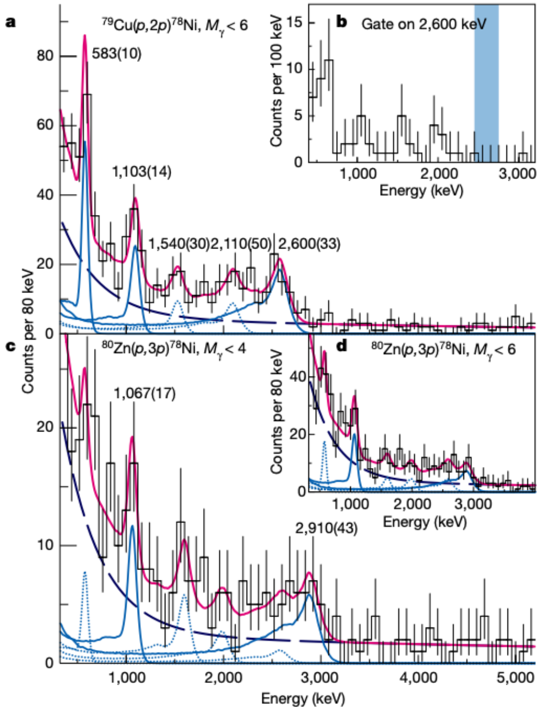

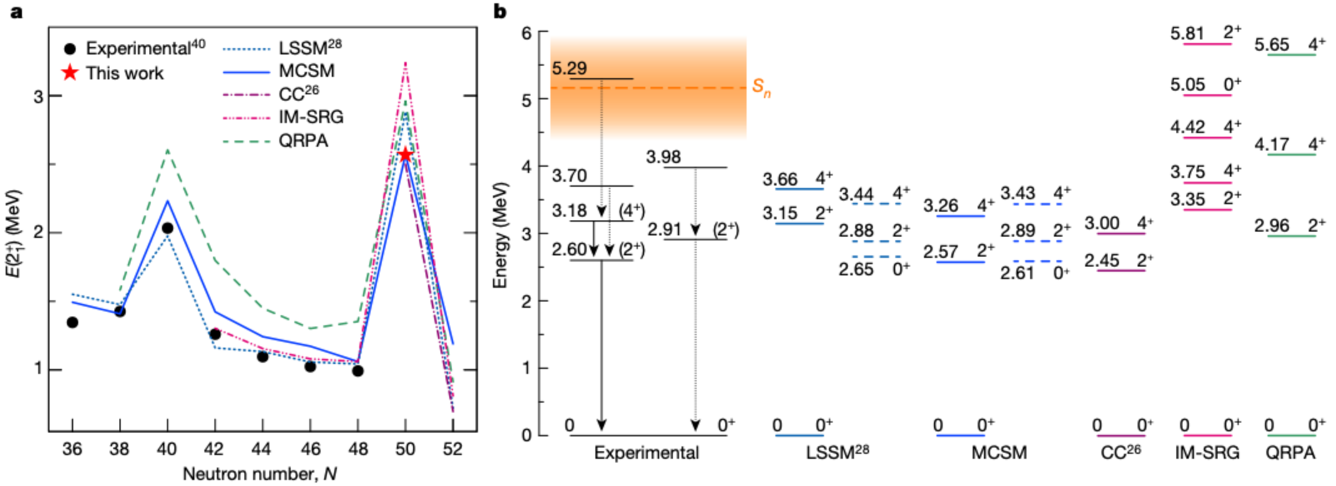

R. Taniuchi et al., Nature 569, 53 (2019)

Shape coexistence in ^{62}Cr

- ^{68}Ni was found to be doubly magic with *N*=40 being a sub-shell closure [see, e.g., R. Broda et al., PRL 74, 868 (1995)]
- However, this neutron sub-shell closure is very fragile and disappears quickly in ^{66}Fe and ^{64}Cr, regarded as the *N*=40 island of inversion (similar to *N*=20 and 28)
  - In those islands of inversion, the competitions between different shapes usually result in an excited 0^+ state at low energy → shape coexistence
  - No such shape coexisting with a 0+ excited state was found in *N*=40
- The experiment was done at FRIB, using in-beam γ-ray spectroscopy (GRETINA) of the two-proton knockout reaction ^{9}Be(^{64}Fe, ^{62}Cr+γ)
  - An excited state is found at 1.38 MeV, with its spin and parity assigned based on the parallel momentum distribution of ^{62}Cr (compared with a direct reaction model)
- Theoretical predictions suggest both 0^+ states are deformed; while the ground state is prolate, the excited state is triaxial

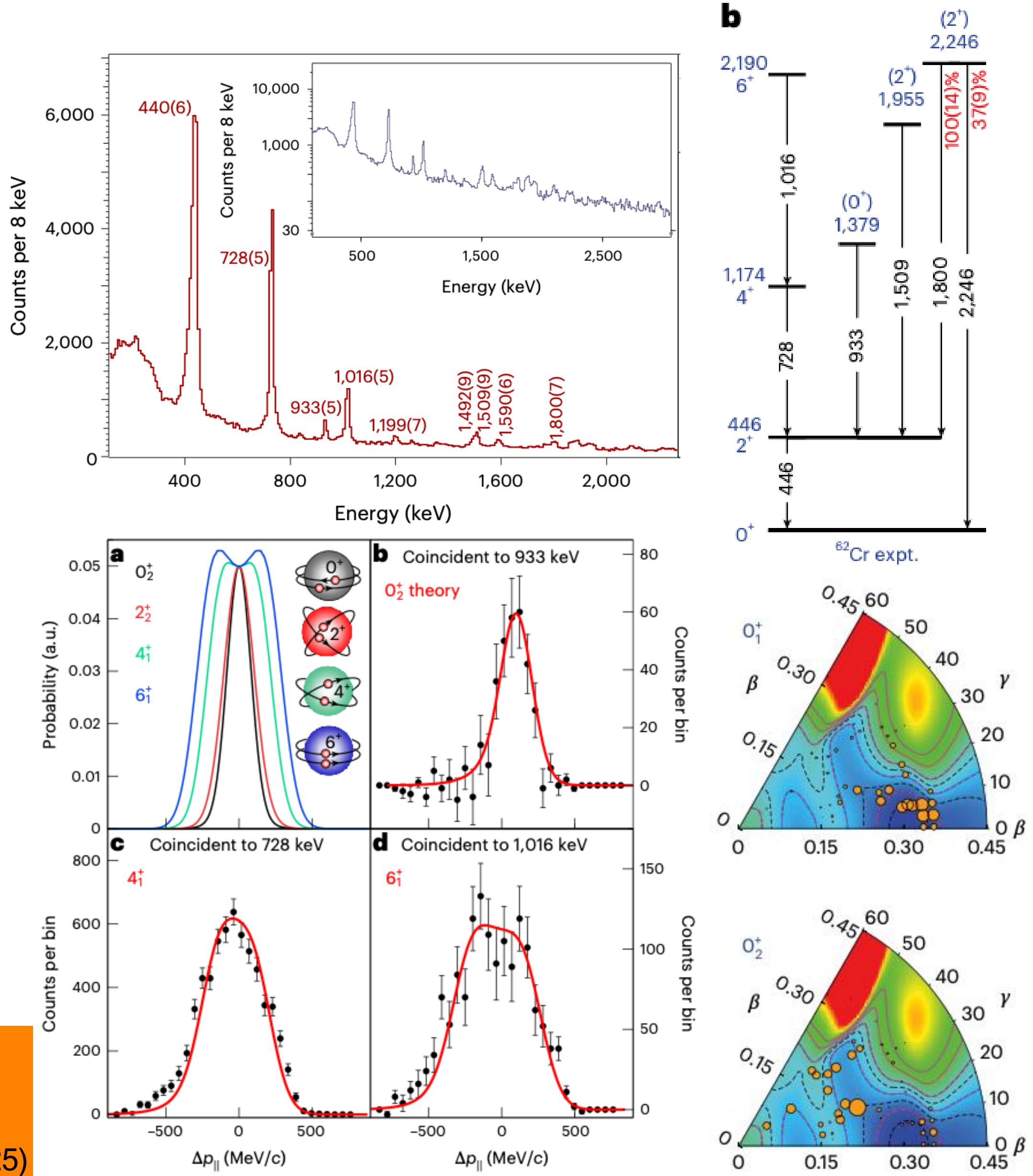

A. Gate et al., Nat. Phys. 21, 37 (2025)

Summary

- Experimental studies on the properties of exotic isotopes aim to benchmark nuclear theories developed via both phenomenological and ab initio methods

- The β decay of exotic nuclei shows rich physics phenomenon that can be linked to the underlying shell structure
    - The systematics of half-lives give the first exploration of shell evolution in the unknown territory (of the nuclear chart)
    - The β-strength function allows for more stringent tests on nuclear theories

- Different experimental observables can probe atomic nuclei from different perspectives
    - Complementary measurements are important to understand nuclear structure comprehensively